NOAA Technical Memorandum NMFS-AFSC-526

Results of the Acoustic-Trawl Survey of Walleye Pollock (*Gadus chalcogrammus*) in Shelikof Strait, Chirikof Shelfbreak, and Marmot Bay March 2025 (DY25-03)

D. Jones and M. Levine

August 2026

U.S. DEPARTMENT OF COMMERCE

National Oceanic and Atmospheric Administration
National Marine Fisheries Service
Alaska Fisheries Science Center

The National Marine Fisheries Service's Alaska Fisheries Science Center uses the NOAA Technical Memorandum series to issue informal scientific and technical publications when complete formal review and editorial processing are not appropriate or feasible. Documents within this series reflect sound professional work and may be referenced in the formal scientific and technical literature.

The NMFS AFSC Technical Memorandum series of the Alaska Fisheries Science Center continues the NMFS F/NWC series established in 1970 by the Northwest Fisheries Center. The NMFS NWFSC series is currently used by the Northwest Fisheries Science Center.

This document should be cited as follows:

Jones, D., Levine, M. 2026. Results of the Acoustic-Trawl Survey of Walleye Pollock (*Gadus chalcogrammus*) in Shelikof Strait, Chirikof Shelfbreak, and Marmot Bay March 2025 (DY25-03). U.S. Department of Commerce, NOAA Technical Memorandum NMFS-AFSC-526, 79 p.

This document is available online at:

Document available: https://repository.library.noaa.gov

Reference in this document to trade names does not imply endorsement by the National Marine Fisheries Service, NOAA.

Results of the Acoustic-Trawl Survey of Walleye Pollock (*Gadus chalcogrammus*) in Shelikof Strait, Chirikof Shelfbreak, and Marmot Bay March 2025 (DY25-03)

D. Jones[1], and M. Levine[1]

[1]Alaska Fisheries Science Center
National Marine Fisheries Service
National Oceanic and Atmospheric Administration
7600 Sand Point Way N.E.
Seattle, WA 98115-6349

U.S. DEPARTMENT OF COMMERCE

National Oceanic and Atmospheric Administration
National Marine Fisheries Service
Alaska Fisheries Science Center

NOAA Technical Memorandum NMFS-TM-AFSC-526

August 2026



U.S. Secretary of Commerce
Howard Lutnick

Under Secretary of Commerce
for Oceans and Atmosphere
Neil Jacobs

Assistant Administrator, National
Marine Fisheries Service.
Eugenio Piñeiro Soler

August 2026

www.nmfs.noaa.gov

OFFICIAL BUSINESS

National Marine
Fisheries Service
Alaska Fisheries Science Center
7600 Sand Point Way N.E.
Seattle, WA 98115 6349

Results of the Acoustic-Trawl Survey of Walleye Pollock (*Gadus chalcogrammus*) in Shelikof Strait, Chirikof Shelfbreak, and Marmot Bay

March 2025

(DY25-03)

by

Darin Jones and Mike Levine

Resource Assessment and Conservation Engineering Division

Alaska Fisheries Science Center

National Marine Fisheries Service

National Oceanic and Atmospheric Administration

7600 Sand Point Way NE

Seattle, WA 98115

August 2026

ABSTRACT

Scientists from the Alaska Fisheries Science Center conducted acoustic-trawl surveys in the Gulf of Alaska during winter 2025 to estimate the distribution and abundance of walleye pollock (*Gadus chalcogrammus*) at three of their primary spawning grounds. These pre-spawning walleye pollock surveys covered the Shelikof Strait, Chirikof Shelfbreak, and Marmot Bay regions. Abundance estimates were based on an analysis where backscatter was attributed to all trawl-captured species and size classes using the biological length-frequency data from the nearest trawl locations. Abundance estimates also included a correction for escapement of fishes and other catch from the survey trawl (i.e., net selectivity).

In the Shelikof Strait region, the amount of pollock was estimated to be 903.2 million fish weighing 323,423.8 t. The majority of the pollock in Shelikof Strait were age-7 and age-5 pollock (from the 2018 and 2020 year classes), which comprised 37.8% and 24.4% of the total pollock biomass, respectively. These adult pollock were primarily observed at 49 cm FL modal length. Age-1 pollock comprised 2.4% of the total pollock biomass (62.4% of total number) and were centered around 12 cm FL. In the Chirikof Shelfbreak region, the amount of pollock was estimated to be 113.3 million fish weighing 95,232.5 t. Pollock were primarily observed at 47 cm FL modal length, consistent with age-4+ pollock. In the Marmot Bay region, the amount of pollock was estimated to be 74.6 million fish weighing 2,256.1 t. Pollock were primarily observed at 13 cm FL modal length, consistent with age-1 pollock.

CONTENTS

ABSTRACT iii

INTRODUCTION 1

METHODS 1
- Acoustic Equipment, Calibration, and Data Collection 1
- Trawl Gear and Oceanographic Equipment 2
- Survey Design 3
- Data Analysis 5

RESULTS AND DISCUSSION 13
- Acoustic System Calibration 13
- Shelikof Strait Survey 13

CITATIONS 17

APPENDIX I. ITINERARY 51

APPENDIX II. SCIENTIFIC PERSONNEL 53

APPENDIX III. ABUNDANCE CALCULATIONS 55

APPENDIX IV. REGIONAL SUMMARIES 59
- Chirikof Shelfbreak 59
- Marmot Bay 67

APPENDIX V. RELATIVE ABUNDANCE OF SHELIKOF AGE-1 POLLOCK 75

INTRODUCTION

The Midwater Assessment and Conservation Engineering (MACE) Program of the Alaska Fisheries Science Center (AFSC) conducts annual acoustic-trawl (AT) surveys in the Gulf of Alaska (GOA) during late winter (Fig. 1). The goal of these surveys is to estimate the distribution and abundance of pre-spawning walleye pollock (*Gadus chalcogrammus*; hereafter pollock) at their main spawning grounds (i.e., pre-spawning surveys). The Shelikof Strait area has been surveyed annually in winter since 1980 (note that no estimates were made in 1980 or 1987, and no surveys were conducted in 1982, 1999, and 2011). These surveys have also intermittently included the Chirikof Shelfbreak and Marmot Bay areas.

This report presents the 2025 AT survey results from the Shelikof Strait area from March 17 to March 25, the Chirikof Shelfbreak area from March 25 to March 28, and the Marmot Bay area from March 28 to March 30.

METHODS

All activities were conducted aboard NOAA Ship *Oscar Dyson*, a 64-m stern trawler equipped for fisheries and oceanographic research. The survey followed established AT methods as specified in NOAA protocols for fisheries acoustics surveys and related sampling[1]. The acoustic units used here are defined in MacLennan et al. (2002). Survey itineraries are listed in Appendix I and scientific personnel in Appendix II.

Acoustic Equipment, Calibration, and Data Collection

Acoustic measurements were collected with a Simrad EK80 scientific echosounder (Bodholt and Solli 1992, Simrad 2018). Data were collected with five split-beam transducers (18, 38, 70, 120, and 200 kHz) mounted on the bottom of the vessel's retractable centerboard, which was extended 9.15 m below the water surface.

Two standard sphere acoustic system calibrations were conducted to measure acoustic system performance (Table 1). The vessel's dynamic positioning system was used to maintain the vessel

[1] National Marine Fisheries Service (NMFS) 2014. NOAA protocols for fisheries acoustics surveys and related sampling (Alaska Fisheries Science Center), 26 p. Prepared by Midwater Assessment and Conservation Engineering Program, Alaska Fish. Sci. Center, Natl. Mar. Fish. Serv., NOAA.

location during calibration. Local water temperature and salinity profiles were measured and used to estimate absorption and sound speed. A tungsten carbide sphere (38.1 mm diameter) suspended below the centerboard-mounted transducers was used to calibrate the 18, 38, 70, 120, and 200 kHz systems. A two-stage calibration approach was followed for each frequency. On-axis sensitivity (i.e., transducer gain and S_a correction) was estimated from measurements with the sphere placed in the center of the beam following the procedure described in Foote et al. (1987). Transducer beam characteristics (i.e., beam angles and angle offsets) were estimated by moving the sphere in a horizontal plane using the EK80's calibration utility (Jech et al. 2005, Simrad 2018). The equivalent beam angle (for characterizing the volume sampled by the beam) and angle sensitivities (for conversion of electrical to mechanical angles) cannot be estimated from the calibration approach used because that requires knowledge of the absolute position of the sphere (see Demer et al. 2015). Therefore, the factory default values for equivalent beam angle and angle sensitivities for each transducer were used during calibration.

Raw narrow and broadband acoustic data were recorded using EK80 software (version 24.6.1) at appropriate ping rates for the survey depths and analyzed from 16 m below the sea surface to within 0.5 m of the sounder-detected bottom to a maximum depth of 1,000 m. Data shallower than 16 m were excluded to account for the acoustic near-field range of the transducers (Simmonds and MacLennan 2005). Data within 0.5 m of the seafloor were also excluded to account for the bottom-associated acoustic dead zone (Ona and Mitson 1996). The raw acoustic data were analyzed using Echoview post-processing software (version 15.0.249, Echoview Software Pty Ltd).

Trawl Gear and Oceanographic Equipment

Midwater and near-bottom acoustic backscatter were sampled using an LFS1421 trawl[2]. The headrope and footrope of the LFS1421 trawl each measure 76.8 m (252.0 ft), with meshes tapering from 650.0 cm (256.0 in.) in the forward sections to 3.8 cm (1.5 in.) in the section immediately preceding the codend (mesh sizes are stretched measurements unless otherwise

[2] LFS1421 trawl (LFS Marine, NOAA, 1421 Research Trawl, designed and built in 2018/2019 to MACE specifications; hereafter LFS1421)

noted). To increase retention of small organisms, the LFS1421 codend was fitted with a knotless nylon 7.9 mm (0.31 in.) mesh, 3.2 mm (0.13 in.) square opening codend liner.

The LFS1421 trawl was fished with four 45.7 m (150.0 ft) bridles (1.9 cm (0.75 in.) dia.), 5 m^2 Series-2000-V trawl doors with 4 in. shoes (918.0 kg (2,024.0 lb) each), and 227 kg (500.0 lb) tom weights attached to each wingtip. Average trawling speed was 1.6 m s^{-1} (3.1 knots). LFS1421 trawl vertical net opening and headrope depth were monitored with a Simrad FS70 third-wire netsonde attached to the headrope. The vertical net opening of the LFS1421 trawl ranged from 15.5 to 32.0 m (50.9 to 105.0 ft) and averaged 19.8 m (65.0 ft) while fishing.

A stereo camera system (CamTrawl; Williams et al. 2010) was attached to the starboard panel forward of the codend on the LFS1421 trawl. The CamTrawl is used to capture stereo images for species identification and length measurement of individual fish and other taxa as they pass through the net toward the codend. The CamTrawl data are useful for determining the depth and size distribution of fish and other taxa when distinct and separate backscatter layers are sampled by a trawl haul as they cannot be differentiated in the codend catch. Images were viewed and annotated using procedures described in Williams et al. (2010).

Physical oceanographic data were collected during the cruise at trawl locations, at calibration locations, and continuously along transects. Water temperature profiles were obtained at trawl locations with a temperature-depth probe (SBE 39, Sea-Bird Scientific) attached to the trawl headrope. Additional temperature-depth measurements were taken from conductivity-temperature-depth (CTD) casts with a Sea-Bird CTD (SBE 911plus) system at the calibration site. Sea surface temperature data were measured using the ship's flow-through system (SBE 38, Sea-Bird Scientific, accuracy $\pm$ 0.002°C) located near the ship's bow, approximately 1.4 m below the surface. At times when the SBE 38 was not operating, sea surface temperatures were taken from the Furuno T-2000 temperature probe (accuracy $\pm$ 0.2°C) located amidships 1.4 m below the surface. These and other environmental data were recorded using the ship's Scientific Computing Systems (SCS).

Survey Design

The survey consisted of a series of predetermined parallel transects except in areas where it was necessary to reorient transects to maintain a perpendicular alignment to the isobaths or navigate

around landmasses. Spatial coverage, transect location, and spacing were chosen to be consistent with previous surveys.

Trawl hauls were conducted to identify the species and size composition of acoustically-observed fish aggregations and to determine biological characteristics of pollock and other specimens. Catches were sorted to species and weighed. When large numbers of juvenile and adult pollock were encountered, the predominant size groups in the catch were sampled separately (e.g., age-1 vs. larger sizes). Fork length (FL), body weight, sex (FL > 20 cm), maturity, age (otoliths), and gonad measurements were collected for a random subset of pollock within each size group. Pollock and other fishes were measured to the nearest 1 mm FL, or standard length (SL) for small specimens, with an electronic measuring board (Towler and Williams 2010). All lengths measured as SL were converted to FL using a SL to FL regression obtained from historic survey data when necessary. Other invertebrate organisms (e.g., jellyfish, squid) were measured to the nearest 1 mm length using accepted measurements for their class (e.g., jellyfish bell diameter, squid mantle length). Gonad maturity was determined by visual inspection and categorized as immature, developing, mature (hereafter, "pre-spawning"), spawning, or spent [3]. The ovary weight was determined for pre-spawning females. An electronic motion-compensating scale (Marel M60) was used to weigh individual pollock and selected ovaries to the nearest 2 g. Otoliths that were collected were stored in 50% glycerin/thymol/water solution and interpreted by AFSC Age and Growth Program researchers to determine fish ages. Trawl station information and biological measurements were electronically recorded using the MACE Program's custom Catch Logger for Acoustic Midwater Surveys (CLAMS) software.

Additional biological samples were collected for special projects. Pollock ovaries were collected from pre-spawning pollock to investigate interannual variation in fecundity of mature females and from female pollock of all maturity stages for a histological study (Sandi Neidetcher, Sandi.Neidetcher@noaa.gov). Pollock stomachs were collected to investigate food habits (Jon Reum, jonathan.reum@noaa.gov). Pacific lamprey (*Entosphenus tridentatus*) were collected to investigate metabarcoding for distribution and dietary studies (Laurie Weitkamp, laurie.weitkamp@noaa.gov). Finally, incidentally caught Chinook salmon (*Oncorhynchus*

[3] 2024 Groundfish Survey Data Codes and Forms. 2024. RACE Division, AFSC, NMFS, NOAA; 7600 Sand Point Way NE, Seattle, WA 98115. DOI: https://doi.org/10.25923/gt9j-rs58.

tshawytscha) were collected to investigate their distribution in the North Pacific (Kathrine Howard, kathrine.howard@noaa.gov).

Data Analysis

Pollock abundance was estimated by combining acoustic and trawl catch information. The analysis method employed here had three principal steps. First, backscatter was associated with the trawl catches from the nearest geographic haul locations within a stratum. Second, a correction was made for net selectivity (escapement from the midwater net, based on relationships derived from recapture nets; Williams et al. 2011). Third, backscatter was converted to estimates of abundance using the nearest-haul catch association (step 1) with sample corrections (step 2) and the expected backscatter from each organism given species and size. Biomass was computed from abundance using the mean weight-at-length from all pollock specimens measured in the survey.

Processing of Acoustic Data

Although acoustic data were recorded at five frequencies, the results of this report and the survey time series are based on the 38 kHz data. The sounder-detected bottom was calculated by averaging the bottom detections for the five frequencies (Jones et al. 2011) and then visually examined to remove any bottom integrations. A minimum S_v threshold of -70 dB re 1 m^{-1} was applied to the 38 kHz acoustic data, which were then echo-integrated from 16 m below the surface to 0.5 m above the sounder-detected bottom, or to a maximum depth of 1,000 m in cases where the bottom depth was > 1,000 m. Data were averaged at 0.5 nmi horizontal by 10 m vertical resolution intervals and exported to a database.

Associating Size and Species Composition with Acoustic Backscatter

Acoustic backscatter was assigned to strata based on the appearance and vertical distribution of the aggregations in the echogram. Strata containing backscatter not considered to be from pollock (e.g., the near-surface mixture of unidentifiable backscatter, backscatter with frequency response indicative of euphausiids or myctophids (De Robertis et al. 2010), or near-bottom backscatter "haystack" morphology indicative of some rockfishes) were excluded from further analyses. Each trawl was associated with a stratum, and the backscatter at a given location was associated with the species and size composition of the geographically-nearest haul within that

stratum (see De Robertis et al. 2017b for details). For example, juvenile pollock can be found in shallow, dense schools with a diffuse layer of adult pollock at deeper depths in the same area. In this case, the backscatter dominated by aggregations of juveniles would be assigned to a shallow stratum (A) and the backscatter dominated by adult layers would be assigned to a deep stratum (B). Hauls that sampled the shallow layer would be assigned to stratum A, and hauls that sampled the deeper layer would be assigned to stratum B. Backscatter was apportioned by species and size within a stratum using the selectivity-corrected catch composition from the geographically nearest trawl in that stratum and converted to abundance.

Accounting for Catch from Non-Targeted Scattering Layers

As noted above, each trawl was associated with an acoustic backscatter stratum. However, trawls may capture animals while passing through non-targeted strata during the trawling process. For example, a trawl targeting a deep stratum may capture acoustically-relevant animals while passing through a shallower stratum during set and retrieval. Because trawls aggregate catch from all the strata sampled, animals from the shallow stratum could then be associated incorrectly with the deeper stratum during analysis. These animals should not be included in the catch that is applied to the deeper stratum.

To avoid incorrectly applying catch from different strata, CamTrawl images collected during LFS1421 trawls were used to identify catch location in the water column. CamTrawl images were captured at a rate of approximately 2 s^{-1} and each image was tagged with collection time and depth. Analysts visually identified and counted animals present in every 100^{th} image (approximately one image per 45 seconds of trawl time) using SEBASTES Stereo Image Analysis software (Williams et al. 2016). For every examined image, the analyst identified all visible fish to the lowest taxonomic level possible, and identified invertebrates to broad taxonomic group (i.e., 'jellyfish,' 'squid,' 'shrimp'). Images were then examined using custom Python applications to identify cases where the trawl retained catch from non-targeted layers. In cases where it was evident that the trawl catch contained acoustically relevant species and/or size classes from outside of the target stratum, these species and/or size class records were excluded during the analysis process from the trawl catch associated with the target stratum (see Fig. 3 and Fig. 4 in Levine et al. (2024) for a summary of the review process).

Selectivity Correction

Previous research has found that smaller pollock are less likely to be retained in large midwater trawls than larger pollock (Williams et al. 2011). To correct for species- and size-related differences in retention, trawl catch compositions were adjusted to that which would be expected from an unselective net. Trawl selectivity was estimated using correction functions developed from catch data collected by recapture nets mounted on the midwater trawl. Net selectivity corrections to trawl species and size composition estimates have been implemented to winter Shelikof Strait AT surveys conducted since 2008 based on the survey vessel, how backscatter was allocated to species, and the type of midwater net used in the survey (Lauffenburger et al. 2019, Stienessen et al. 2019, McCarthy et al. 2022, Honkalehto et al. 2024). Trawl selectivity in the 2025 survey was estimated for all species observed in the codend using correction functions developed from catch data collected by recapture nets mounted on the LFS1421 trawl during the 2020 and 2021 winter Shelikof Strait AT surveys (see Appendix IV in Honkalehto et al. 2024). The counts and weights of fish and other taxa caught in the recapture nets were expanded to provide an estimate of escapement from the entire trawl. The catch of all species was corrected for the estimated probability of escapement by dividing the abundance of a given species and size class by the estimated probability of retention of that species and size class. The probability of retention was calculated using either species-specific trawl selectivity correction functions for the most abundant species or more generic selectivity functions for less abundant species that were pooled together (De Robertis et al. 2017b, Honkalehto et al. 2024). Thus, the 2025 survey estimates reflect adjustments to the trawl-derived estimates of species and size composition which incorporate the estimated escapement of all organisms from the LFS1421 catch (e.g., De Robertis et al. 2017a).

Specimen Weighting

Pollock specimen data collected from catches were used to compute length-weight keys and age-length keys (which are used to convert pollock abundance-at-length into biomass-at-length, numbers-at-age, and biomass-at-age; see Appendix III) and pollock maturity parameters (maturity-at-length, maturity-at-age, and proportion-at-maturity stage). Each specimen was weighted by a factor computed to express how it represented the total surveyed population. This process consisted of two scalars. The first scalar is the proportion of all the fish in the haul that

each specimen represents, which accounts for catch subsampling for specimens by age subcategory and also for length-dependent retention by the trawl, or trawl selectivity. The second scalar is the local abundance as estimated by the survey, computed as the total number of pollock estimated in the "nearest-haul" stratum associated with a particular trawl sample. For a full description of this process see McGowan et al. (in prep.).

Abundance Calculations

A series of target strength (TS, dB re 1 m^2; the expected backscatter from each organism) to length (hereafter TS-length) relationships from the literature (Table A1) were used along with size and species distributions from selectivity-corrected trawl catches to estimate the proportion of the observed acoustic scattering attributable to each of the species captured in the trawls (Appendix III). For species for which the TS-length relationship was derived using a different length measurement type than the one used for measuring the trawl catch specimens, an appropriate length conversion was applied (e.g., total length to fork length). Species-specific TS-length relationships from the literature were used for pollock, Pacific capelin, eulachon, Pacific herring, and for any species whose contribution to the total backscatter used in survey estimates was > 5% when available. Otherwise, species were assigned to one of five group TS-length relationships: fishes with swim bladders, fishes without swim bladders, jellyfish, squid, and pelagic crustaceans (Table A1).

Biomass-at-length was computed from abundance-at-length using the mean weight-at-length from all pollock specimens included in the length-weight key, which in winter is typically all specimens lengthed and weighed in the survey trawl catches (Appendix III). When < 5 pollock occurred within a 1-cm length interval, weight at that length interval was estimated from a linear regression of the natural logs of the length and weight data and corrected for a small bias due to back-transformation (Appendix III; Miller 1984, De Robertis and Williams 2008).

An age-length key and a proportion-at-age matrix were applied to the population numbers-at-length and biomass-at-length to estimate numbers- and biomass-at-age (Appendix III; Jones et al. 2019). For population estimates at lengths where no otolith specimens were collected, the proportion at age was estimated using a Gaussian-model approach based on historical age at length data (2000-2014).

Processing of Maturity Data

As previously noted, maturity data by haul were weighted by the local acoustically-estimated abundance of pollock (McGowan et al. in prep.). A > 40 cm fork length cutoff was used in computing local pollock abundance for consistency with reporting from past surveys. The proportion of pollock at each maturity stage (immature, developing, pre-spawning, spawning or spent) was determined for both male and female pollock. Additionally, the length at 50% maturity ($L50$) was estimated for female pollock as a logistic regression using a weighted generalized linear model following Williams (2007) with the inclusion of the haul weights, W_h, into the model (function glm, R Core Team 2021).

Relative Estimation Error

Relative estimation errors for the acoustic-based estimates were derived using a one-dimensional (1-D) geostatistical method (Petitgas 1993, Williamson and Traynor 1996, Walline 2007). "Relative estimation error" is defined as the ratio of the square root of the 1-D estimation variance ($variance_{sum}$) to the biomass estimate (i.e., the sum of biomass over all transects, $biomass_{sum}$, kg):

$$Relative\ estimation\ error_{1-D} = \frac{\sqrt{variance_{sum}}}{biomass_{sum}} \quad . \qquad \text{(Eq. 1)}$$

Because sampling resolution affects the variance estimate, and the 1-D method assumes equal transect spacing, estimation variance was determined separately in each area with unique transect spacing. Relative estimation error for an entire survey area (among n survey areas with different transect spacings) was computed by summing the estimation variance for each area j, taking the square root, and then dividing by the sum of the biomass over all areas, assuming independence among estimation errors for each survey area (Rivoirard et al. 2000):

$$Relative\ estimation\ error_{1-D\ survey} = \frac{\sqrt{\sum_{j=1}^{n} variance_{sum_j}}}{\sum_{j=1}^{n} biomass_{sum_j}} \quad . \qquad \text{(Eq. 2)}$$

Geostatistical methods were used to compute estimation error to account for estimation uncertainty arising from the observed spatial structure in the fish distribution. These errors,

however, quantify only across-transect sampling variability of the acoustic data (Rivoirard et al. 2000). Other sources of error (e.g., target strength, trawl sampling) were not evaluated.

Spatial Patterns Analysis

To examine pollock horizontal distribution in the Shelikof Strait relative to prior surveys, geostatistical measures of the mean location (center of gravity) and dispersion of the distribution around its center of gravity (inertia) were calculated for each Shelikof Strait survey from 2008 to 2025 (Woillez et al. 2007). To account for interannual changes in survey coverage, center of gravity and inertia were estimated using acoustic samples located within a standardized area of Shelikof Strait based on a minimum convex polygon that encompassed 95% of all samples collected between 2008 and 2025. The minimum convex polygon was estimated using the smoothed cross-validation bandwidth selector and kernel density estimator functions in the 'KS' R package (Duong 2022). Center of gravity and inertia were calculated using the 'gstlearn' R package (MINES Paris – PSL University 2025).

Additional Analyses

Pollock vertical distribution patterns were examined using two metrics: 1) mean weighted depth (MWD) of pollock from the surface-referenced primary analysis, and 2) height above bottom (HAB) calculated from a 'bottom-referenced' analysis in which pollock vertical position was measured in terms of distance above the seafloor. The MWD in each along-track interval i is computed as:

$$MWD_i = \sum_j \left(\left(\frac{B_{i,j}}{\sum_j B_{i,j}} \right) d_{i,j} \right) \quad , \qquad \text{(Eq. 3)}$$

where $B_{i,j}$ is observed biomass in 0.5 nmi along-track interval i and 10 m depth bin j, and d is the depth in meters of bin i from the sea surface. In contrast to the surface-referenced primary analysis, the bottom-referenced analysis data were exported using Echoview in 10 m vertical bins referenced to the scrutinized line 0.5 m above the sounder-detected bottom. The HAB is computed in a similar fashion:

$$HAB_i = \sum_j \left(\left(\frac{B_{i,j}}{\sum_j B_{i,j}} \right) h_{i,j} \right) \quad , \qquad \text{(Eq. 4)}$$

where the terms are as described above and h is the height in meters of bin i above the sounder-detected bottom. MWD and HAB were summarized for a given survey area by first summing biomass over all intervals i in the area and then computing the MWD and HAB using the equations above. The bottom-referenced analysis was generated for previous years to allow for inter-annual comparison of vertical distribution. All other parts of this analysis were the same as the primary analysis.

Revisions to Survey Time Series

While the current report is focused on the results of the winter 2025 AT survey, results from previous surveys are referenced to provide historical context. Two recent revisions have improved this historical survey time series.

In the period from 1981-2000, many Shelikof Strait surveys were conducted using multiple vessel passes within the Strait (Fig. 2a; note years with multiple dashed lines), with abundance and biomass values derived in various ways depending on the survey year and extent of the individual passes. The original method used to combine multiple passes in 1997 and 2000 was unclear, which impacts the reproducibility of these two survey estimates. Therefore, it was more straightforward for reproducibility to simply use the results from a single pass in each of these years to represent the survey biomass. This had minimal impact on the reported estimates: in both 1997 and 2000, the newly reported biomass values from a single pass were within 3% of the previously reported values from combining two passes. Furthermore, the observed proportions at length and age were very similar for each pass in these two years, so the choice to only use a single survey pass did not impact the reported proportions at length and age.

The current MACE AT survey and analysis methods incorporate multiple technical advancements introduced over the course of the survey time series. Advances have encompassed improved hardware (i.e. trawl net improvements, updated echosounder systems) and analytical approaches (including associating backscatter with the spatially nearest haul, estimating species- and size- specific escapement of organisms from the trawl net, apportioning acoustic backscatter to all organisms captured in trawls, using species-specific target strength-to-length relationships for a larger range of species, and weighting specimen data by local abundance). These updates have been incorporated on an incremental basis, resulting in the Shelikof Strait survey time

series abundance and biomass values previously presented in routine survey reports (i.e. Levine and Jones 2024) and provided for annual stock assessments (i.e. Monnahan et al. 2024) being estimated using various approaches. The period from 2008-2025 has recently been re-analyzed using the most up-to-date methods to produce a standardized index (McGowan et al. in prep.). While standardized pollock abundance and biomass estimates have generally changed by < 5% on a per-survey basis, the updated estimates increase accuracy, precision, and more completely account for sampling bias as compared to the historical estimates (McGowan et al. in prep.). Therefore, updated results for the 2008-2025 Shelikof Strait time series are presented in the current report and provided for management advice.

RESULTS AND DISCUSSION

The biomass and age composition data from the Shelikof Strait region are used directly as an input to the pollock annual stock assessment model (Monnahan et al. 2023), while data from the remaining surveyed regions (Chirikof Shelfbreak and Marmot Bay) are used to help managers apportion the total allowable catch between fishery management areas. The structure of this report reflects this division, with the Shelikof Strait presented in the body of the report and all other surveyed regions presented separately in Appendix IV.

Acoustic System Calibration

Pre-survey calibration measurements of the 38 kHz echosounder showed no notable differences in on-axis gain parameters or beam pattern characteristics, confirming that the acoustic system was stable throughout the survey (Table 1). At 38 kHz the integration gain differed by < 0.10 dB across the two measurements. On-axis acoustic system gain, S_a correction values, and EK80 calibration utility 3 dB beamwidths and offset angles measured during the winter 2025 calibrations were averaged in the linear domain. These averaged values were used with the nominal sound speed and absorption values appropriate for the survey areas in the final parameter set for survey data analysis. The measured equivalent beam angle recorded on the 38 kHz transducer's specification sheet was adjusted (Bodholt 2002) using the sound speed assumed during survey conditions for data analysis (Table 1).

Shelikof Strait Survey

Survey Timing and Extent

The 2025 winter AT survey of pre-spawning pollock in Shelikof Strait was conducted between 17 March and 25 March (Fig. 2a). Since 2019, Shelikof Strait has been surveyed a few days earlier than in prior years because of the relatively high percentages of spawning and spent female pollock observed in the 2017-2018 winter Shelikof Strait surveys (Fig. 2b). An earlier start date in Shelikof Strait was intended to increase the chances of surveying when most pollock were in the mature (or pre-spawning) stage, as well as to increase the chances that < 10% of female pollock were in the spawning or spent stages, a timing consistent with most prior surveys. However, in 2025 vessel mechanical delays resulted in the survey being conducted approximately a week later than originally planned.

The entire survey area encompassed 23,120 km^2 (6,741 nmi^2). Acoustic backscatter was measured along 1,634.4 km (882.5 nmi) of transects spaced primarily 13.9 km (7.5 nmi) apart, with spacing varying from 11.3 km to 15.6 km (6.1 to 8.4 nmi) in the survey area where the transects transition to a more southerly orientation (Fig. 3). Bottom depths in the survey area ranged from 46 m to 325 m.

Environmental Conditions

Sea surface temperatures (SST) measured in Shelikof Strait in 2025 indicated relatively warmer thermal conditions during the survey. SST ranged from 3.1°C to 5.5°C as measured by the ship's flow-through instrumentation along acoustic transects and averaged 4.8°C (Fig. 4). The average SST measured by the SBE 39 at all haul locations was 4.8°C (Table 2), which was 1.6°C warmer than the mean SST in 2024 and 1.2°C warmer than the long-term 1989-2024 historical mean (Fig. 5). The average temperature at 100 m depth, used as an indicator of thermal conditions at depth, was 5.4°C, which was 1.4°C warmer than the haul-based mean temperature at 100 m depth in 2024 and 1.2°C warmer than the long-term 1989-2024 historical mean (Fig. 5). Mean temperature between the surface and deepest trawl (i.e., headrope) depth at all haul locations varied by approximately 0.9°C (Fig. 6).

Trawl Catch Summary

Biological data and specimens were collected in Shelikof Strait from 22 LFS1421 hauls (Table 2, Fig. 3). Pollock were randomly sampled for length (n = 6,006), body weight (n = 1,070), maturity (n = 835), and age (n = 597 otoliths collected) measurements (Table 3). Pollock and Pacific ocean perch were the most abundant species by weight in the LFS1421 hauls, contributing 83.9% and 6.1% of the total catch by weight respectively (Table 4). Euphausiids and pollock were the most abundant species by numbers with 46.6% and 18.8% of the total catch by numbers, respectively (Table 4).

Pollock Maturity

Most female pollock in Shelikof Strait were in the pre-spawning stage of maturity and substantially fewer were spawning or spent, which suggests that the timing of the 2025 Shelikof Strait survey relative to the spawning period was appropriate (Fig. 2b). The maturity composition of females > 40 cm FL (n = 534) was 0% immature, 2% developing, 91% pre-spawning, 6%

spawning, and 1% spent, while the maturity composition of males > 40 cm FL (n = 204) was 1% immature, 1% developing, 22% pre-spawning, 75% spawning, and 1% spent (Fig. 7a). The length at which 50% of female pollock were determined to be reproductively mature (i.e., pre-spawning, spawning, or spent) was 41.8 cm FL (Fig. 7b).

Distribution and Abundance

Adult pollock (defined as age-3+ and comprising 97.6% of the total biomass and 37.6% of the total numbers in the Shelikof Strait) were detected throughout the Strait, with the largest aggregations concentrated in the western central portion of the sea valley ranging from Katmai Bay to the north to Wide Bay to the south (Fig. 8). Juvenile pollock (largely comprised of age-1 fish and comprising 2.4% of the total biomass and 62.4% of the total numbers) were observed in moderate numbers throughout the Strait, with aggregations observed primarily near the eastern ends of the northern transects near Kodiak Island. The center of gravity for pollock biomass shifted 0.8 km to the east and 0.8 km to the south from the 2024 distribution, which continued a more pronounced shift of 21.0 km to the west and 5.6 km to the south from the historical mean center of gravity between 2008 and 2024 (Fig. 9).

Most adult pollock were detected between depths of 195-275 m from the surface (Fig. 10a). Most juvenile pollock were between depths of 65-165 m (Fig. 10b) from the surface. The 'bottom-referenced' analysis indicated that adult pollock were primarily observed within 55 m of the seafloor with most juveniles found within 125 m of the seafloor (Fig. 10c, d). Adult pollock depth distributions in 2025 were similar to 2024 (Fig. 10a, c), with 24.5% of the biomass observed within 10 m of the seafloor, and 81.6% percent of biomass within 50 m of the seafloor (Fig. 10c).

A total of 903.2 million pollock weighing 323,423.8 t were estimated to be in Shelikof Strait at the time of the survey (Tables 5, 6, & 7). The 2025 biomass was 12.2% higher than that observed in 2024 (288,237.7 t) and was 40.6% less than the historical mean of 544,847.1 t (Table 5, Fig. 16). The relative estimation error of the 2025 biomass estimate based on the 1-D geostatistical analysis was 7.6% (Table 5).

The majority of the pollock population was comprised of age-7 and age-5 pollock (from the 2018 and 2020 year classes, respectively), which comprised 37.8% and 24.4% of the total pollock

biomass. These pollock were primarily observed at 49 cm modal length (Tables 6 & 7, Fig. 11; for the progression of specific year classes also see Figs. 13 and 14). Compared to previous surveys, the pollock from these primary age classes were within 1 standard deviation of the historical mean weight and length for age-7 and age-5 pollock, respectively (Fig. 15).

Historic Population Trends

Historic population trends in Shelikof Strait, as observed by winter pre-spawning AT surveys, track the strong year classes well through time starting from relatively small sizes and young ages (Figs. 13 & 14). McKelvey (1996) showed that there was a strong relationship between the estimated number of age-1 pollock from the Shelikof Strait pre-spawning survey and year-class strength for GOA pollock. The McKelvey index was based on data that did not include a correction for escapement of age-1 pollock (i.e. data were not corrected for trawl selectivity). A recent analysis of selectivity-corrected data in surveys from 2008-2022 indicated that, as in the historic McKelvey index, the abundance of age-1 pollock continues to be positively correlated with age-3 abundance for the same year class ($r^2 = 0.51$, n = 13; Appendix V). Given this continued correlation, age-1 year class strength is now estimated as 'low', 'medium', or 'high' based on the normal deviate ("Z-score") of age-1 abundance relative to the time period from 2008-2023 (2023 represents the most recent survey year from which the cohort first observed as age-1 fish were subsequently observed as age-3 fish).

In 2025 age-1 pollock contributed 2.4% by biomass and 62.3% by number (Fig. 17). This represents a medium strength year class (Z = 0.23, n = 14). The relationship between age-1 abundance and age-3 abundance for the same year class remains positive but variable (for the period from 2008-2023, $r^2 = 0.48$, n = 14).

CITATIONS

Bodholt, H. 2002. The effect of water temperature and salinity on echo sounder measurements. ICES Symposium on Acoustics in Fisheries, Montpellier, France, 10–14 June 2002.

Bodholt, H., and H. Solli. 1992. Split beam techniques used in Simrad EK500 to measure target strength. Pages 16–31 *In* World Fisheries Congress. May 1992, Athens, Greece.

De Robertis, A., D. R. McKelvey, and P. H. Ressler. 2010. Development and application of an empirical multifrequency method for backscatter classification. Can. J. Fish. Aquat. Sci. 67:1459–1474.

De Robertis, A., and K. Taylor. 2014. *In situ* target strength measurements of the scyphomedusa *Chrysaora melanaster*. Fish. Res. 153:18–23.

De Robertis, A., K. Taylor, K. Williams, and C. D. Wilson. 2017a. Species and size selectivity of two midwater trawls used in an acoustic survey of the Alaska Arctic. Deep Sea Res. Pt. II 135:40–50.

De Robertis, A., K. Taylor, C. D. Wilson, and E. V. Farley. 2017b. Abundance and distribution of Arctic cod (*Boreogadus saida*) and other pelagic fishes over the U.S. Continental shelf of the northern Bering and Chukchi Seas. Deep Sea Res. Part II 135:51–65.

De Robertis, A., and K. Williams. 2008. Weight-length relationships in fisheries studies: The standard allometric model should be applied with caution. Trans. Am. Fish. Soc. 137:707–719.

Demer, D. A., L. Berger, M. Bernasconi, E. Bethke, K. Boswell, D. Chu, R. Domokos, A. Dunford, S. Fässler, S. Gauthier, L. T. Hufnagle, J. M. Jech, N. Bouffant, A. Lebourges-Dhaussy, X. Lurton, G. J. Macaulay, Y. Perrot, T. Ryan, S. Parker-Stetter, S. Stienessen, T. Weber, and N. Williamson. 2015. Calibration of acoustic instruments. ICES Coop. Res. Rep. 326. 133p.

Demer, D. A., and S. G. Conti. 2005. New target-strength model indicates more krill in the Southern Ocean. ICES J. Mar. Sci. 62:25–32.

Duong, T. 2022. Ks: Kernel smoothing.

Foote, K. G. 1987. Fish target strengths for use in echo integrator surveys. J. Acoust. Soc. Am. 82:981–987.

Foote, K. G., H. P. Knudson, G. Vestnes, and E. J. Simmonds. 1987. Calibration of acoustic instruments for fish density estimation: A practical guide. ICES Coop. Res. Rep. 144:69.

Foote, K. G., and J. J. Traynor. 1988. Comparisons of walleye pollock target strength estimates determined from *in situ* measurements and calculations based on swimbladder form. J. Acoust. Soc. Am. 83:9–17.

Gauthier, S., and J. K. Horne. 2004. Acoustic characteristics of forage fish species in the Gulf of Alaska and Bering Sea based on Kirchhoff-approximation models. Can. J. Fish. Aquat. Sci. 61:1839–1850.

Guttormsen, M. A., and C. D. Wilson. 2009. *In situ* measurements of capelin (*Mallotus villosus*) target strength in the North Pacific Ocean. ICES J. Mar. Sci. 66:258–263.

Honkalehto, T., A. McCarthy, M. Levine, D. Jones, and K. Williams. 2024. Results of the acoustic-trawl survey of walleye pollock (*Gadus chalcogrammus*) in Shelikof Strait and Marmot Bay March 2021 (DY-202102). AFSC Processed Rep. 2024-08, 68 p. Alaska Fish. Sci. Cent., NOAA, Natl. Mar. Fish. Serv., 7600 Sand Point Way NE, Seattle WA 98115.

Jech, J. M., K. G. Foote, D. Chu, and L. C. Hufnagle. 2005. Comparing two 38-kHz scientific echosounders. ICES J. Mar. Sci. 62:1168–1179.

Jones, D. T., A. De Robertis, and N. J. Williamson. 2011. Statistical combination of multi-frequency sounder-detected bottom lines reduces bottom integrations. U.S. Dep. Commer., NOAA Tech. Memo. NMFS-AFSC-219:13 p.

Jones, D. T., N. E. Lauffenburger, K. Williams, and A. De Robertis. 2019. Results of the acoustic-trawl survey of walleye pollock (*Gadus chalcogrammus*) in the Gulf of Alaska, June-August 2017 (DY2017-06). AFSC Processed Rep. 2019-08, 110 p. Alaska Fish. Sci. Cent., NOAA, Natl. Mar. Fish. Serv., 7600 Sand Point Way NE, Seattle WA 98115.

Kang, D., T. Mukai, K. Iida, D. Hwang, and J.-G. Myoung. 2005. The influence of tilt angle on the acoustic target strength of the Japanese common squid (*Todarodes pacificus*). ICES J. Mar. Sci. 62:779–789.

Lauffenburger, N., K. Williams, and D. Jones. 2019. Results of the acoustic-trawl surveys of walleye pollock (*Gadus chalcogrammus*) in the Gulf of Alaska, March 2019 (SH2019-04). AFSC Processed Rep. 2019-10, 76 p. Alaska Fish. Sci. Cent., NOAA, Natl. Mar. Fish. Serv., 7600 Sand Point Way NE, Seattle WA 98115.

Levine, M., and D. Jones. 2024. Results of the acoustic-trawl survey of walleye pollock (*gadus* chalcogrammus) in the Shumagin Islands, Shelikof Strait, and Chirikof shelfbreak, February and March 2024 (DY2024-01 and DY2024-03). AFSC Processed Rep. 2025-07, 82 p. Alaska Fish. Sci. Cent., NOAA, Natl. Mar. Fish. Serv., 7600 Sand Point Way NE, Seattle WA 98115.

Levine, M., D. Jones, and D. McGowan. 2024. Results of the acoustic-trawl survey of walleye pollock (*Gadus chalcogrammus*) in the Gulf of Alaska, June-July 2021 (DY2021-04). AFSC Processed Rep. 2024-07, 100 p. Alaska Fish. Sci. Cent., NOAA, Natl. Mar. Fish. Serv., 7600 Sand Point Way NE, Seattle WA 98115.

MacLennan, D. N., P. G. Fernandes, and J. Dalen. 2002. A consistent approach to definitions and symbols in fisheries acoustics. ICES J. Mar. Sci. 59:365–369.

McCarthy, A., M. Levine, and D. Jones. 2022. Results of the acoustic-trawl surveys of walleye pollock (*Gadus chalcogrammus*) in the Shumagin Islands and Shelikof Strait, February and March 2020 (DY-202001 and DY-202003). AFSC Processed Rep. 2022-08, 78 p. Alaska Fish. Sci. Cent., NOAA, Natl. Mar. Fish. Serv., 7600 Sand Point Way NE, Seattle WA 98115.

McGowan, D. W., K. William, D. T. Jones, N. E. Lauffenburger, M. Levine, and M. Phillips. in prep. Reanalysis of winter and summer Gulf of Alaska walleye pollock acoustic-trawl surveys. U.S. Dept. Commer., Seattle, WA.

McKelvey, D. R. 1996. Juvenile walleye pollock, *Theragra chalcogramma*, distribution and abundance in Shelikof Strait—what can we learn from acoustic surveys. Ecology of juvenile walleye pollock, *Theragra chalcogramma*. U.S. Dep. Commer., NOAA Tech. Rep. NMFS 126. Alaska Fish. Sci. Cent., NOAA, Natl. Mar. Fish. Serv., 7600 Sand Point Way NE, Seattle WA 98115.

Miller, D. M. 1984. Reducing transformation bias in curve fitting. Am. Stat. 38:124–126.

MINES Paris – PSL University. 2025. gstlearn/gstlearn: Release v1.9.0 (stable_1.9.0). MINES Paris – PSL University; Zenodo. https://doi.org/10.5281/zenodo.13343742.

Monnahan, C. C., G. D. Adams, B. E. Ferriss, S. K. Shotwell, D. R. McKelvey, and D. W. McGowan. 2023. 1. Assessment of the Walleye Pollock Stock in the Gulf of Alaska. North Pacific Stock Assessment and Fishery Evaluation Report. North Pacific Fishery Management Council, 1007 West 3rd Ave., Suite 400, L92 Building, 4th floor, Anchorage, AK 99501.

Monnahan, C. C., B. E. Ferriss, S. K. Shotwell, Z. Oyafuso, M. Levine, J. T. Thorson, L. Rogers, J. Sullivan, and J. Champagnat. 2024. 1. Assessment of the Walleye Pollock Stock in the Gulf of Alaska. North Pacific Stock Assessment and Fishery Evaluation Report. North Pacific Fishery Management Council, 1007 West 3rd Ave., Suite 400, L92 Building, 4th floor, Anchorage, AK 99501.

Ona, E. 2003. An expanded target-strength relationship for herring. ICES J. Mar. Sci. 60:493–499.

Ona, E., and R. B. Mitson. 1996. Acoustic sampling and signal processing near the seabed: The deadzone revisited. ICES J. Mar. Sci. 53:677–690.

Petitgas, P. 1993. Geostatistics for fish stock assessments: A review and an acoustic application. ICES J. Mar. Sci. 50:285–298.

R Core Team. 2021. R: A language and environment for statistical computing. R Foundation for Statistical Computing, Vienna, Austria.

Ricker, W. E. 1973. Linear regressions in fishery research. J. Fish. Res. Board Can. 30: 409-434.

Rivoirard, J., J. Simmonds, K. G. Foote, P. Fernandes, and N. Bez. 2000. Geostatistics for estimating fish abundance. Page 206. Blackwell Science Ltd, Oxford, UK.

Simmonds, E. J., and D. N. MacLennan. 2005. Fisheries acoustics: Theory and practice. 2nd edition. Page 473. Blackwell Science Ltd, Oxford, UK.

Simrad. 2018. Reference manual for Simrad EK80 scientific echo sounder application. Strandpromenenaden 50, Box 111, N-3191 Horten, Norway.

Stienessen, S. C., N. Lauffenburger, and A. De Robertis. 2019. Results of the acoustic-trawl surveys of walleye pollock (*Gadus chalcogrammus*) in the Gulf of Alaska, February-March 2018 (DY2018-01 and DY2018-03). AFSC Processed Rep. 2019-05, 109 p. Alaska Fish. Sci. Cent., NOAA, Natl. Mar. Fish. Serv., 7600 Sand Point Way NE, Seattle WA 98115.

Towler, R., and K. Williams. 2010. An inexpensive millimeter-accuracy electronic length measuring board. Fish. Res. 106:107–111.

Traynor, J. J. 1996. Target-strength measurements of walleye pollock (*Theragra chalcogramma*) and Pacific whiting (*Merluccius productus*). ICES J. Mar. Sci. 53:253–258.

Walline, P. D. 2007. Geostatistical simulations of eastern Bering Sea walleye pollock spatial distributions, to estimate sampling precision. ICES J. Mar. Sci. 64:559–569.

Williams, K. 2007. Evaluation of the macroscopic staging method for determining maturity of female walleye pollock *Theragra chalcogramma* in Shelikof Strait, Alaska. Alsk. Fish. Res. Bull. 12:252–263.

Williams, K., A. E. Punt, C. D. Wilson, and J. K. Horne. 2011. Length-selective retention of walleye pollock, *Theragra chalcogramma*, by midwater trawls. ICES J. Mar. Sci. 68:119–129.

Williams, K., C. N. Rooper, and R. Towler. 2010. Use of stereo camera systems for assessment of rockfish abundance in untrawlable areas and for recording pollock behavior during midwater trawls. Fish. Bull., U.S. 108:352–362.

Williams, K., R. Towler, P. Goddard, R. Wilborn, and C. Rooper. 2016. Sebastes Stereo Image Analysis Software. AFSC Processed Rep. 2016-03, 42 p. Alaska Fish. Sci. Cent., NOAA, Natl. Mar. Fish. Serv., 7600 Sand Point Way NE, Seattle WA 98115.

Williamson, N. J., and J. J. Traynor. 1996. Application of a one-dimensional geostatistical procedure to fisheries acoustic surveys of Alaskan pollock. ICES J. Mar. Sci. 53:423–428.

Woillez, M., J.-C. Poulard, J. Rivoirard, P. Petitgas, and N. Bez. 2007. Indices for capturing spatial patterns and their evolution in time, with application to European hake (*Merluccius merluccius*) in the Bay of Biscay. ICES J. Mar. Sci. 64:537–550.

Table 1. Simrad EK80 38 kHz acoustic system description and settings used during the 2025 winter acoustic-trawl surveys. These include environmental parameters and results from standard sphere acoustic system calibrations conducted in association with the survey and final values used to calculate biomass and abundance data. The collection settings column contains 5 February EK80 calibration utility results. Other columns are a combination of on-axis and EK80 calibration utility results (see Methods and Results and Discussion sections of text for details).

	Survey collection settings	16 March Kalsin Bay Kodiak	30 March Kalsin Bay Kodiak	Final analysis settings
Echosounder	Simrad EK80	Simrad EK80	Simrad EK80	Simrad EK80
Transducer	ES38-7 s/n 324	ES38-7 s/n 324	ES38-7 s/n 324	ES38-7 s/n 324
Frequency (kHz)	38.00	38.00	38.00	38.00
Transducer depth (m)	9.15	9.15	9.15	9.15
Pulse length (ms)	1.024	1.024	1.024	1.024
Transmitted power (W)	400	400	400	400
Angle sensitivity along	18.00	18.00	18.00	18.00
Angle sensitivity athwart	18.00	18.00	18.00	18.00
2-way beam angle (dB re 1 steradian)	-20.70	-20.70	-20.70	-20.52
Gain (dB)	27.08	27.02	26.99	27.00
S_a correction (dB)	-0.09	-0.10	-0.07	-0.08
Integration gain (dB)	26.99	26.92	26.92	26.92
3 dB beamwidth along	6.33	6.33	6.30	6.32
3 dB beamwidth athwart	6.50	6.50	6.42	6.46
Angle offset along	-0.04	-0.04	-0.02	-0.03
Angle offset athwart	0.05	0.05	0.05	0.05
Post-processing S_v threshold (dB re 1 m^{-1})	-70.00	--	--	-70.00
Standard sphere TS (dB re 1 m^2)	--	-42.08	-42.38	--
Sphere range from transducer (m)	--	20.48	30.75	--
Absorption coefficient (dB m^{-1})	0.00986	0.00978	0.00977	0.00986
Sound velocity (m s^{-1})	1466.0	1466.5	1467.0	1466.0
Water temp at transducer (°C)	--	4.75	4.83	--

Note: Gain and beam pattern terms are defined in the Operator Manual for Simrad EK80 Scientific echosounder application, which is available from Simrad Strandpromenaden 50, Box 111, N-3191 Horten, Norway.
-- symbol indicates the value is not applicable for the noted survey collection or calibration setting.

Table 2. Trawl stations and catch data summary from the 2025 acoustic-trawl survey of pollock in the Shelikof Strait, Chirikof Shelfbreak, and Marmot Bay regions.

Haul	Area	Gear	Date	Time	Duration	Start Position		Depth (m)		Temp (°C)		pollock		Other
No.		Type[a]	(GMT)	(GMT)	(mins)	Lat. (N)	Long. (W)	Headrope[b]	Bottom	Headrope	Surface[c]	(kg)	Number	(kg)
1	Shelikof Strait	LFS1421	17-Mar	17:27	6.3	58.4215	-153.0186	136	205	5.8	5.1	216.4	15,561	19.6
2	Shelikof Strait	LFS1421	18-Mar	02:43	4.5	58.2309	-153.3371	128	217	5.8	5.2	296.2	21,009	15.0
3	Shelikof Strait	LFS1421	18-Mar	08:43	8.1	58.3085	-153.9518	151	212	5.6	3.5	1,257.7	1,074	13.8
4	Shelikof Strait	LFS1421	18-Mar	16:08	25.4	57.9299	-153.7791	116	171	5.7	5.2	373.6	865	29.9
5	Shelikof Strait	LFS1421	18-Mar	21:15	5.2	58.0942	-154.2115	196	233	5.8	4.1	1,304.2	1,059	4.8
6	Shelikof Strait	LFS1421	19-Mar	05:36	11.3	57.9282	-154.6244	207	258	5.6	4.6	1,945.8	1,819	14.1
7	Shelikof Strait	LFS1421	19-Mar	09:29	9.4	57.8860	-154.8581	208	248	5.6	4.6	410.4	371	18.0
8	Shelikof Strait	LFS1421	19-Mar	16:37	36.0	57.6708	-154.7002	189	217	5.9	4.6	148.7	794	486.7
9	Shelikof Strait	LFS1421	19-Mar	22:22	8.1	57.7089	-155.2262	245	291	5.7	4.7	464.9	486	144.0
10	Shelikof Strait	LFS1421	20-Mar	06:41	6.6	57.6217	-155.3749	226	272	5.8	4.8	2,222.8	2,344	45.6
11	Shelikof Strait	LFS1421	20-Mar	12:14	3.0	57.4805	-155.4859	222	300	5.7	5.1	2,133.2	2,167	43.8
12	Shelikof Strait	LFS1421	20-Mar	23:34	8.6	57.3427	-155.4770	213	271	5.7	5.0	577.6	621	153.3
13	Shelikof Strait	LFS1421	21-Mar	06:30	4.2	57.2006	-155.4300	221	256	5.6	5.0	1,906.7	2,266	88.1
14	Shelikof Strait	LFS1421	21-Mar	19:03	16.9	56.9787	-155.6689	251	284	5.6	4.7	498.4	542	267.3
15	Shelikof Strait	LFS1421	22-Mar	02:43	7.8	56.8621	-155.7303	255	287	5.8	4.7	504.9	480	47.5
16	Shelikof Strait	LFS1421	22-Mar	06:13	4.8	56.9206	-156.0138	105	213	5.2	4.7	65.8	5,176	8.2
17	Shelikof Strait	LFS1421	22-Mar	16:42	22.6	56.6769	-156.0835	245	285	5.9	4.6	430.4	386	46.0
18	Shelikof Strait	LFS1421	23-Mar	03:00	10.0	56.4852	-155.8515	189	216	5.9	5.1	152.1	377	55.2
19	Shelikof Strait	LFS1421	23-Mar	05:17	23.2	56.4724	-155.7906	74	182	5.0	5.1	7.3	643	214.7
20	Shelikof Strait	LFS1421	23-Mar	17:14	29.1	56.2730	-156.1093	209	243	5.6	5.0	481.0	446	100.5
22	Shelikof Strait	LFS1421	25-Mar	06:20	4.0	55.5079	-156.2888	187	212	5.6	4.8	7.4	7	1,125.8
23	Shelikof Strait	LFS1421	25-Mar	12:26	22.7	55.7043	-155.9740	41	192	5.0	4.8	-	-	12.3
24	Chirikof Shelfbreak	LFS1421	26-Mar	03:07	19.8	55.9038	-154.8963	250	279	5.2	5.2	31.0	52	659.9
25	Chirikof Shelfbreak	LFS1421	26-Mar	13:49	10.9	55.9114	-154.3407	304	654	4.9	5.2	451.6	523	50.9
26	Chirikof Shelfbreak	LFS1421	26-Mar	23:15	3.0	55.8930	-153.9829	326	601	5.0	6.0	147.6	191	228.7
27	Chirikof Shelfbreak	LFS1421	27-Mar	06:45	0.3	56.1237	-153.7835	227	266	5.4	5.8	12.4	17	611.2
28	Chirikof Shelfbreak	LFS1421	27-Mar	17:07	15.8	56.2323	-152.8099	309	250	4.7	5.8	1,204.4	1,581	51.4
29	Chirikof Shelfbreak	LFS1421	27-Mar	22:40	12.8	56.3515	-152.4886	342	500	4.7	6.2	473.9	573	305.2
30	Marmot Bay	LFS1421	28-Mar	16:16	21.9	57.9274	-152.6934	73	122	5.3	5.2	522.4	14,017	35.6
31	Marmot Bay	LFS1421	28-Mar	22:44	21.9	58.0147	-152.5223	150	203	5.5	5.5	199.4	8,784	13.8
32	Marmot Bay	LFS1421	29-Mar	07:04	15.5	57.9899	-152.3250	46	216	5.6	5.6	141.8	8,436	32.7
33	Marmot Bay	LFS1421	29-Mar	12:21	14.9	57.9651	-152.2561	196	252	5.5	5.6	760.0	1,338	37.6
34	Marmot Bay	LFS1421	29-Mar	17:20	11.0	58.0264	-152.0900	115	156	5.5	5.7	211.8	8,253	1.5
35	Marmot Bay	LFS1421	30-Mar	03:19	10.7	58.0565	-151.7770	120	167	5.7	5.7	74.6	4,847	42.0

[a]LFS1421 = LFS1421 midwater trawl.

[b]Headrope depth obtained from temperature-depth probe. In hauls without temperature-depth probe records, depth was obtained from scientist notes when possible.

[c]Average temperature measured from a temperature-depth probe (SBE 39, Sea-Bird Scientific).

Table 3. Numbers of pollock measured and biological samples collected during the winter 2025 acoustic-trawl survey of Shelikof Strait, Chirikof Shelfbreak, and Marmot Bay.

Haul no.	Region name	Catch lengths	Weights	Maturities	Otoliths	Ovary weights	Ovaries collected	Stomachs collected
1	Shelikof Strait	299	36	1	6	-	1	9
2	Shelikof Strait	80	19	-	5	-	-	7
3	Shelikof Strait	301	49	49	34	31	11	17
4	Shelikof Strait	389	75	60	35	7	15	24
5	Shelikof Strait	362	51	51	26	51	15	18
6	Shelikof Strait	340	87	56	40	48	5	-
7	Shelikof Strait	371	70	50	30	45	6	19
8	Shelikof Strait	176	75	54	30	28	7	20
9	Shelikof Strait	486	55	55	35	25	5	18
10	Shelikof Strait	395	72	51	40	44	6	9
11	Shelikof Strait	377	53	50	38	39	3	12
12	Shelikof Strait	350	51	51	35	20	4	9
13	Shelikof Strait	307	54	50	39	2	2	12
14	Shelikof Strait	347	51	50	36	27	7	13
15	Shelikof Strait	310	51	50	36	29	5	10
16	Shelikof Strait	90	20	-	5	-	-	-
17	Shelikof Strait	330	59	50	40	34	5	18
18	Shelikof Strait	304	65	50	40	4	6	13
19	Shelikof Strait	38	20	-	5	-	-	-
20	Shelikof Strait	347	50	50	35	24	5	11
22	Shelikof Strait	7	7	7	7	1	-	-
24	Chirikof Shelfbreak	52	52	52	34	7	1	14
25	Chirikof Shelfbreak	328	50	50	35	20	4	15
26	Chirikof Shelfbreak	191	50	50	35	17	1	8
27	Chirikof Shelfbreak	17	17	17	17	4	2	9
28	Chirikof Shelfbreak	406	50	50	35	7	14	12
29	Chirikof Shelfbreak	345	56	56	41	20	-	-
30	Marmot Bay	494	48	43	33	-	11	20
31	Marmot Bay	309	64	44	34	1	-	10
32	Marmot Bay	128	85	64	35	2	-	13
33	Marmot Bay	476	70	50	40	17	-	-
34	Marmot Bay	380	70	50	40	3	-	8
35	Marmot Bay	77	30	10	-	4	-	-
Total		9,209	1,712	1,371	976	561	141	348

Table 4. Catch by species and numbers of length and weight measurements taken from 22 LFS1421 hauls during the 2025 acoustic-trawl survey of pollock in Shelikof Strait.

		Catch				Measurements	
Species name	Scientific name	Weight (kg)	%	Number	%	Length	Weight
pollock	*Gadus chalcogrammus*	15,405.5	83.9	58,493	18.8	6,006	1,070
Pacific ocean perch	*Sebastes alutus*	1,125.2	6.1	1,639	0.5	76	25
eulachon	*Thaleichthys pacificus*	686.4	3.7	22,914	7.4	454	149
northern smoothtongue	*Leuroglossus schmidti*	367.2	2.0	42,131	13.5	345	131
magistrate armhook squid	*Berryteuthis magister*	193.5	1.1	2,271	0.7	202	113
squids	Cephalopoda (class)	189.5	1.0	5,123	1.6	125	70
Pacific capelin	*Mallotus catervarius*	165.5	0.9	19,989	6.4	337	224
salmon shark	*Lamna ditropis*	62.6	0.3	1	<0.1	1	1
Chinook salmon	*Oncorhynchus tshawytscha*	59.3	0.3	41	<0.1	38	38
smooth lumpsucker	*Aptocyclus ventricosus*	46.6	0.3	38	<0.1	34	33
Pacific glass shrimp	*Pasiphaea pacifica*	14.7	<0.1	11,222	3.6	121	8
Pacific herring	*Clupea pallasii*	11.7	<0.1	1,735	0.6	94	56
chrysaora jellyfish	*Chrysaora sp.*	9.5	<0.1	42	<0.1	40	40
euphausiids	Euphausiacea (order)	7.9	<0.1	145,021	46.6	-	-
arrowtooth flounder	*Atheresthes stomias*	6.5	<0.1	6	<0.1	6	6
Pacific cod	*Gadus macrocephalus*	5.7	<0.1	3	<0.1	3	3
Pacific lamprey	*Lampetra tridentata*	0.8	<0.1	21	<0.1	18	18
aurelia jellyfish	*Aurelia sp.*	0.3	<0.1	2	<0.1	1	1
lanternfishes	Myctophidae (family)	0.3	<0.1	231	<0.1	16	11
egg yolk jelly	*Phacellophora camtschatica*	0.2	<0.1	1	<0.1	1	1
flathead sole	*Hippoglossoides elassodon*	0.2	<0.1	1	<0.1	1	1
pricklebacks	Stichaeidae (family)	0.1	<0.1	91	<0.1	11	11
jellyfishes	Scyphozoa (class)	<0.1	<0.1	1	<0.1	1	1
yellow Irish lord	*Hemilepidotus jordani*	<0.1	<0.1	1	<0.1	1	1
pandalus sp.	*Pandalus sp.*	<0.1	<0.1	25	<0.1	3	3
eelpouts	Zoarcidae (family)	<0.1	<0.1	5	<0.1	1	1
Alaskan pink shrimp	*Pandalus eous*	<0.1	<0.1	8	<0.1	8	8
sidestripe shrimp	*Pandalopsis dispar*	<0.1	<0.1	1	<0.1	1	1
crangonid shrimps	Crangonidae (family)	<0.1	<0.1	3	<0.1	3	-
Total		18,359.6		311,060		7,948	2,025

Table 5. Estimates of pollock biomass (thousands of metric tons) and relative estimation error for Shelikof Strait. Estimates for 2008-2025 reflect selectivity corrections for escapement of juveniles.

Year	Shelikof Strait		
	Area (nmi^2)	Biomass (thousand t)[1]	Est. error (%)
1981	2,529	2,784.0	-
1982	-	-	-
1983	5,128	2,277.0	-
1984	4,830	1,757.0	-
1985	4,778	1,175.0	-
1986	4,702	584.0	-
1987	-	-	-
1988	6,510	302.0	-
1989	6,350	290.0	-
1990	5,252	374.0	-
1991	5,018	379.0	-
1992	-	713.0	3.6
1993	5,357	436.0	4.6
1994	-	493.0	4.5
1995	5,672	763.5	4.5
1996	6,002	777.1	3.7
1997	5,579	566.9	3.7
1998	5,501	504.6	3.8
1999	-	-	-
2000	5,580	461.0	4.6
2001	5,772	432.7	4.5
2002	5,728	257.8	6.9
2003	5,775	312.7	5.2
2004	4,859	330.8	9.2
2005	5,393	356.7	4.1
2006	7,175	294.1	4.0
2007	5,330	181.1	5.8
2008	4,994	166.3	5.6
2009	5,140	248.9	5.9
2010	5,363	413.4	2.6
2011	-	-	-
2012	5,626	327.1	7.9
2013	5,001	714.9	5.3
2014	5,793	809.1	4.7
2015	5,434	844.3	4.3
2016	6,169	665.3	6.5
2017	6,255	1,422.2	4.3
2018	6,688	1,262.0	3.9
2019	6,861	1,244.2	6.6
2020	6,463	457.1	2.9
2021	7,119	523.0	2.9
2022	6,262	369.6	10.3
2023	6,832	261.2	4.6
2024	6,872	288.2	7.0
2025	6,741	323.4	7.6

[1]Values from 2008-2024 have been standardized to use the most up-to-date analytical methods (See McGowan et al. in prep).

Table 6. Numbers-at-length estimates (millions of fish) from acoustic-trawl surveys of pollock in the Shelikof Strait from 2015-2025. Note that years prior to 2015 are excluded due to space constraints.

Length (cm)	2015	2016	2017	2018	2019	2020	2021	2022	2023	2024	2025
5	0	0	0	0	0	0	0	0	0	0	0
6	0	0	0	0	0	0	0	0	0	0	0
7	0	0	0	0	0	0	0	0	0	0	0
8	<1	0	0	0	40.0	0	11.0	2.9	0	0	0
9	0	0	1.8	137.5	194.3	0	249.3	<1	0	0	<1
10	10.6	0	72.6	1,049.6	2,701.5	<1	1,392.2	<1	0	0	5.4
11	7.9	0	187.8	1,492.5	4,100.4	<1	2,756.4	<1	<1	0	72.3
12	7.1	0	444.1	683.9	2,241.8	1.8	2,144.8	2.5	<1	<1	169.7
13	6.7	0	264.3	67.7	361.6	3.2	935.0	2.0	0	<1	166.3
14	3.7	0	54.4	11.0	68.5	4.0	216.1	1.1	0	<1	114.4
15	<1	0	21.9	2.4	0	1.6	60.0	<1	0	<1	31.4
16	<1	0	<1	1.2	<1	<1	7.0	<1	0	<1	3.3
17	<1	0	0	0	4.3	<1	0	4.3	0	0	0
18	<1	0	0	<1	29.6	<1	0	11.8	0	0	<1
19	<1	0	0	3.5	133.5	<1	0	41.7	0	0	0
20	1.6	0	<1	5.4	338.5	8.9	<1	57.0	0	<1	0
21	8.5	0	0	15.4	341.1	19.3	<1	41.8	0	<1	0
22	16.1	<1	0	24.3	231.9	23.7	<1	22.4	0	<1	0
23	14.7	0	<1	25.9	135.7	17.1	<1	7.9	0	<1	0
24	18.2	<1	<1	21.6	61.7	11.7	1.6	3.1	0	<1	<1
25	15.4	<1	<1	17.5	31.5	19.0	3.5	2.2	<1	1.4	<1
26	33.5	<1	0	7.3	11.7	23.4	2.7	<1	<1	1.4	<1
27	85.2	<1	0	7.5	3.4	44.5	1.8	<1	<1	1.2	<1
28	170.1	<1	<1	4.0	5.6	53.6	3.0	<1	<1	1.0	<1
29	271.2	<1	0	0	14.7	77.6	4.4	<1	<1	<1	<1
30	293.4	1.9	0	1.2	16.3	53.6	7.2	<1	<1	<1	<1
31	241.1	3.0	0	<1	19.9	43.7	10.5	<1	<1	<1	<1
32	190.7	10.1	0	<1	25.9	23.2	15.5	<1	<1	<1	<1
33	127.2	22.3	<1	<1	15.1	16.8	17.3	1.1	<1	<1	<1
34	67.5	45.8	<1	0	11.2	16.9	21.0	2.0	<1	<1	<1
35	49.2	81.5	<1	0	5.7	9.6	21.1	2.6	1.3	<1	1.8
36	26.1	124.6	4.4	0	1.8	14.3	28.0	6.5	1.1	<1	3.0
37	18.9	195.3	8.6	1.2	3.9	10.3	31.2	12.8	1.5	1.4	3.1
38	13.1	270.4	54.6	1.7	1.9	5.6	28.1	22.4	1.9	2.9	3.5
39	10.7	273.1	126.5	9.9	1.4	4.4	23.5	24.4	3.6	5.4	4.2
40	7.7	209.6	341.2	43.5	1.4	3.3	19.9	33.1	4.9	13.4	2.5
41	4.9	146.4	514.2	98.0	4.8	2.3	14.9	31.0	11.1	19.8	1.7
42	5.6	83.1	562.0	191.6	33.2	7.9	15.1	28.8	14.1	29.7	5.7
43	9.0	48.3	530.0	290.3	100.3	15.2	12.0	22.6	18.1	33.6	7.1
44	12.6	21.8	319.0	350.3	173.2	34.4	9.4	21.4	20.7	34.5	12.5

Length (cm)	2015	2016	2017	2018	2019	2020	2021	2022	2023	2024	2025
45	19.4	13.5	165.1	334.7	239.3	67.2	16.7	19.6	23.3	35.9	24.1
46	29.9	11.6	78.2	252.1	238.1	78.5	31.8	18.4	21.1	34.0	27.2
47	32.0	6.5	45.5	181.9	215.7	74.8	29.4	25.7	19.2	28.3	30.5
48	37.8	6.7	23.3	111.9	165.2	62.2	42.9	27.6	19.9	22.1	34.8
49	32.8	9.6	8.7	59.9	119.4	41.0	45.4	29.2	16.2	21.7	32.3
50	25.7	6.6	6.7	29.6	66.1	33.2	37.8	26.3	15.8	15.3	28.8
51	24.8	5.0	3.4	28.2	33.8	20.5	28.8	21.3	13.9	12.0	26.2
52	20.6	5.3	2.4	9.5	24.5	13.2	27.9	18.4	12.5	10.5	19.4
53	23.4	1.9	<1	9.3	10.2	5.7	23.9	15.7	11.0	7.9	15.7
54	22.4	3.3	2.8	3.7	5.2	4.9	16.8	15.7	10.7	7.4	12.0
55	27.5	2.4	4.4	6.5	4.6	3.0	13.9	13.1	9.7	6.1	10.7
56	24.7	2.1	4.3	1.8	<1	1.4	8.5	8.9	8.8	3.7	8.9
57	22.4	2.3	<1	<1	<1	<1	5.7	5.9	7.6	5.0	6.9
58	19.5	1.4	1.9	0	<1	<1	4.3	2.1	5.7	3.0	4.4
59	14.8	<1	<1	0	<1	<1	3.1	2.6	3.3	1.8	3.6
60	13.7	2.1	<1	<1	<1	<1	<1	<1	2.3	1.4	2.5
61	8.1	<1	<1	0	<1	<1	<1	<1	1.8	<1	1.6
62	6.6	<1	<1	<1	0	<1	<1	<1	1.4	<1	1.4
63	3.7	<1	<1	0	0	<1	0	<1	<1	<1	<1
64	1.5	0	0	0	0	0	<1	<1	<1	<1	<1
65	2.1	0	0	0	0	0	<1	0	<1	<1	<1
66	<1	0	0	0	0	0	0	0	0	<1	<1
67	<1	0	0	0	0	0	0	0	<1	0	0
68	<1	0	0	0	0	0	0	0	0	<1	0
69	<1	0	0	0	0	0	0	0	0	0	<1
70	0	0	0	0	0	0	0	0	0	0	0
71	0	0	0	0	0	0	0	0	0	0	0
72	0	0	0	0	0	0	0	0	0	0	0
73	0	0	0	0	0	0	0	0	0	0	0
74	0	0	0	0	0	0	0	0	0	0	0
75	0	0	0	0	0	0	0	0	0	0	0
76	0	0	0	0	0	0	0	0	0	0	0
Total	2,164.7	1,620.7	3,859.5	5,596.9	12,592.5	982.1	8,405.3	667.9	287.4	367.7	903.2

Table 7. Biomass-at-length estimates (thousands of metric tons) from acoustic-trawl surveys of pollock in the Shelikof Strait from 2015-2025. Note that years prior to 2015 are excluded due to space constraints.

Length (cm)	2015	2016	2017	2018	2019	2020	2021	2022	2023	2024	2025
5	0	0	0	0	0	0	0	0	0	0	0
6	0	0	0	0	0	0	0	0	0	0	0
7	0	0	0	0	0	0	0	0	0	0	0
8	<1	0	0	0	<1	0	<1	<1	0	0	0
9	0	0	<1	<1	<1	0	1.1	<1	0	0	<1
10	<1	0	<1	6.5	17.8	<1	8.7	<1	0	0	<1
11	<1	0	1.4	11.9	33.3	<1	22.6	<1	<1	0	<1
12	<1	0	4.4	7.2	22.0	<1	21.6	<1	<1	<1	2.0
13	<1	0	3.3	<1	4.1	<1	11.4	<1	0	<1	2.3
14	<1	0	<1	<1	1.2	<1	3.2	<1	0	<1	1.9
15	<1	0	<1	<1	0	<1	1.2	<1	0	<1	<1
16	<1	0	<1	<1	<1	<1	<1	<1	0	<1	<1
17	<1	0	0	0	<1	<1	0	<1	0	0	0
18	<1	0	0	<1	1.1	<1	0	<1	0	0	<1
19	<1	0	0	<1	5.8	<1	0	1.8	0	0	0
20	<1	0	<1	<1	17.0	<1	<1	2.7	0	<1	0
21	<1	0	0	<1	19.6	1.1	<1	2.3	0	<1	0
22	1.1	<1	0	1.7	15.3	1.6	<1	1.4	0	<1	0
23	1.1	0	<1	2.2	10.6	1.3	<1	<1	0	<1	0
24	1.5	<1	<1	2.0	5.3	1.1	<1	<1	0	<1	<1
25	1.7	<1	<1	1.9	3.0	1.9	<1	<1	<1	<1	<1
26	3.9	<1	0	<1	1.3	2.7	<1	<1	<1	<1	<1
27	10.9	<1	0	<1	<1	5.9	<1	<1	<1	<1	<1
28	25.6	<1	<1	<1	<1	7.9	<1	<1	<1	<1	<1
29	43.8	<1	0	0	2.3	12.8	<1	<1	<1	<1	<1
30	53.9	<1	0	<1	3.1	9.8	1.4	<1	<1	<1	<1
31	48.5	<1	0	<1	3.8	8.8	2.2	<1	<1	<1	<1
32	42.5	2.2	0	<1	5.8	5.2	3.6	<1	<1	<1	<1
33	31.3	5.4	<1	<1	3.7	4.1	4.4	<1	<1	<1	<1
34	18.5	12.1	<1	0	3.2	4.6	5.9	<1	<1	<1	<1
35	14.9	23.7	<1	0	1.9	2.9	6.5	<1	<1	<1	<1
36	9.1	40.0	1.3	0	<1	4.8	9.6	2.2	<1	<1	1.1
37	6.9	67.4	2.8	<1	1.5	3.8	11.5	4.7	<1	<1	1.2
38	5.3	101.1	20.5	<1	<1	2.2	11.2	8.9	<1	1.2	1.5
39	4.7	109.5	49.4	3.9	<1	1.9	10.8	10.4	1.5	2.4	2.1
40	3.9	89.7	143.0	19.8	<1	1.6	9.8	15.1	2.2	6.7	1.2
41	2.5	67.5	240.2	46.5	2.4	1.1	7.8	15.4	5.7	10.7	<1
42	3.2	41.0	274.4	94.1	17.9	4.2	8.9	15.4	7.5	16.7	3.2
43	5.6	25.1	271.6	156.2	56.1	9.0	7.4	13.2	10.7	20.3	4.1
44	8.3	12.4	175.6	202.8	103.7	21.8	6.4	13.3	13.5	22.9	8.0

Length (cm)	2015	2016	2017	2018	2019	2020	2021	2022	2023	2024	2025
45	14.2	8.3	94.5	202.7	155.4	44.3	12.5	13.2	16.5	25.4	16.1
46	23.4	7.2	50.5	162.1	164.7	53.9	24.3	13.9	16.3	25.5	20.2
47	26.9	4.1	30.2	123.1	160.7	57.3	24.9	19.9	15.4	22.7	24.0
48	32.8	5.0	18.7	80.2	138.5	52.0	37.4	22.7	17.4	18.9	27.7
49	31.1	8.1	7.6	45.5	105.5	36.2	40.9	26.1	15.4	20.0	29.0
50	26.0	5.3	7.0	22.8	64.3	31.2	37.7	24.9	15.3	15.6	27.7
51	27.1	4.4	3.0	28.8	34.3	22.2	29.4	23.0	14.2	12.4	26.8
52	23.0	4.7	2.0	9.0	25.5	14.8	31.8	20.4	13.7	12.1	22.7
53	28.9	2.1	<1	9.4	11.2	6.2	27.7	19.6	13.2	9.6	18.6
54	28.7	3.5	3.0	3.9	5.9	6.0	21.9	20.4	13.4	9.3	15.7
55	36.6	2.5	5.1	7.3	6.5	4.1	18.6	19.1	13.5	8.6	14.6
56	36.0	2.1	5.3	2.1	<1	1.9	10.3	14.3	13.0	5.2	13.0
57	34.3	2.5	<1	<1	1.2	1.1	8.4	9.1	12.3	7.2	9.6
58	31.4	1.9	2.6	0	<1	<1	7.3	3.3	8.6	4.6	6.5
59	24.5	1.2	1.1	0	<1	<1	5.5	4.3	5.6	2.8	6.3
60	24.1	2.6	<1	<1	<1	<1	1.5	1.3	4.3	2.4	4.1
61	15.2	<1	<1	0	<1	1.4	1.5	1.8	3.6	1.5	3.0
62	12.4	<1	<1	<1	0	<1	1.3	1.0	2.9	<1	3.0
63	7.7	<1	<1	0	0	<1	0	<1	1.0	<1	1.7
64	3.5	0	0	0	0	0	<1	<1	1.1	<1	<1
65	4.6	0	0	0	0	0	<1	0	<1	<1	<1
66	1.7	0	0	0	0	0	0	0	0	<1	<1
67	<1	0	0	0	0	0	0	0	<1	0	0
68	<1	0	0	0	0	0	0	0	0	<1	0
69	<1	0	0	0	0	0	0	0	0	0	<1
70	0	0	0	0	0	0	0	0	0	0	0
71	0	0	0	0	0	0	0	0	0	0	0
72	0	0	0	0	0	0	0	0	0	0	0
73	0	0	0	0	0	0	0	0	0	0	0
74	0	0	0	0	0	0	0	0	0	0	0
75	0	0	0	0	0	0	0	0	0	0	0
76	0	0	0	0	0	0	0	0	0	0	0
Total	844.3	665.3	1,422.2	1,262.0	1,244.2	457.1	523.0	369.6	261.2	288.2	323.4

Table 8. Biomass-at-age estimates (thousands of metric tons) from acoustic-trawl surveys of pollock in the Shelikof Strait. Numbers from 2008-2025 reflect selectivity corrections for escapement of juveniles.

Year	1	2	3	4	5	6	7	8	9	10	11	12+	Total
1981	1.0	309.0	342.0	255.0	1,068.0	496.0	133.0	92.0	68.0	19.0	1.0	<1	2,784.0
1983	<1	71.0	117.0	529.0	650.0	455.0	332.0	94.0	11.0	12.0	5.0	1.0	2,277.0
1984	1.0	6.0	83.0	78.0	373.0	684.0	331.0	161.0	36.0	3.0	<1	1.0	1,757.0
1985	24.0	54.0	41.0	159.0	109.0	253.0	353.0	138.0	35.0	6.0	2.0	1.0	1,175.0
1986	4.0	139.0	40.0	17.0	56.0	41.0	76.0	140.0	58.0	11.0	2.0	<1	584.0
1988	<1	8.0	130.0	91.0	31.0	9.0	6.0	6.0	5.0	11.0	2.0	3.0	302.0
1989	4.0	8.0	21.0	86.0	111.0	27.0	12.0	4.0	3.0	1.0	12.0	1.0	290.0
1990	<1	67.0	15.0	23.0	61.0	120.0	36.0	24.0	9.0	11.0	1.0	7.0	374.0
1991	<1	12.0	85.0	13.0	33.0	54.0	106.0	23.0	36.0	3.0	6.0	8.0	379.0
1992	3.0	3.0	16.0	60.0	144.0	68.0	92.0	194.0	36.0	71.0	3.0	23.0	713.0
1993	1.0	6.0	11.0	34.0	136.0	90.0	28.0	43.0	46.0	21.0	10.0	10.0	436.0
1994	2.0	3.0	14.0	20.0	127.0	75.0	48.0	34.0	64.0	68.0	21.0	17.0	493.0
1995	114.2	46.2	23.4	40.8	83.1	220.3	115.5	55.4	19.1	15.3	19.6	10.6	763.5
1996	<1	180.4	24.5	11.8	49.8	73.2	211.6	132.1	48.4	17.5	15.7	11.5	777.1
1997	<1	16.2	190.7	27.7	13.4	51.0	59.9	115.9	64.0	18.2	3.0	6.1	566.9
1998	4.4	7.9	28.2	152.5	52.5	12.3	38.8	47.0	95.0	33.3	20.8	11.9	504.6
2000	55.8	64.8	63.5	9.3	56.2	110.1	17.6	17.3	15.3	11.8	22.6	16.7	461.0
2001	2.5	214.3	60.3	25.4	26.6	24.4	40.4	18.0	8.3	4.6	2.0	5.9	432.7
2002	<1	13.4	164.7	29.1	11.7	15.9	9.2	8.5	2.3	1.0	<1	1.2	257.8
2003	<1	8.4	41.4	218.3	24.9	7.3	5.1	2.1	1.6	<1	<1	<1	311.4
2004	<1	7.9	14.2	77.0	179.1	35.4	3.6	3.3	4.1	<1	<1	<1	326.9
2005	17.9	13.1	17.0	19.0	132.9	119.5	28.8	4.2	2.9	0	1.4	0	356.7
2006	1.5	54.4	10.7	5.0	14.5	63.2	87.6	42.9	10.3	1.1	1.6	1.3	294.1
2007	<1	14.5	39.0	13.3	8.5	21.6	47.5	30.1	2.8	1.9	1.4	0	181.1
2008	34.1	23.8	50.2	25.3	7.6	<1	2.9	12.6	7.0	1.3	<1	0	166.3
2009	11.7	80.7	28.1	43.6	45.5	9.8	3.5	2.1	9.3	11.0	2.9	<1	248.6
2010	2.3	22.8	127.1	61.0	81.9	41.7	19.8	9.2	10.3	13.0	16.5	6.6	412.3
2012	4.2	65.2	7.2	44.9	107.0	44.5	48.1	3.8	<1	<1	0	<1	327.1
2013	96.9	15.3	209.0	17.5	77.2	133.8	67.0	61.3	20.0	8.3	1.4	7.1	714.9
2014	19.6	199.5	5.4	146.9	50.9	71.4	140.5	86.4	48.9	21.3	14.1	4.1	809.1
2015	<1	7.9	311.8	53.0	122.5	80.5	67.1	124.9	41.9	18.0	7.2	9.2	844.3
2016	0	<1	14.3	567.7	18.2	23.7	23.6	5.8	9.8	2.3	0	0	665.3
2017	10.7	0	8.3	82.2	1,225.9	64.3	20.5	10.0	0	0	0	0	1,422.0
2018	27.3	11.8	<1	2.3	82.4	1,032.3	65.4	39.7	0	0	0	0	1,261.5
2019	79.5	77.0	30.8	<1	<1	110.0	906.1	32.2	7.5	<1	0	0	1,244.2
2020	<1	5.6	63.3	22.5	4.4	24.6	54.7	164.1	74.7	31.3	8.6	3.0	457.1
2021	70.0	1.8	22.7	75.3	27.1	5.2	10.4	67.2	141.7	80.1	19.8	1.8	523.0
2022	<1	9.9	6.0	57.4	79.9	23.3	<1	10.5	28.4	118.7	29.7	5.4	369.6
2023	<1	<1	2.4	26.9	77.7	31.3	8.3	<1	6.0	33.8	60.9	13.3	261.2

Year	1	2	3	4	5	6	7	8	9	10	11	12+	Total
2024	<1	1.0	3.4	86.5	34.7	88.3	18.9	2.8	<1	11.4	19.2	21.7	288.2
2025	7.7	<1	7.1	14.1	78.9	30.8	122.2	23.6	<1	<1	7.1	30.9	323.4

Table 9. Numbers-at-age estimates (millions of fish) from acoustic-trawl surveys of pollock in the Shelikof Strait. Numbers from 2008-2025 reflect selectivity corrections for escapement of juveniles.

Year	1	2	3	4	5	6	7	8	9	10	11	12+	Total
1981	78.0	3,481.0	1,511.0	769.0	2,786.0	1,052.0	210.0	129.0	79.0	25.0	2.0	<1	10,122.0
1983	1.0	902.0	380.0	1,297.0	1,171.0	698.0	599.0	132.0	14.0	12.0	4.0	2.0	5,212.0
1984	62.0	58.0	324.0	142.0	635.0	988.0	450.0	224.0	41.0	3.0	<1	1.0	2,928.0
1985	2,092.0	544.0	123.0	315.0	181.0	347.0	439.0	167.0	43.0	6.0	2.0	1.0	4,260.0
1986	575.0	2,115.0	184.0	46.0	75.0	49.0	86.0	149.0	60.0	11.0	1.0	<1	3,351.0
1988	17.0	110.0	694.0	322.0	78.0	17.0	6.0	6.0	4.0	9.0	2.0	2.0	1,267.0
1989	399.0	90.0	90.0	216.0	249.0	43.0	14.0	4.0	2.0	1.0	10.0	1.0	1,119.0
1990	49.0	1,210.0	72.0	63.0	116.0	180.0	46.0	22.0	8.0	8.0	1.0	6.0	1,781.0
1991	22.0	174.0	550.0	48.0	65.0	70.0	116.0	24.0	29.0	2.0	4.0	5.0	1,109.0
1992	228.0	34.0	74.0	188.0	368.0	84.0	85.0	171.0	33.0	56.0	2.0	16.0	1,339.0
1993	63.0	76.0	37.0	72.0	233.0	126.0	27.0	36.0	39.0	16.0	8.0	7.0	740.0
1994	186.0	36.0	49.0	32.0	155.0	84.0	42.0	27.0	44.0	48.0	15.0	10.0	728.0
1995	10,687.6	510.3	79.4	77.7	103.3	245.2	121.7	53.6	16.6	10.7	14.6	8.4	11,929.1
1996	56.1	3,306.4	118.9	25.1	54.0	71.0	201.0	118.5	39.8	13.0	11.3	8.2	4,023.4
1997	71.6	206.1	1,217.2	79.7	18.6	43.2	51.6	95.4	50.7	13.2	2.2	3.9	1,853.6
1998	395.0	88.5	125.5	474.2	136.1	14.2	31.9	36.3	74.1	25.9	14.3	8.3	1,424.1
2000	4,401.6	770.6	227.8	16.4	69.3	135.8	17.4	13.1	10.2	8.2	14.4	10.3	5,695.0
2001	288.6	4,103.9	351.7	61.0	41.5	23.0	34.6	13.1	6.2	2.7	1.2	3.3	4,930.8
2002	8.2	163.5	1,111.7	97.0	16.3	16.2	7.7	6.8	1.5	<1	<1	<1	1,430.5
2003	49.9	93.1	202.6	791.1	56.0	8.2	4.3	1.6	1.0	<1	<1	<1	1,208.9
2004	52.6	94.0	57.6	158.8	356.8	48.0	2.7	2.5	2.8	<1	<1	<1	777.1
2005	1,613.1	156.1	55.6	34.7	173.3	162.9	36.1	3.6	2.4	0	<1	0	2,238.7
2006	160.8	828.9	40.9	11.6	17.5	56.2	75.3	32.4	6.9	<1	<1	<1	1,232.6
2007	53.2	230.3	175.3	29.7	10.2	17.3	34.4	20.9	1.5	1.0	<1	0	574.4
2008	2,622.6	227.3	176.2	56.5	10.0	<1	1.6	7.1	3.6	<1	<1	0	3,106.7
2009	1,133.8	1,045.5	112.8	78.3	64.7	8.7	2.0	1.1	4.5	5.4	1.4	<1	2,458.2
2010	243.2	289.8	537.5	90.6	74.7	32.6	11.2	4.5	4.4	6.6	7.3	2.9	1,305.2
2012	354.8	831.7	25.2	68.4	114.0	34.6	34.4	2.6	<1	<1	0	<1	1,466.8
2013	11,047.5	116.3	610.7	27.6	65.6	99.2	44.3	34.2	11.7	4.3	<1	3.0	12,065.2
2014	1,915.4	3,442.1	17.3	245.3	70.4	62.7	108.7	57.5	31.7	13.9	9.5	2.0	5,976.3
2015	37.1	86.3	1,567.4	76.0	141.3	75.4	48.2	83.3	28.7	11.1	4.5	5.4	2,164.7
2016	0	1.1	46.7	1,457.6	35.0	31.8	32.0	5.3	9.4	1.8	0	0	1,620.7
2017	1,047.7	0	21.8	173.1	2,458.5	114.4	20.0	9.3	0	0	0	0	3,844.8
2018	3,442.2	133.1	<1	4.0	151.5	1,713.2	102.5	44.2	0	0	0	0	5,591.7
2019	9,708.7	1,295.0	150.9	1.8	<1	161.6	1,222.2	42.0	10.0	<1	0	0	12,592.5
2020	12.7	79.4	366.8	62.4	7.2	32.5	70.4	203.6	95.3	39.2	10.7	1.9	982.1
2021	7,771.8	15.0	83.1	165.2	49.6	5.8	11.7	63.0	142.4	77.3	18.5	1.9	8,405.3
2022	11.1	193.2	17.2	110.4	135.0	25.0	<1	9.3	26.6	107.0	27.9	4.8	667.9
2023	<1	1.4	7.3	41.8	105.2	35.1	7.0	<1	4.7	26.9	47.1	10.6	287.4

Year	1	2	3	4	5	6	7	8	9	10	11	12+	Total
2024	<1	7.6	7.9	138.5	43.6	106.4	19.6	2.0	<1	11.0	14.4	15.9	367.7
2025	562.7	<1	17.2	22.7	95.4	30.9	124.8	21.7	<1	<1	4.5	21.6	903.2

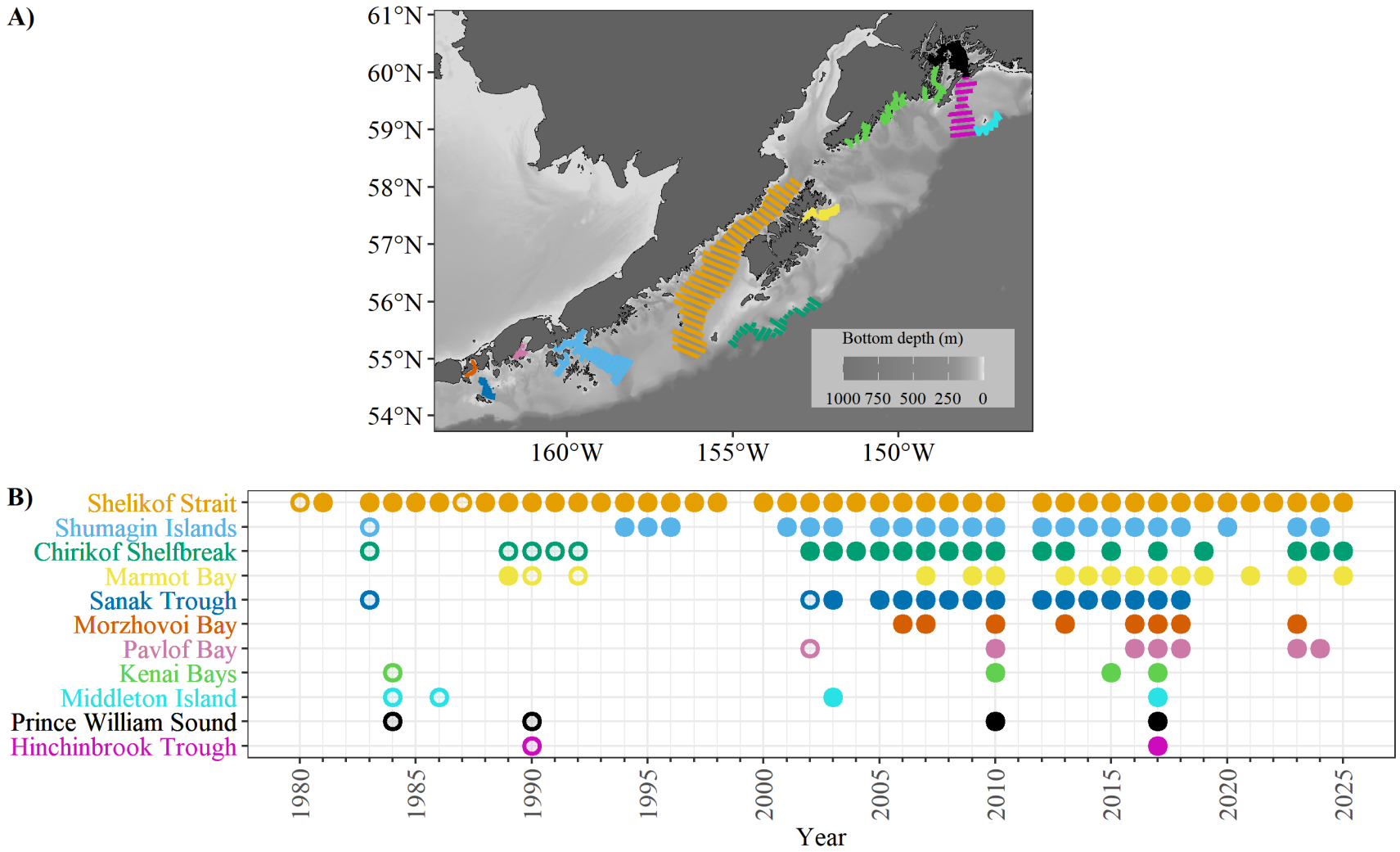


Figure 1. Gulf of Alaska pre-spawning pollock acoustic-trawl surveys from 1980-2025. A) acoustic-trawl survey regions. Bottom depths are indicated in greyscale. Note that this scale is used in all maps throughout report. B) Survey years for each region. Unfilled circles indicate years in which a survey was conducted but no biomass estimate was made; filled circles indicate complete surveys in which biomass was successfully estimated.

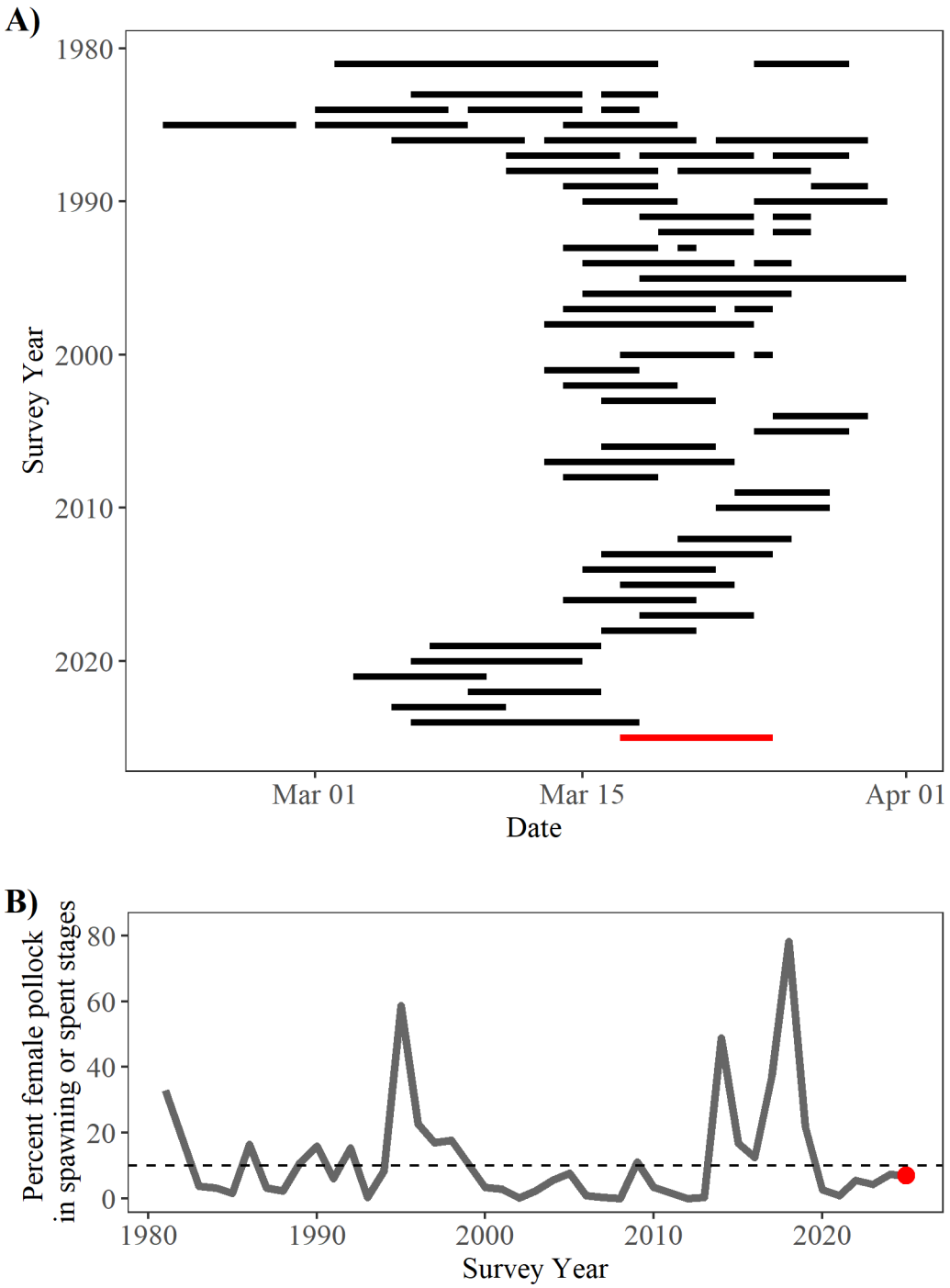


Figure 2. Shelikof Strait survey timing. A) acoustic-trawl survey timing from 1980-2025. B) percent of female pollock > 40 cm FL in spawning or spent maturity stages. The 2025 survey timing and maturity status are highlighted in red. The dashed line indicates where 10% of female pollock are in spawning or spent maturity stages.

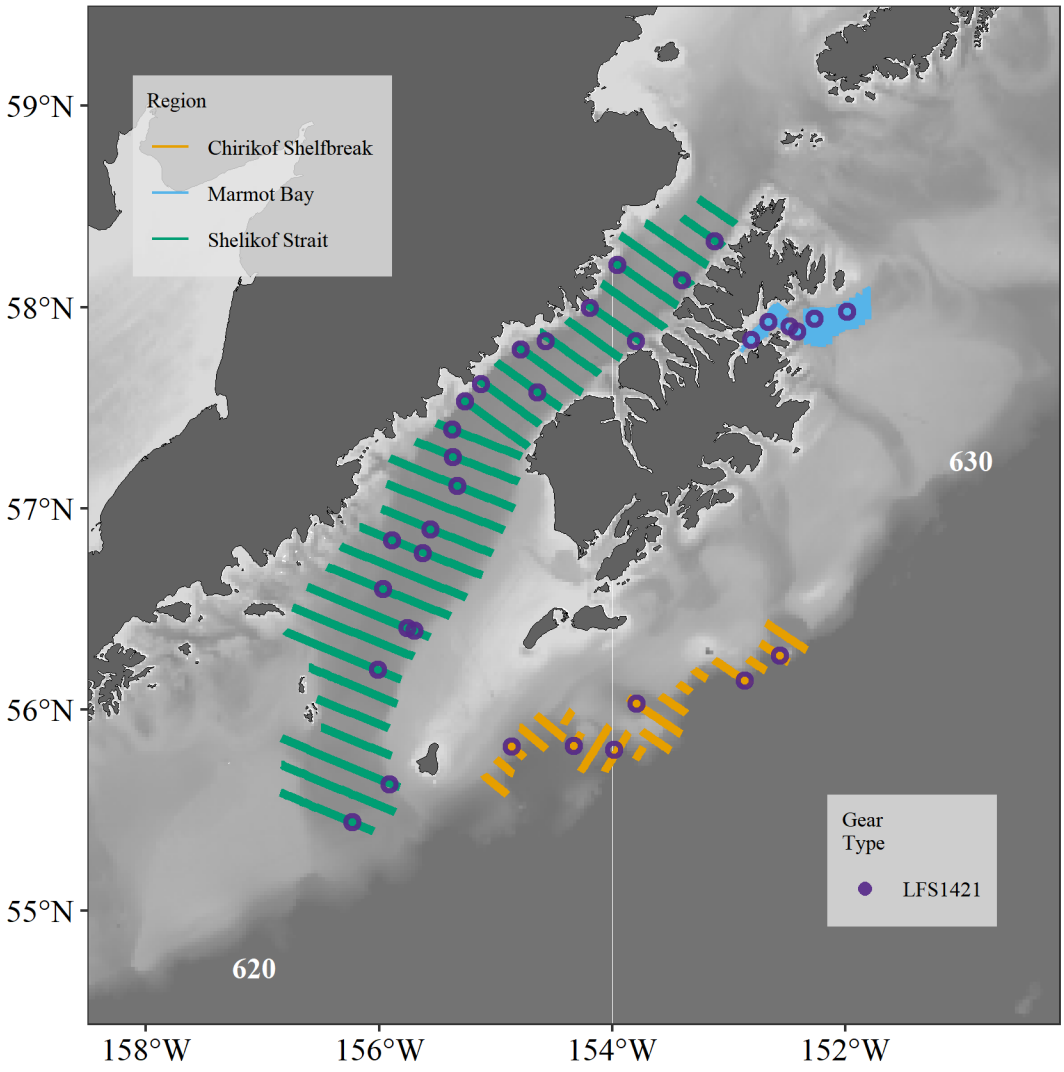


Figure 3. Transect lines and trawl haul locations from the 2025 winter pre-spawning acoustic-trawl surveys. The survey region associated with each transect is indicated by the transect color. The locations of trawl events are indicated with purple markers. NMFS reporting areas are noted in white text.

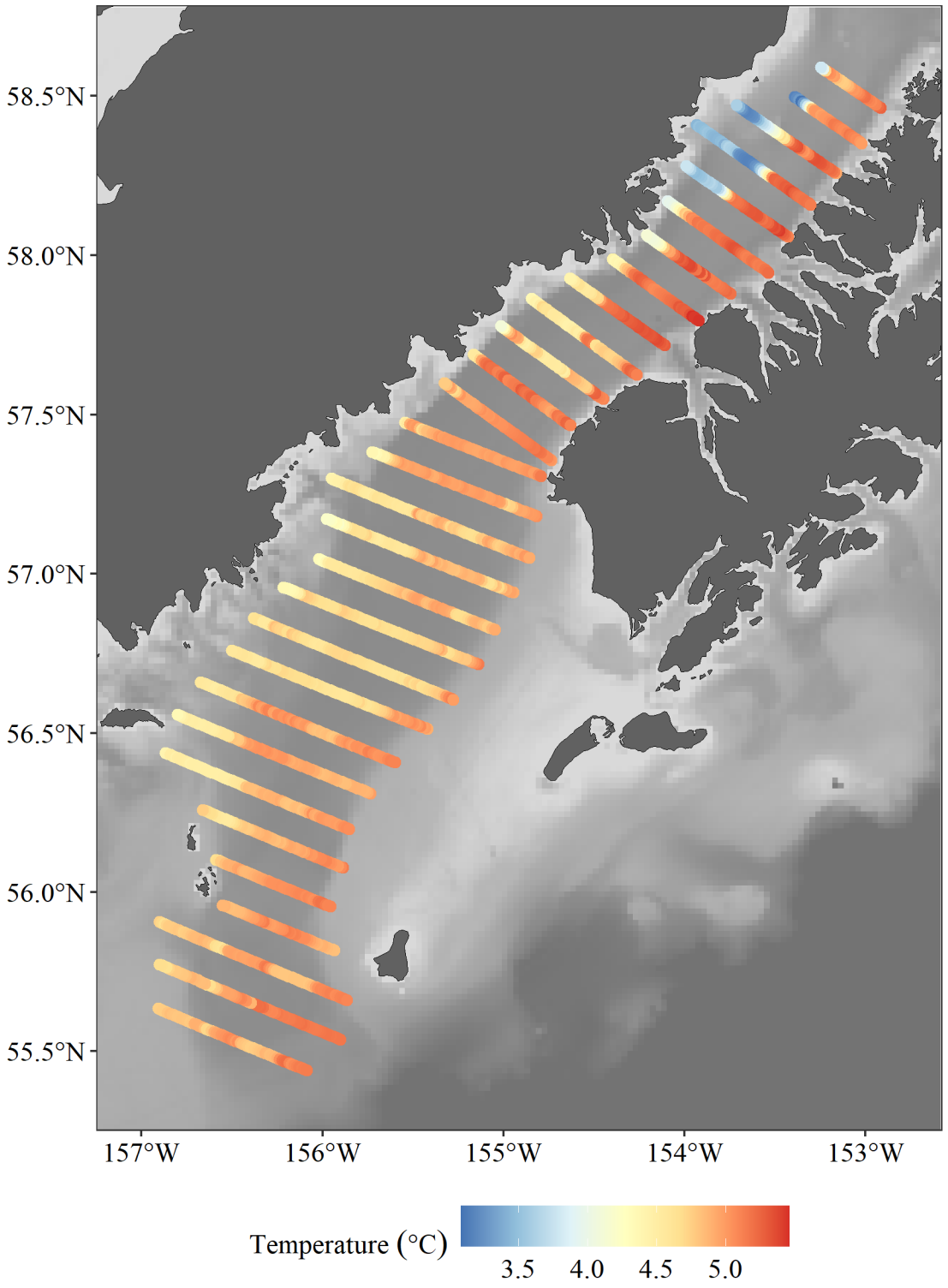


Figure 4. Surface water temperatures (°C) recorded at 5-second intervals during the winter 2025 acoustic-trawl survey in Shelikof Strait.

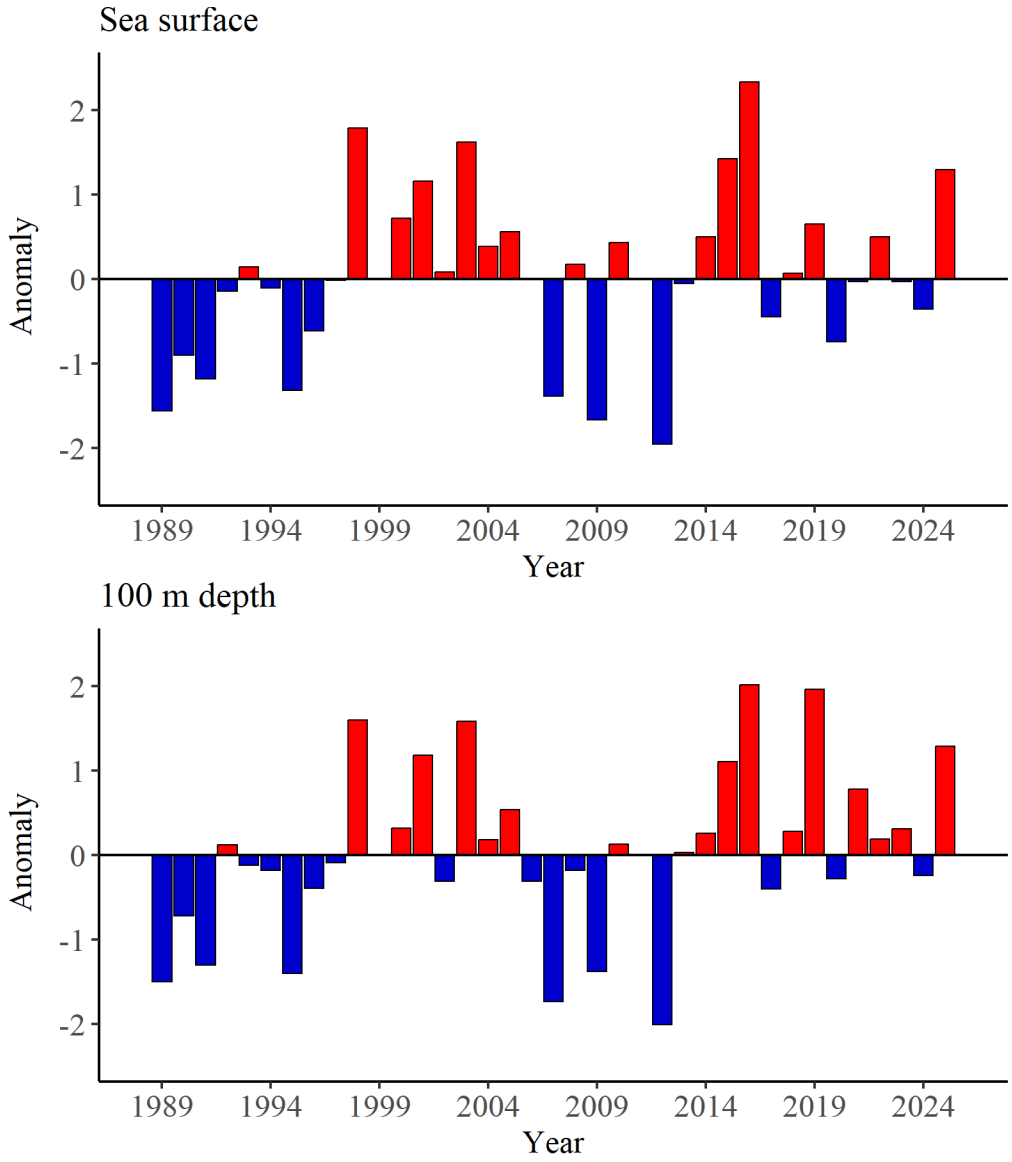


Figure 5. Temperature anomalies at the sea surface (upper panel) and 100 m depth (lower panel) in Shelikof Strait. Anomalies for each temperature source are centered and scaled by their respective mean temperature and standard deviation from the 1989-2024 period. Positive and negative anomalies are indicated by red and blue bars, respectively.

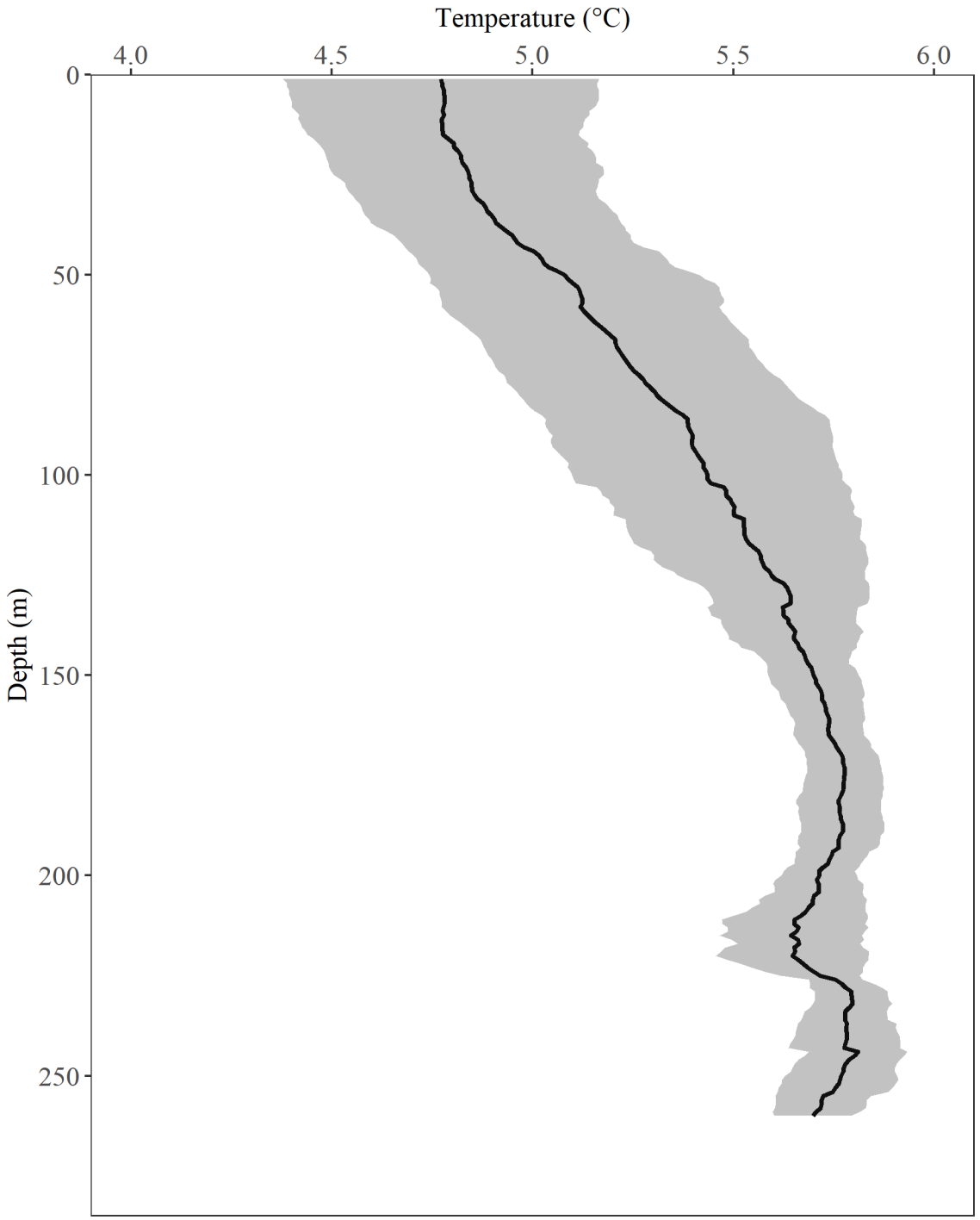


Figure 6. Mean water temperature (°C; solid line) by 1-m depth intervals measured at 22 trawl locations during the 2025 acoustic-trawl survey of walleye pollock in Shelikof Strait. The shaded area indicates ± 1 standard deviation.

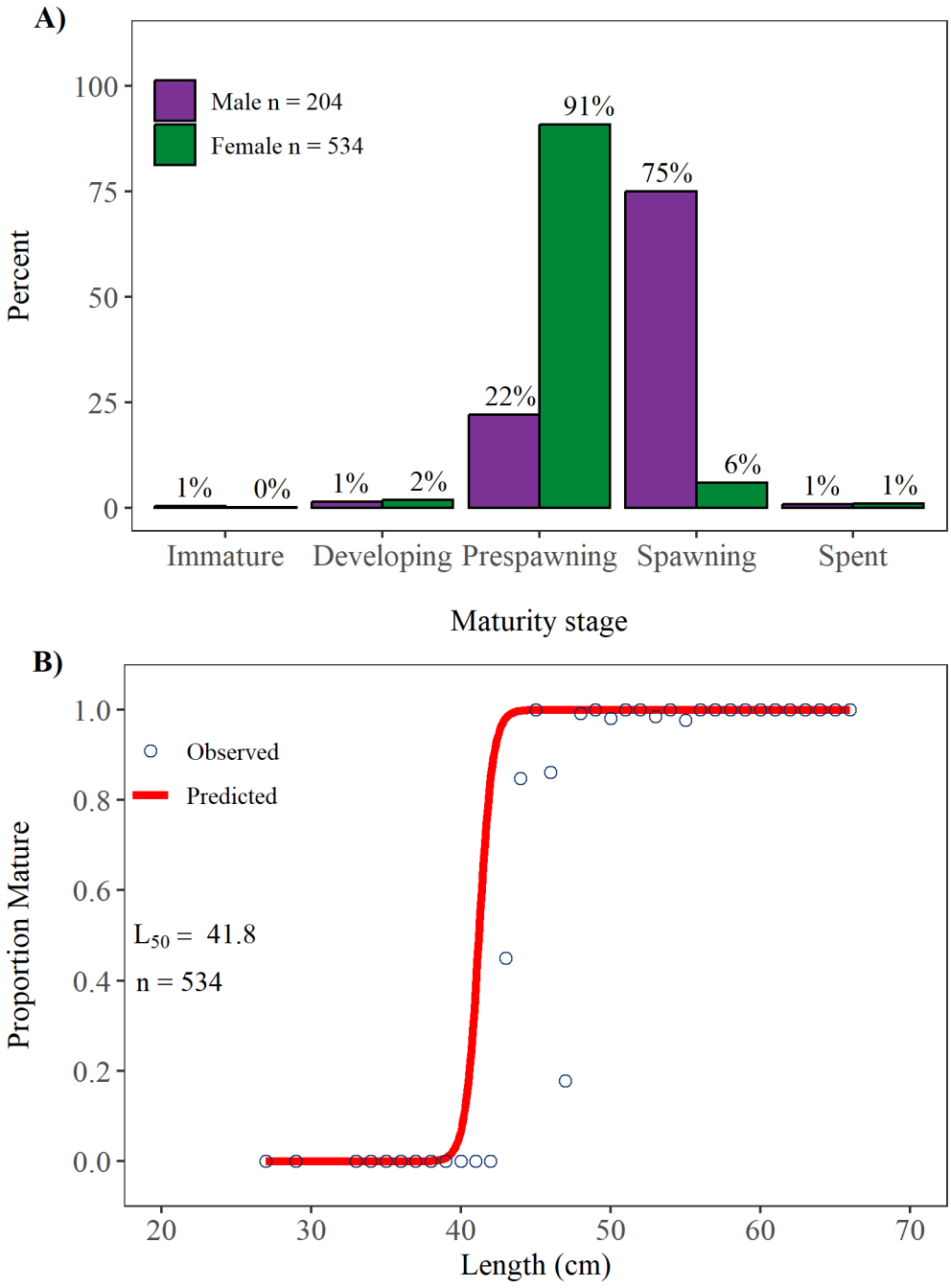


Figure 7. Pollock maturity in Shelikof Strait. A) maturity composition for male and female pollock > 40 cm fork length (FL) within each stage; B) proportion mature (i.e., pre-spawning, spawning, or spent) by 1-cm size group for female pollock. All maturity quantities are weighted by local pollock abundance.

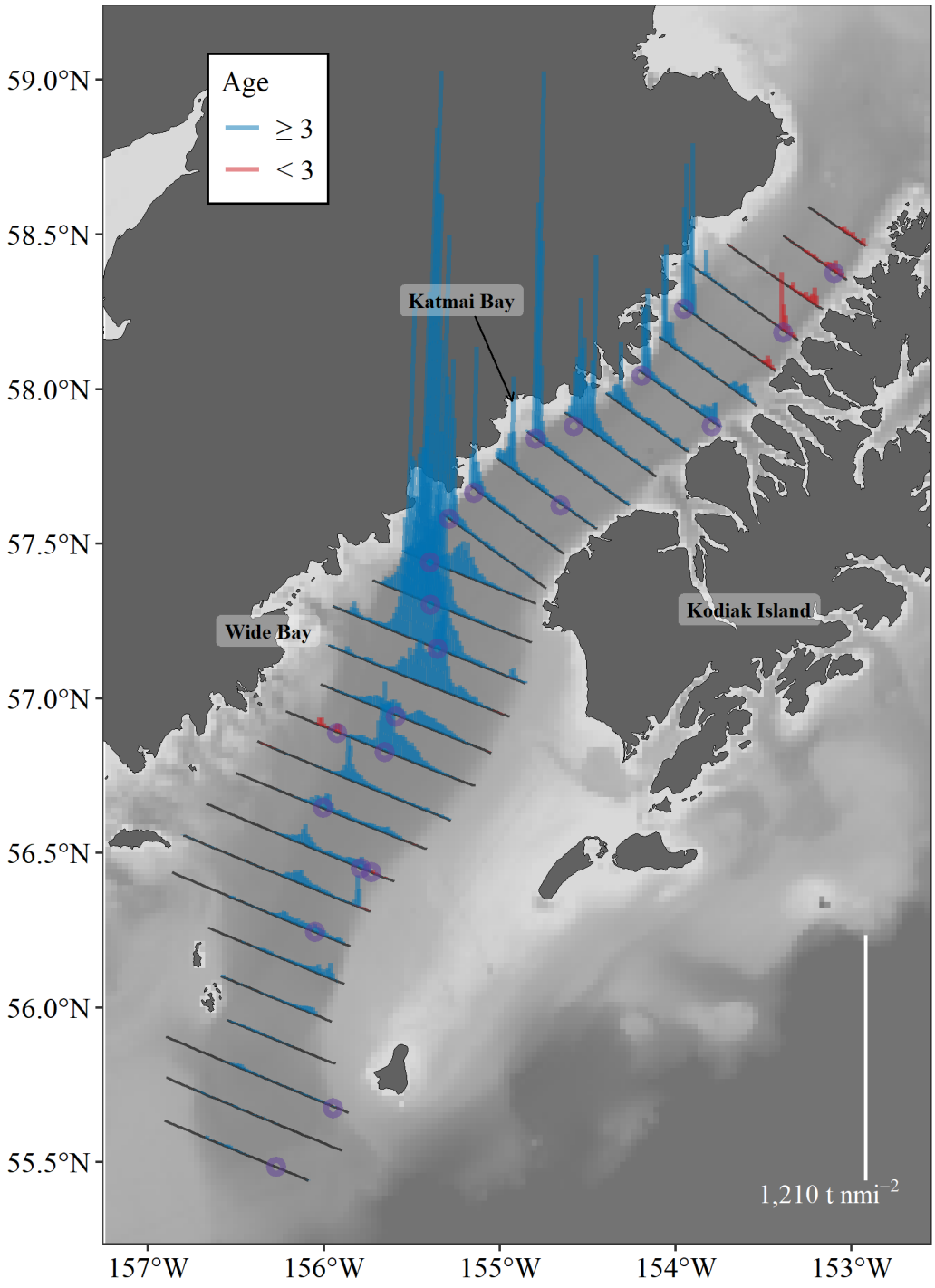


Figure 8. Biomass (t nmi^{-2}) attributed to pollock (vertical lines) along tracklines surveyed during the 2025 acoustic-trawl survey of Shelikof Strait. The locations of trawl events are indicated with purple markers. Biomass is categorized based on haul catches comprised of mostly adult (≥ 3 years old, blue) or juvenile (< 3 years old, red) pollock.

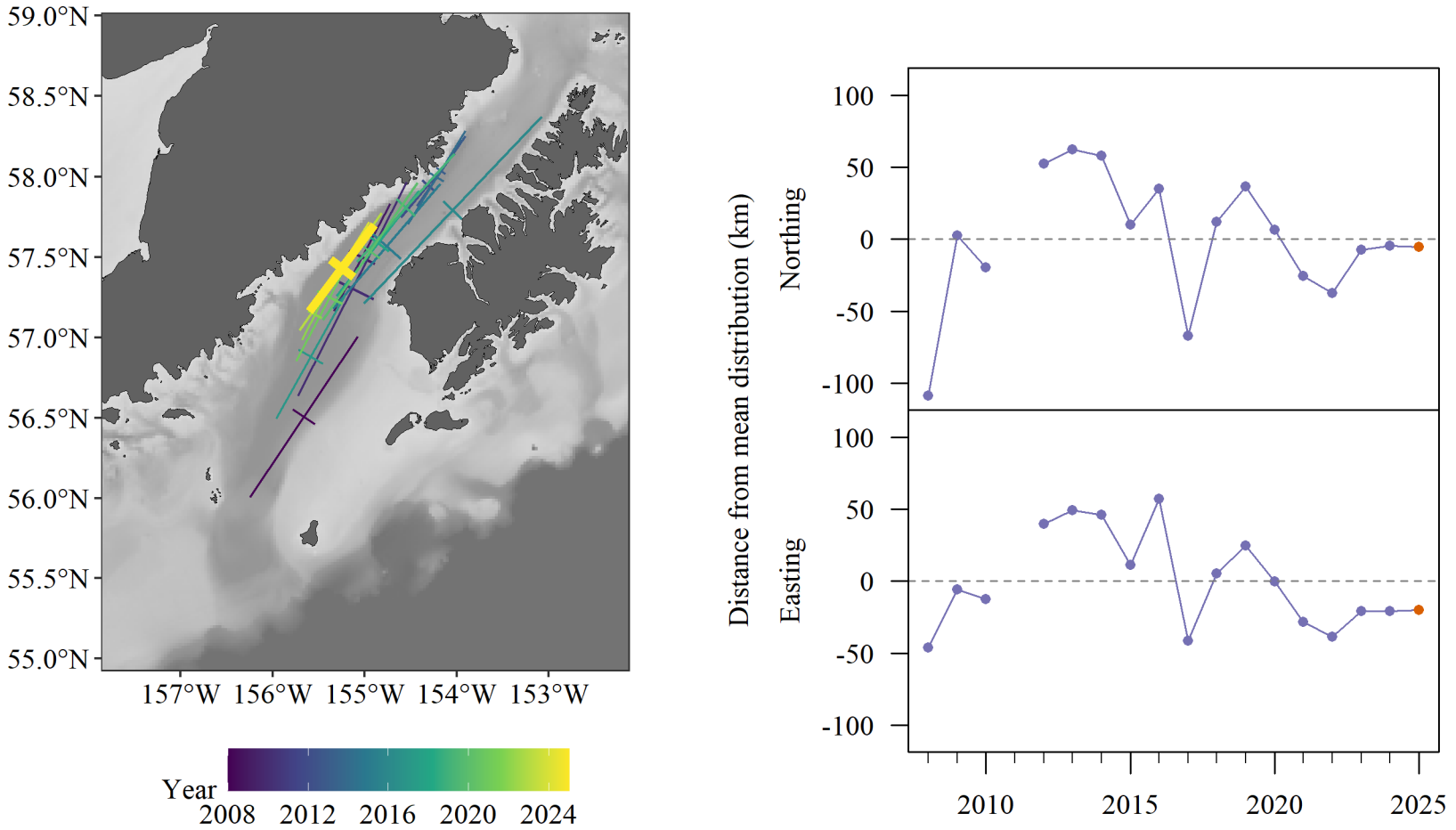


Figure 9. Geostatistical characterizations of pollock biomass distributions from 2008-2025. Center of gravity (line intersection) and inertia (line length) estimates (left map) indicate the mean location and dispersion of the distribution around its center of gravity during the 2025 survey (yellow; thickest line) and each of the other survey years (colors vary by survey year; thinner lines). Time series of center of gravity estimates (right plots) centered by the 15-year mean are shown along latitudinal ('Northing') and longitudinal ('Easting') axes.

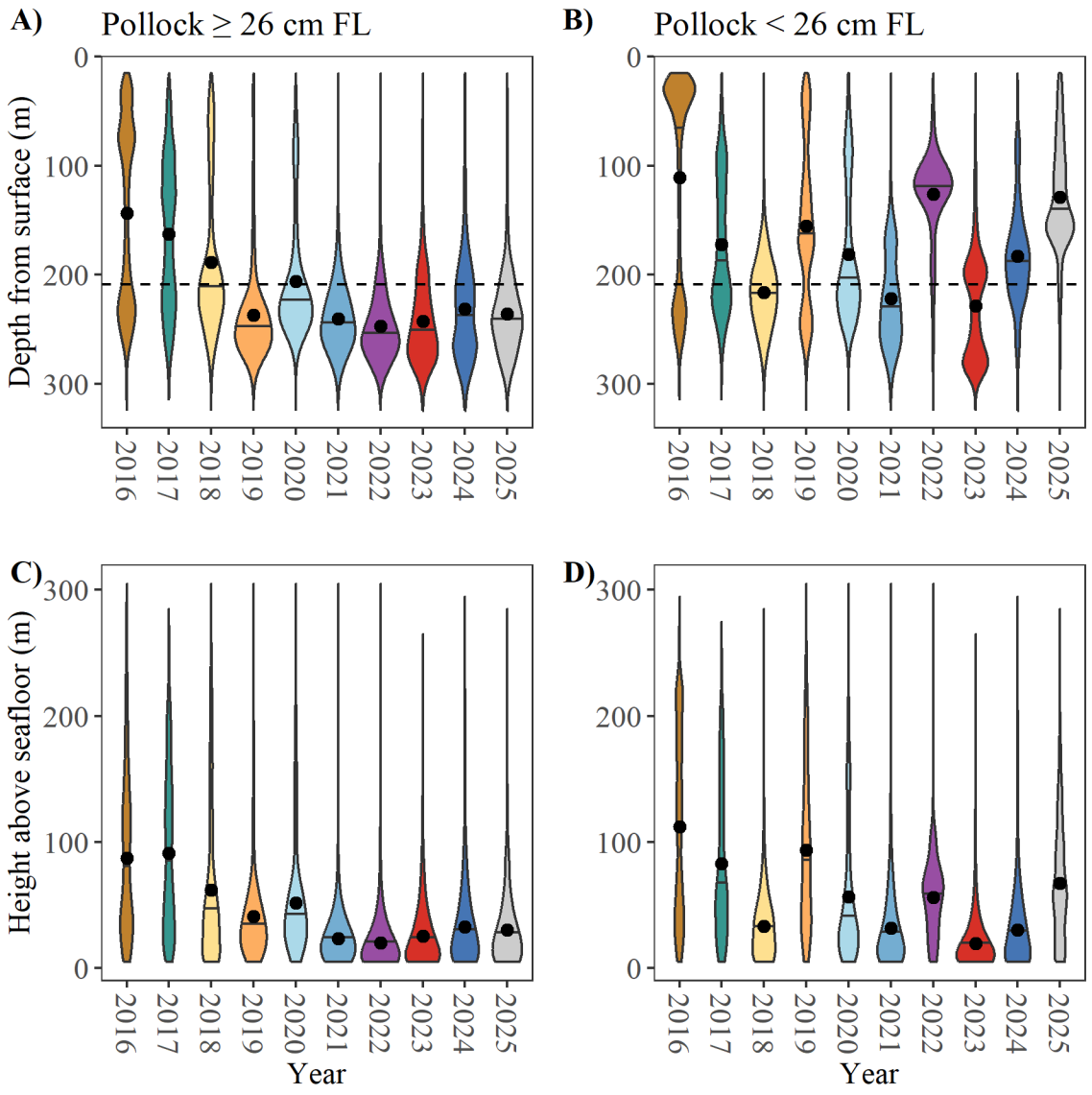


Figure 10. Estimated biomass distributions of adult (≥ 26 cm FL) and juvenile (< 26 cm FL) pollock A, B) depth and C, D) height above the seafloor in the 2025 acoustic-trawl survey of Shelikof Strait. Results for the 2016-2024 acoustic-trawl surveys are included for comparison. Depth is referenced to the surface and height is referenced to the bottom. Data were averaged in 10-m depth bins. Mean bottom depth for 2025 is shown in panels A) and B) (dashed line). Plots show the probability density of pollock distribution, with median pollock depth noted by black horizontal lines, and the mean weighted pollock depth indicated by black points.

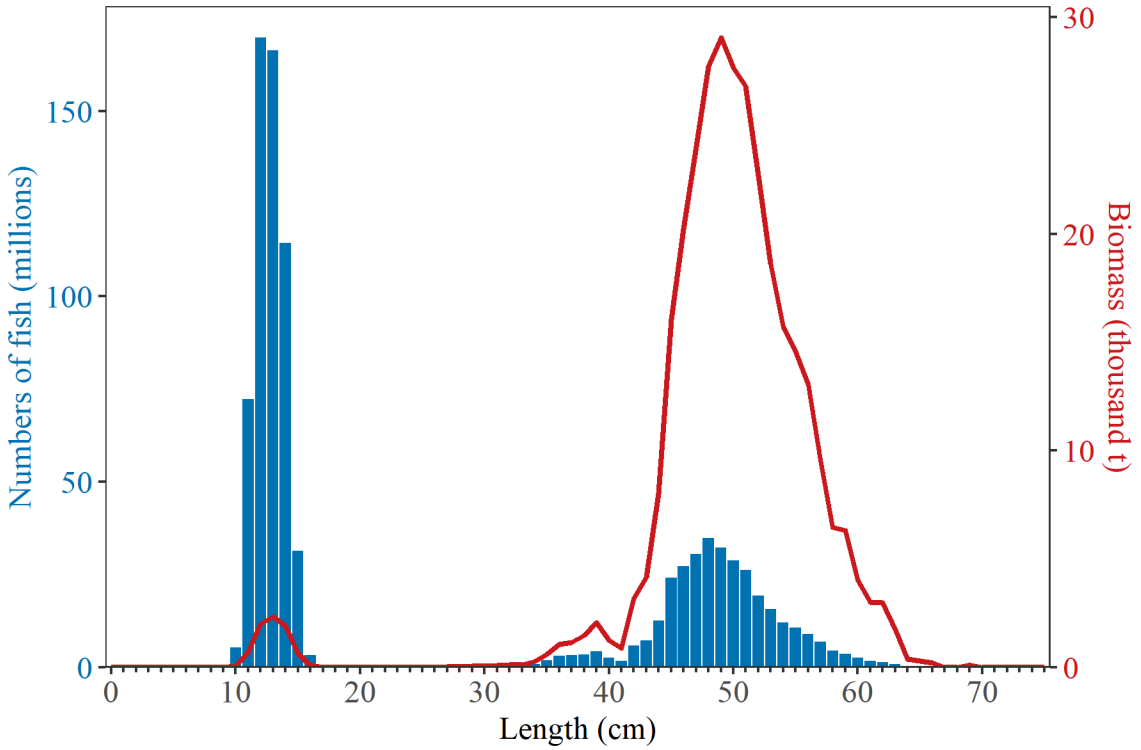


Figure 11. Numbers- (blue bars) and biomass- (red line) at-length estimates of pollock for the 2025 acoustic-trawl survey of Shelikof Strait.

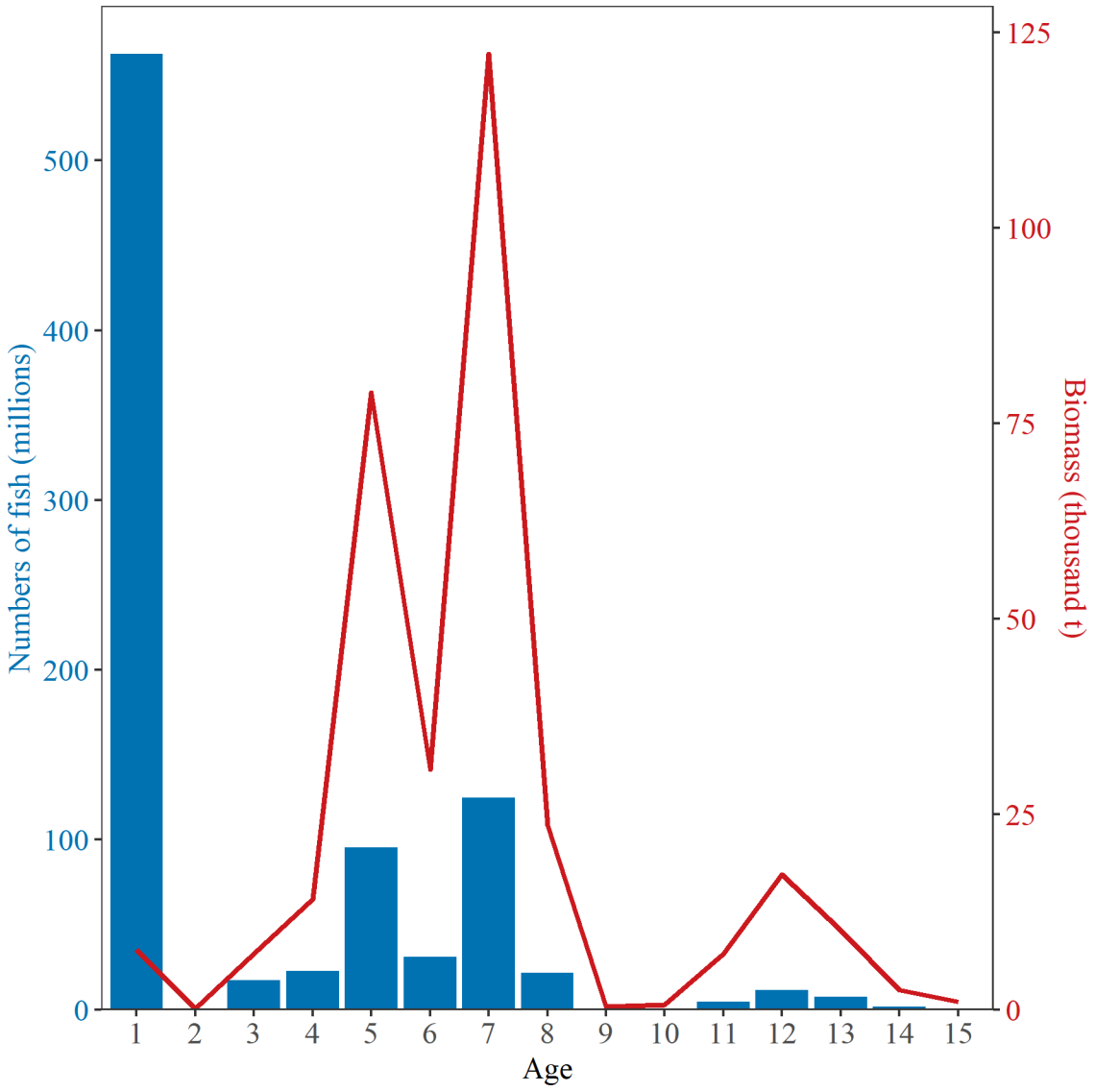


Figure 12. Numbers- (millions of fish, blue bars) and biomass- (1000s t, red line) at-age estimates of pollock for the 2025 acoustic-trawl survey of Shelikof Strait.

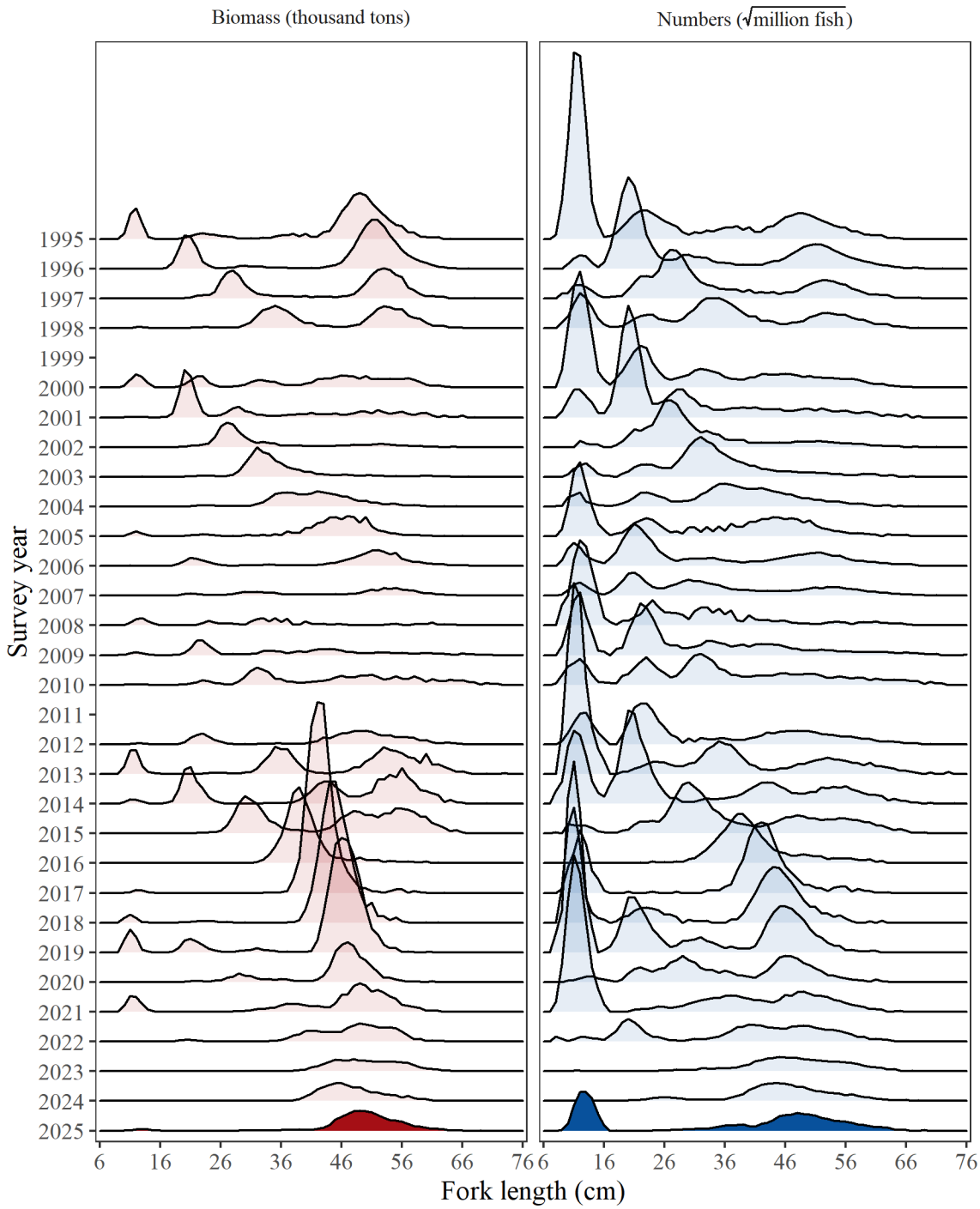


Figure 13. Time series of pollock population length composition by weight (left panel, thousand tons) and numbers (right panel, million fish) from acoustic-trawl surveys of Shelikof Strait for 1995-2025. Estimates for 2008-2025 include selectivity corrections for juvenile escapement (see text for explanation). The 2025 estimates are highlighted in solid colors for comparison.

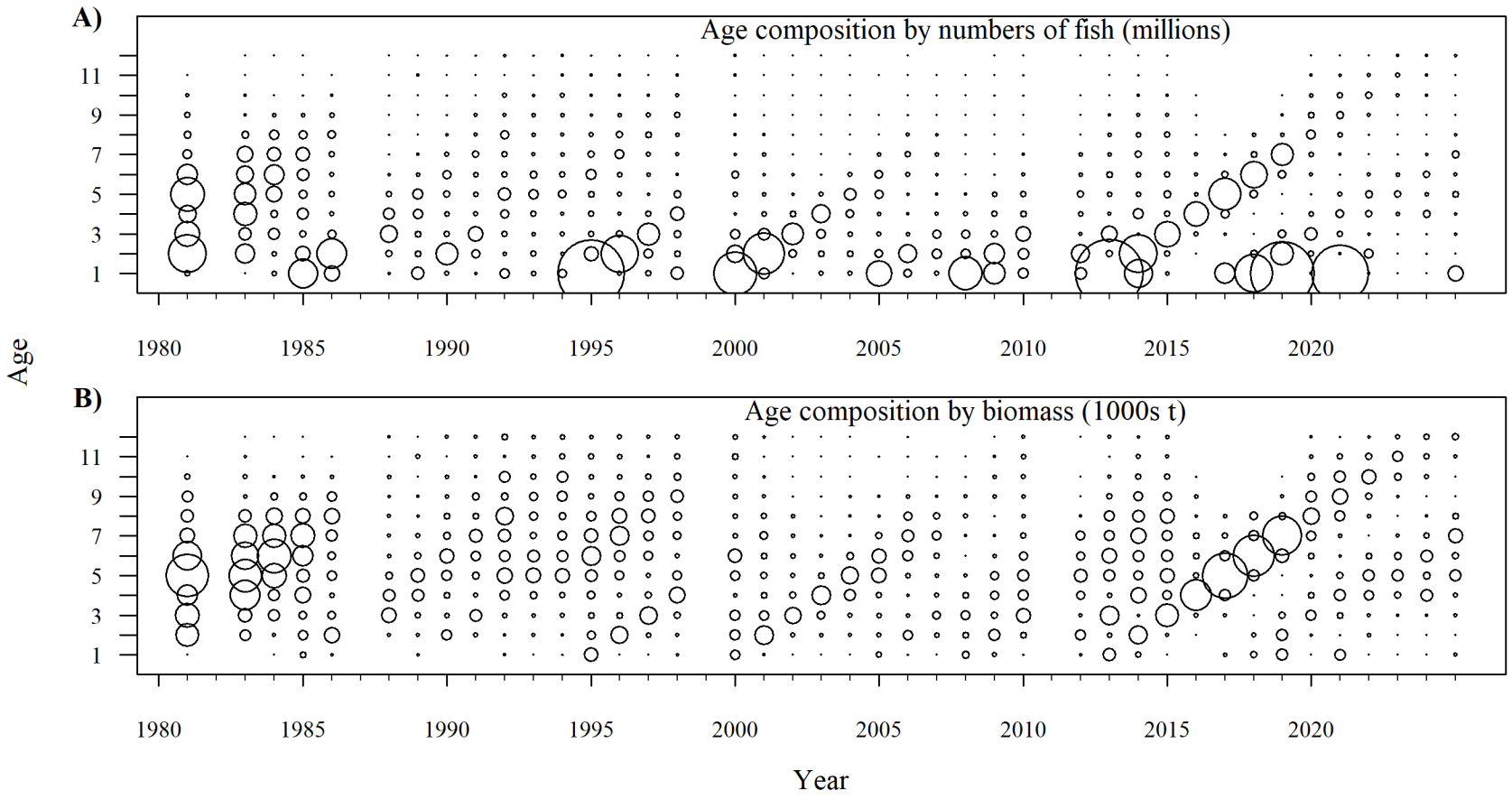


Figure 14. Time series of pollock population age composition by A) numbers (millions of fish) and B) biomass (1000s t) from acoustic-trawl surveys of Shelikof Strait. Estimates for 2008-2025 include selectivity corrections for juvenile escapement (see text for explanation). Bubble size is scaled based on square root transform of numbers/biomass estimate by age.

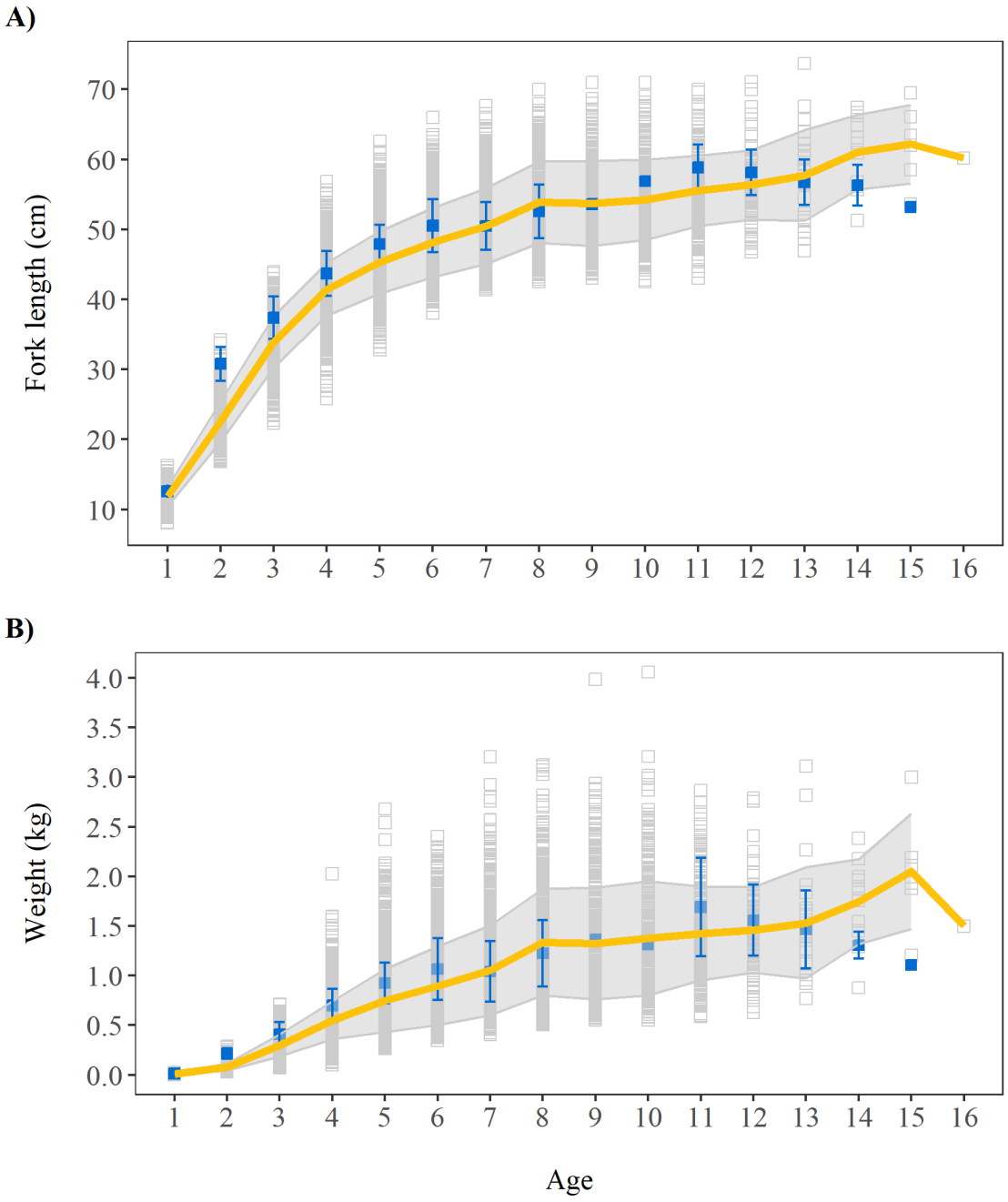


Figure 15. Pollock A) length- and B) weight-at-age for Shelikof Strait. The 2025 survey is highlighted in blue (mean ± 1 standard deviation). Gray squares indicate the range of observations in previous surveys (2008-2024), and the yellow line and gray ribbon indicate mean length- or weight-at-age in previous surveys ± 1 standard deviation.

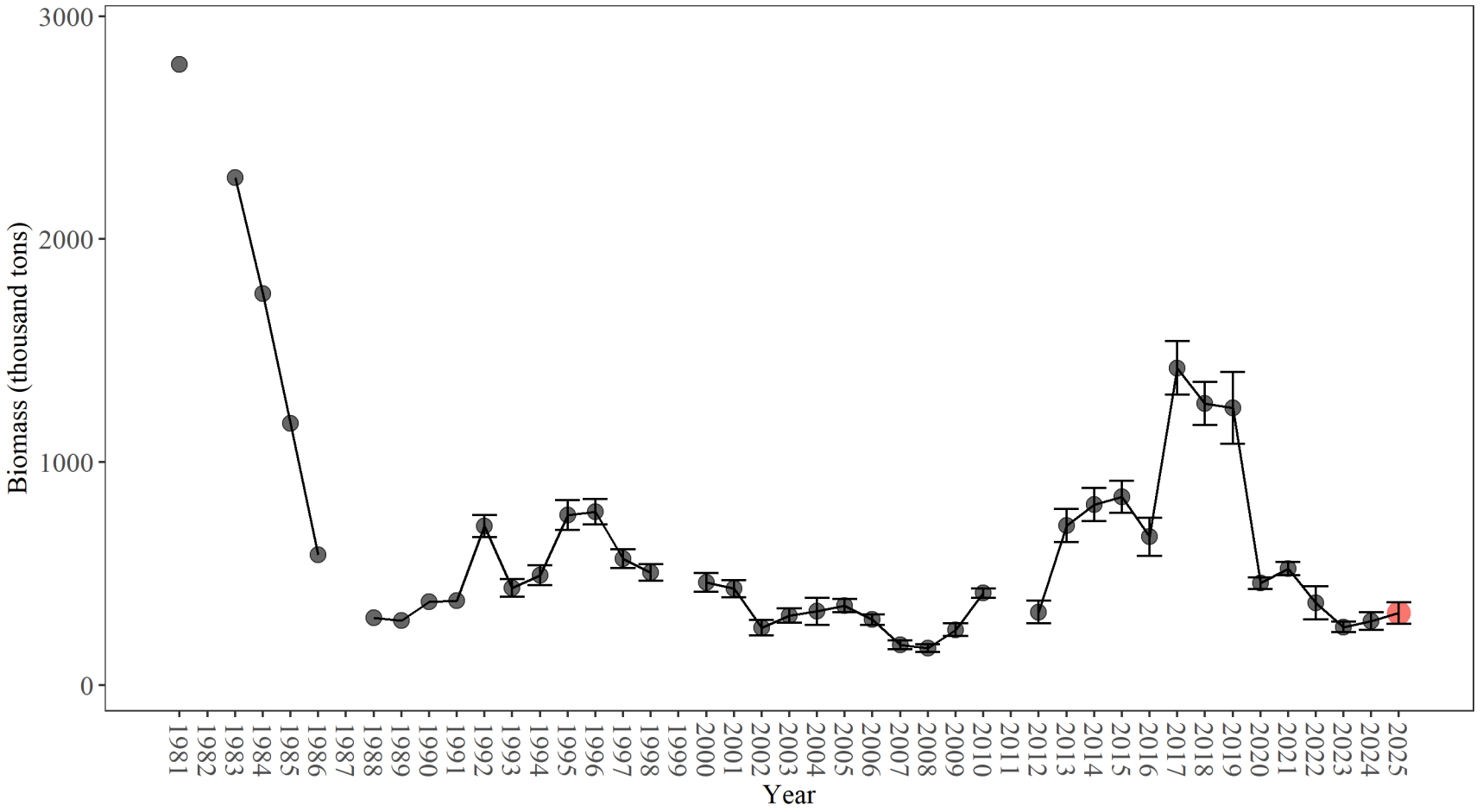


Figure 16. Summary of age-1+ pollock biomass estimates (thousands of metric tons) for Shelikof Strait based on acoustic-trawl surveys from 1981-2025 (except 1999 and 2011). Estimates for 2008-2025 include selectivity corrections for juvenile escapement (see text for explanation). Current survey estimate in red, and shaded area indicate 1-D geostatistical 95% confidence intervals from 1992-2025.

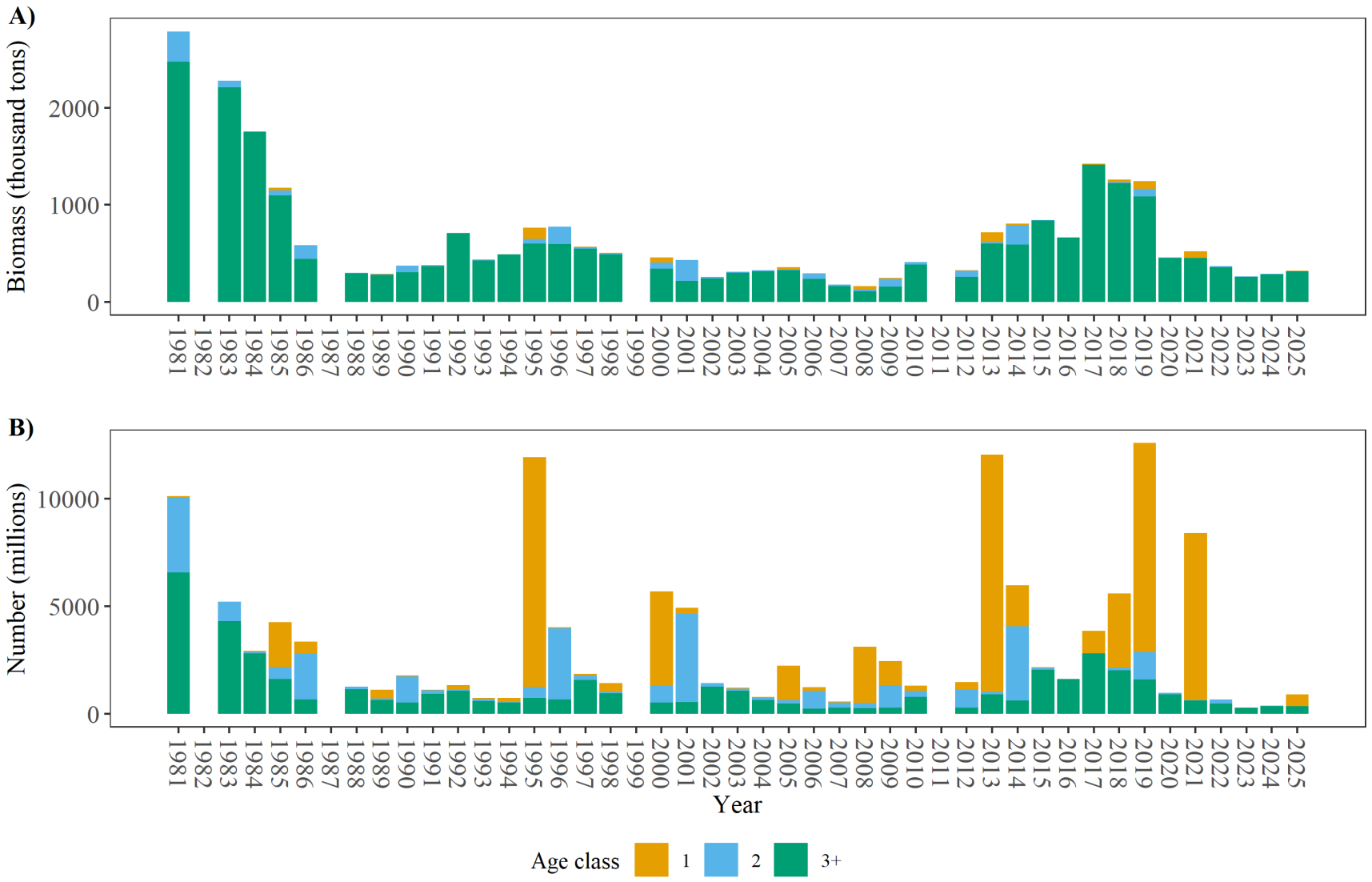


Figure 17. Pollock A) biomass and B) abundance estimates by age class in Shelikof Strait from 1981-2025. Age classes are defined as age-1, age-2, and age-3+ pollock.

APPENDIX I. ITINERARY

Shelikof Strait

16 March	Depart Kodiak, AK
16 March-17 March	Acoustic sphere calibration and mooring deployment in Kalsin Bay, AK
17 March	Transit to survey start area
17 March-25 March	Acoustic-trawl survey of the Shelikof Strait
25 March-28 March	Acoustic-trawl survey of the Chirikof Shelfbreak
28 March-30 March	Acoustic-trawl survey of Marmot Bay
30 March	Transit to Kalsin Bay
30 March-31 March	Acoustic sphere calibration and mooring recovery and redeployment in Kalsin Bay, AK
31 March	In port Kodiak

APPENDIX II. SCIENTIFIC PERSONNEL

Shelikof Strait

Name	Position	Organization
Darin Jones	Chief Scientist	AFSC
Denise McKelvey	Biologist	AFSC
Scott Furnish	Computer Spec.	AFSC
Matthew Phillips	Biologist	AFSC
Dave McGowan	Biologist	AFSC
Robert Levine	Biologist	AFSC
David Bryan	Biologist	AFSC

AFSC = Alaska Fisheries Science Center, National Marine Fisheries Service, Seattle, WA

APPENDIX III. ABUNDANCE CALCULATIONS

The abundance of target species was calculated by combining the echosounder measurements with size and species distributions from trawl catches and TS-length relationships from the literature (see De Robertis et al. 2017b for details). The echosounder measures volume backscattering strength, which is integrated vertically to produce the nautical area scattering coefficient, s_A (units of m^2 nmi^{-2}; MacLennan et al. 2002). The backscatter from an individual fish of species s at length l is referred to as its backscattering cross-section, $\sigma_{bs_{s,l}}$ (m^2), or in logarithmic terms as its target strength, $TS_{s,l}$ (dB re 1 m^2):

$$TS_{s,l} = 10\log_{10}\left(\sigma_{bs_{s,l}}\right) . \qquad \text{(Eq. } i\text{)}$$

The numbers of individuals of species s in length class l ($N_{s,l}$) captured in the nearest haul h were used to compute the proportion of acoustic backscatter associated with each species and length. First, the number of individuals in the catch were converted to a proportion ($P_{s.l,h}$):

$$P_{s,l,h} = \frac{N_{s,l,h}}{\sum_{s,l} N_{s,l,h}} , \quad \text{where} \sum_{s,l} P_{s,l,h} = 1 . \qquad \text{(Eq. } ii\text{)}$$

In analyses where trawl selectivity was considered, the selectivity-corrected numbers $N_{s_{corr,}l,h}$ were used in place of $N_{s,l,h}$ in Eq. ii. This correction corrects the catch for trawl escapement. The corrected catch is that expected for an unselective sampling device. Refer to the main text for a description of the selectivity corrections applied.

The mean backscattering cross-section (an areal measure of acoustic scattering in m^2; MacLennan et al 2002) of species s of length class l is:

$$\sigma_{bs_{s,l}} = 10^{(0.1 \cdot TS_{s,l})} , \qquad \text{(Eq. } iii\text{)}$$

where TS is the target strength (dB re 1 m^2) of species *s* at size *l* (Table 1).

The proportion of backscatter from species s of length class l in haul h ($PB_{s,l,h}$) is computed from the proportion of individuals of species s and length class l estimated from haul h ($P_{s,l,h}$) and their backscattering cross-section:

$$PB_{s,l,h} = \frac{P_{s,l,h} \cdot \sigma_{bs_{s,l}}}{\sum_{s,l}\left(P_{s,l,h} \cdot \sigma_{bs_{s,l}}\right)} \ . \qquad \text{(Eq. } iv\text{)}$$

The measured nautical area scattering coefficient (s_A) at interval i was allocated to species s and length l as follows:

$$s_{A_{s,l,i}} = s_{A_i} \cdot PB_{s,l,h} \ , \qquad \text{(Eq. } v\text{)}$$

where haul h is the nearest haul within a stratum assigned to represent the species composition in a given 0.5 nmi along-track interval i. The nearest geographic haul was determined by using the great-circle distance to find the nearest trawl location (defined as the location where the net is at depth and begins to catch fish) out of the pool of hauls assigned to the same stratum (see above for details) closest to the start of interval i.

The abundance of species of length l in an area encompassing a series of transect intervals i was estimated from the area represented by that interval (A_i, nmi^2), the mean areal backscatter attributed to species s in given length/size class l ($s_{A_{s,l,i}}$, m^2 nmi^{-2}), and mean backscattering cross-section of species s at that size ($\sigma_{bs_{s,l}}$ m^2) as follows:

$$\text{Numbers-at-length } l\text{: } N_{s,l} = \sum_i \left(\frac{s_{A_{s,l,i}}}{4\pi\sigma_{bs_{s,l,i}}} \times A_i\right) \qquad \text{(Eq. } vi\text{)}$$

$$\text{Biomass-at-length } l\text{: } B_{s,l} = \sum_i \left(W_{s,l} \times N_{s,l,i}\right) \ , \qquad \text{(Eq. } vii\text{)}$$

where $W_{s,l}$ is the mean weight-at-length for species s in each 1-cm length l derived from length-weight regressions. In the case of pollock, when five or more individuals were measured within a length interval, the mean weight-at-length was used. Otherwise (i.e., for length classes of pollock with < 5 weight measurements, or other species), weight-at-length was estimated using a linear regression of the natural log-transformed length-weight data (De Robertis and Williams 2008).

The abundance-at-age was computed from $Q_{s,l,j}$, the proportion of j-aged individuals of species s in length class l, and the abundance of that species and age class in each surveyed interval follows:

$$\text{Numbers-at-age } j\text{: } N_{s,j} = \sum_{i} \left(Q_{s,l,j} \times N_{s,l}\right) \qquad \text{(Eq. } viii\text{)}$$

$$\text{Biomass-at-age } j\text{: } B_{s,j} = \sum_{i} \left(Q_{s,l,j} \times B_{s,l}\right) \text{ .} \qquad \text{(Eq. } ix\text{)}$$

Table A1. Target strength (TS) to size relationships from the literature used to allocate 38 kHz acoustic backscatter to most species in this report. The symbols in the equations are as follows: r is the bell radius in cm and L is length in cm for all groups except pelagic crustaceans, in which case L is in m.

Group	TS (dB re 1 m^2)	Length type	TS derived for which species	Reference
pollock	$TS = 20 \log_{10} L - 66$	L = fork length	*Gadus chalcogrammus*	Foote and Traynor (1988), Traynor (1996)
Pacific capelin	$TS = 20 \log_{10} L - 70.3$	L = total length	*Mallotus catervarius*	Guttormsen and Wilson (2009)
Pacific herring[1]	$TS = 20 \log_{10} L - 2.3 \log_{10}(1 + depth/10) - 65.4$	L = fork length	*Clupea harengus*	Ona (2003)
eulachon	$TS = 20 \log_{10} L - 84.5$	L = total length	*Thaleichthys pacificus*	Gauthier and Horne (2004)
fish with swim bladders	$TS = 20 \log_{10} L - 67.4$	L = total length	Physoclist fishes	Foote (1987)
fish without swim bladders	$TS = 20 \log_{10} L - 83.2$	L = total length	*Pleurogrammus monopterygius*	Gauthier and Horne (2004)
jellyfish	$TS = 10 \log_{10}(\pi r^2) - 86.8$	r = bell radius	*Chrysaora melanaster*	De Robertis and Taylor (2014)
squid	$TS = 20 \log_{10} L - 75.4$	L = mantle length	*Todarodes pacificus*	Kang et al. (2005)
pelagic crustaceans[2]	$TS = A * (\log_{10}(BkL)/(BkL))^c + D((kL)^6) + E((kL)^5) + F((kL)^4) + G((kL)^3) + H((kL)^2) + I(kL) + J + 20 \log_{10}(L/L_0)$	L = total length	*Euphausia superba*	Demer and Conti (2005)

[1] *depth* (m) is fixed at 75 m.

[2] A = -930.429983; B = 3.21027896; C = 1.74003785; D = 1.36133896 x 10^{-8}; E = -2.26958555 x 10^{-6}
F= 1.50291244 x 10^{-4}; G = -4.86306872 x 10^{-3}; H = 0.0738748423; I = -0.408004891; J = -73.9078690; and L_0 = 0.03835
If L < 0.015 m, TS = -105 dB; and if L > 0.065 m, TS = -73 dB.
k = 2πfc, where f = 38,000 (frequency in Hz) and c = 1470 (sound speed in m s^{-1}).

APPENDIX IV. REGIONAL SUMMARIES

Chirikof Shelfbreak

The Chirikof Shelfbreak region (Fig. 3) was surveyed between 25 March and 28 March. The survey region encompassed 4,044 km^2 (1,179 nmi^2). Acoustic backscatter was measured along 347.1 km (187.4 nmi) of transects spaced 11.1 km (6.0 nmi) apart (Fig. 3). Bottom depths in the survey area ranged from 79 m to 1,010 m.

Sea surface temperatures (SST) measured in the Chirikof Shelfbreak region indicated relatively warmer thermal conditions during the 2025 survey. SST ranged from 5.0°C to 6.3°C as measured by the ship's flow-through instrumentation along acoustic transects and averaged 5.7°C (Fig. A4.1a). Mean temperature between the surface and deepest trawl (i.e., headrope) depth at all haul locations varied by approximately 0.7°C (Fig. A4.1b). The average SST measured by the SBE 39 at all haul locations was 5.7°C (Table 2), which was 1.2°C warmer than the mean SST in 2024 and 1.3°C warmer than the long-term 1989-2024 historical mean (Fig. A4.2). The average temperature at 100 m depth, used as an indicator of thermal conditions at depth, was 5.7°C, which was 0.7°C warmer than the mean temperature at 100 m depth in 2024 and 1°C warmer than the long-term 1989-2024 historical mean (Fig. A4. 2).

Biological data and specimens were collected in the Chirikof Shelfbreak region from 6 LFS1421 hauls (Table 2, Fig. 3). Pollock were randomly sampled for length (n = 1,339), body weight (n = 275) and maturity (n = 275) measurements (Table 3). Pollock and Pacific ocean perch were the most abundant species by weight in the LFS1421 hauls, contributing 54.9% and 43.5% of the catch by weight, respectively (Table A4.1). Pollock and Pacific ocean perch were the most abundant species by number, contributing 52.3% and 42.6% of the catch by number, respectively (Table A4.1).

Pollock observed in the Chirikof Shelfbreak region were generally in pre-spawning (females) or spawning (males) maturity stages. The abundance weighted maturity composition for males > 40 cm FL (n = 114) was 0% immature, 2% developing, 30% pre-spawning, 69% spawning, and 0% spent, and for females > 40 cm FL (n = 150) the abundance weighted maturity composition was 0% immature, 7% developing, 47% pre-spawning, 14% spawning, and 32% spent (Fig. A4.3).

Pollock with lengths < 17 cm FL, indicative of age-1 pollock, were not observed in the Chirikof Shelfbreak region. Pollock 17-26 cm FL, indicative of age-2 pollock, were not observed in the Chirikof Shelfbreak region. Pollock ≥ 26 cm FL, indicative of age-3+ pollock, accounted for 100.0% and 100.0% of the numbers and biomass, respectively (Fig. A4.4a). The distribution of pollock in the Chirikof Shelfbreak region is summarized in Fig A4.5.

A total of 113.3 million pollock weighing 95,232.5 t were estimated to be in the Chirikof Shelfbreak region. The 2025 biomass was 18.4% less than that observed in 2024 (116,740.3 t) and 148.8% greater than the historic mean of 38,282.4 t (Fig. A4.4b). The relative estimation error of the 2025 biomass estimate based on the 1-D geostatistical analysis was 11.2%.

Table A4.1. Catch by species and numbers of length and weight measurements taken from 6 LFS1421 hauls during the 2025 acoustic-trawl survey of pollock in Chirikof Shelfbreak.

		Catch				Measurements	
Species name	Scientific name	Weight (kg)	%	Number	%	Length	Weight
pollock	*Gadus chalcogrammus*	2,320.8	54.9	2,937	52.3	1,339	275
Pacific ocean perch	*Sebastes alutus*	1,837.8	43.5	2,394	42.6	429	129
shortraker rockfish	*Sebastes borealis*	22.8	0.5	5	<0.1	5	5
rougheye rockfish	*Sebastes aleutianus*	20.3	0.5	11	0.2	11	11
chrysaora jellyfish	*Chrysaora sp.*	6.1	0.1	18	0.3	18	18
Chinook salmon	*Oncorhynchus tshawytscha*	4.7	0.1	2	<0.1	2	2
giant grenadier	*Coryphaenoides pectoralis*	3.2	<0.1	1	<0.1	1	1
smooth lumpsucker	*Aptocyclus ventricosus*	3.0	<0.1	3	<0.1	3	3
northern rockfish	*Sebastes polyspinis*	1.8	<0.1	2	<0.1	2	2
dusky rockfish	*Sebastes variabilis*	1.7	<0.1	1	<0.1	1	1
egg yolk jelly	*Phacellophora camtschatica*	1.5	<0.1	7	0.1	7	7
aurelia jellyfish	*Aurelia sp.*	1.3	<0.1	7	0.1	7	7
lanternfishes	Myctophidae (family)	1.1	<0.1	121	2.2	34	19
arrowtooth flounder	*Atheresthes stomias*	0.8	<0.1	1	<0.1	1	1
magistrate armhook squid	*Berryteuthis magister*	0.4	<0.1	27	0.5	6	6
eulachon	*Thaleichthys pacificus*	0.3	<0.1	6	0.1	6	6
Pacific capelin	*Mallotus catervarius*	0.3	<0.1	33	0.6	30	24
northern smoothtongue	*Leuroglossus schmidti*	0.1	<0.1	8	0.1	2	2
Pacific glass shrimp	*Pasiphaea pacifica*	<0.1	<0.1	23	0.4	1	1
Pacific lamprey	*Lampetra tridentata*	<0.1	<0.1	1	<0.1	1	1
lampreys	Petromyzontidae (family)	<0.1	<0.1	2	<0.1	2	2
viperfishes	Stomiidae (family)	<0.1	<0.1	3	<0.1	3	3
flatfish larvae	*Pleuronectiform larvae*	<0.1	<0.1	1	<0.1	1	1
Total		4,228.2		5,614		1,912	527

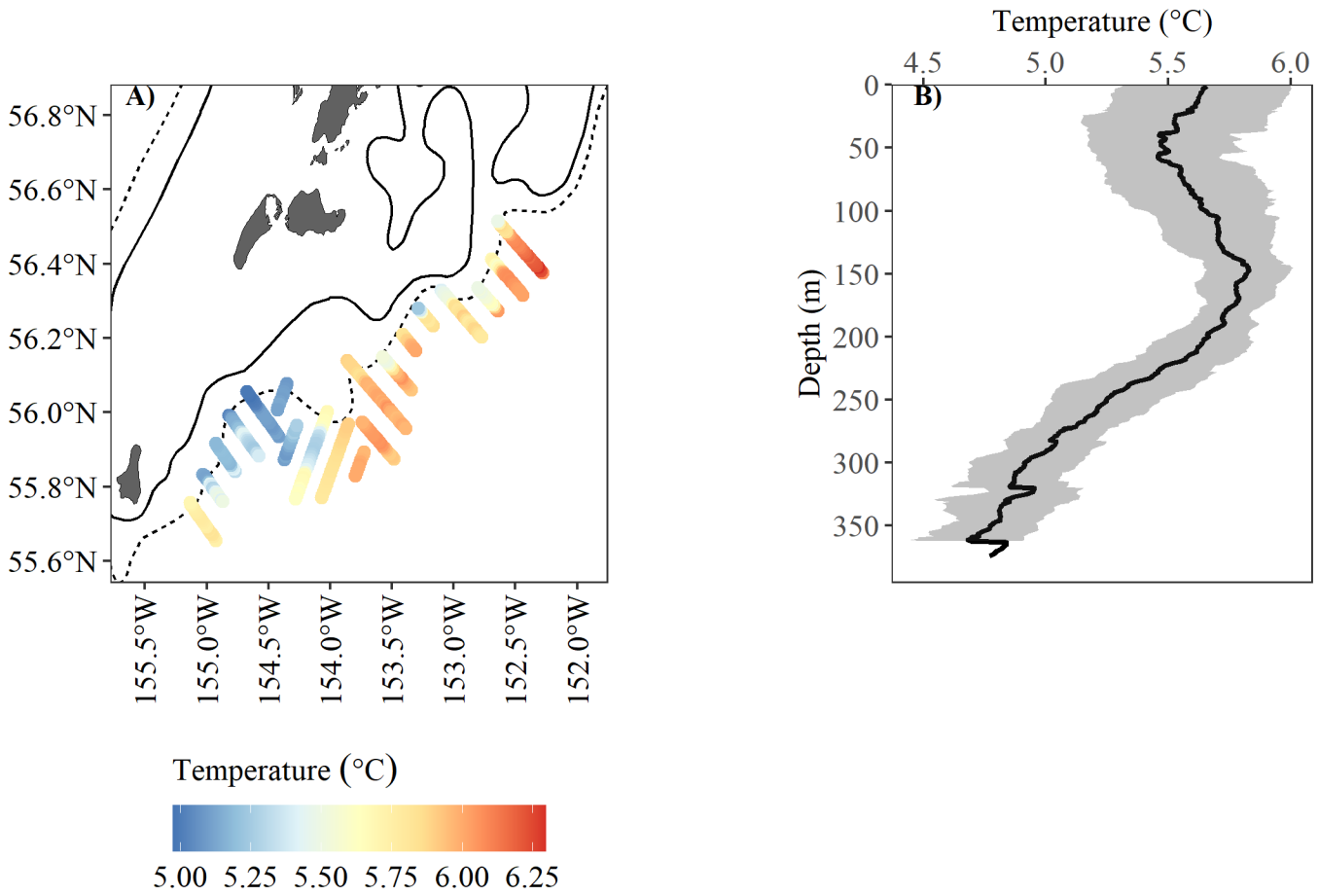


Figure A4.1. 2025 Chirikof Shelfbreak temperature summary. A) surface water temperatures (°C) recorded at 5-second intervals. B) mean water temperature (°C; solid line) by 1-m depth intervals. The shaded area indicates ± 1 standard deviation.

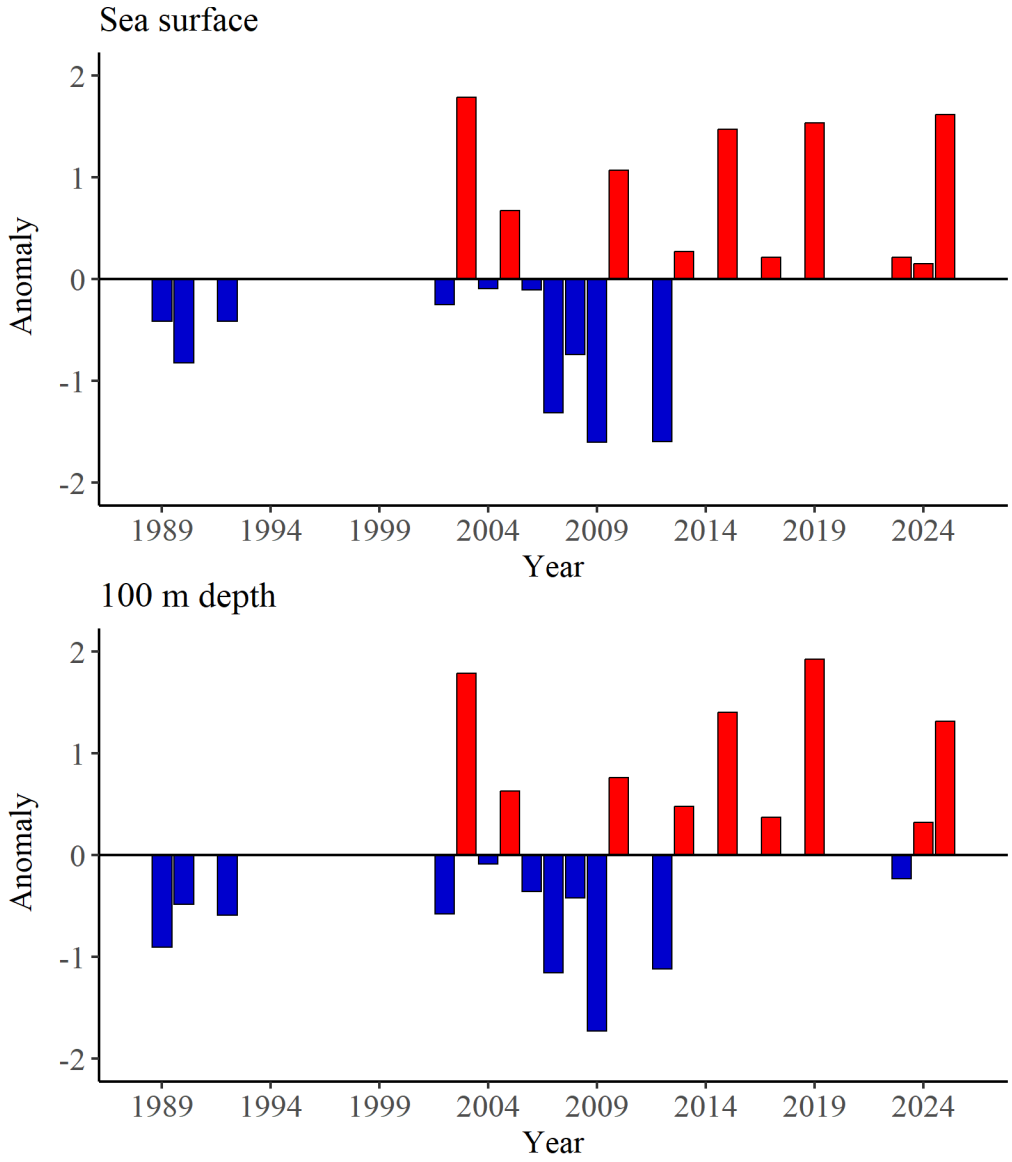


Figure A4.2. Temperature anomalies at the sea surface (upper panel) and 100 m depth (lower panel) in the Chirikof Shelfbreak region. Anomalies for each temperature source are centered and scaled by their respective mean temperature and standard deviation from the 1989-2024 period. Positive and negative anomalies are indicated by red and blue bars, respectively.

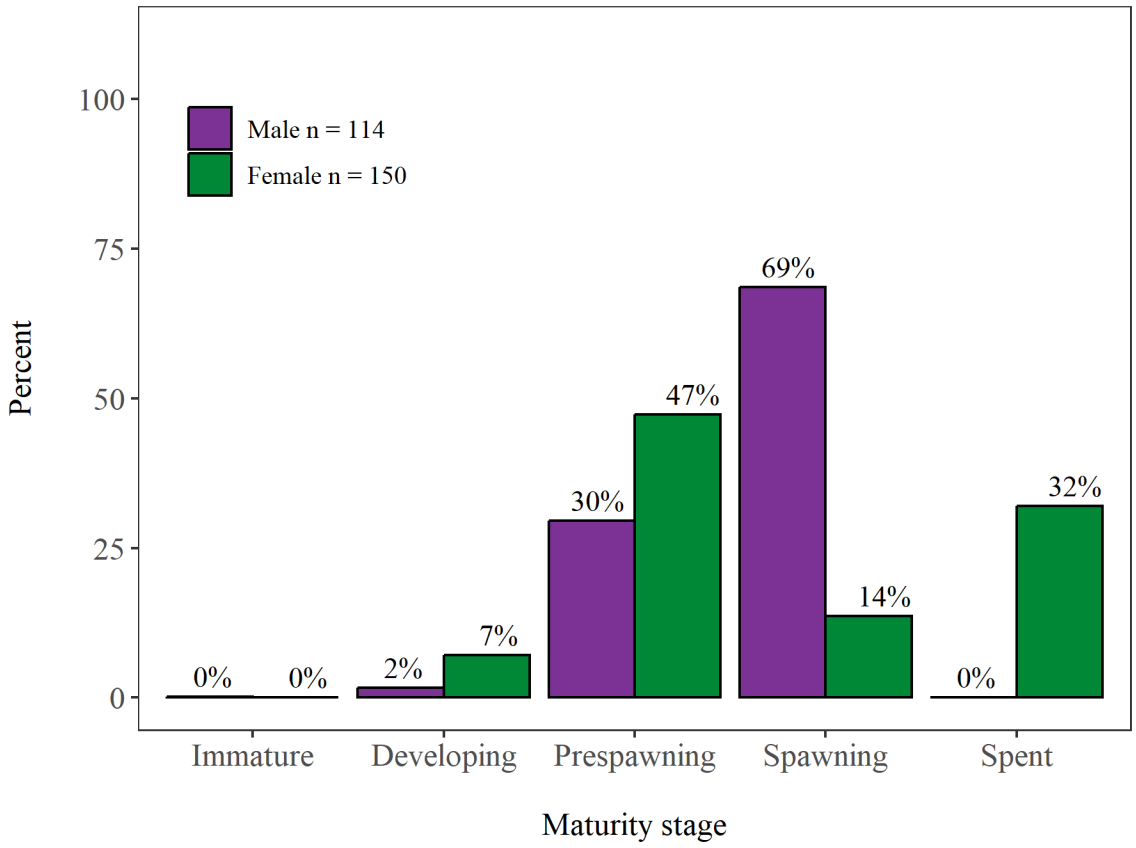


Figure A4.3. Pollock maturity composition for male and female pollock > 40 cm fork length (FL) within each stage in the Chirikof Shelfbreak region.

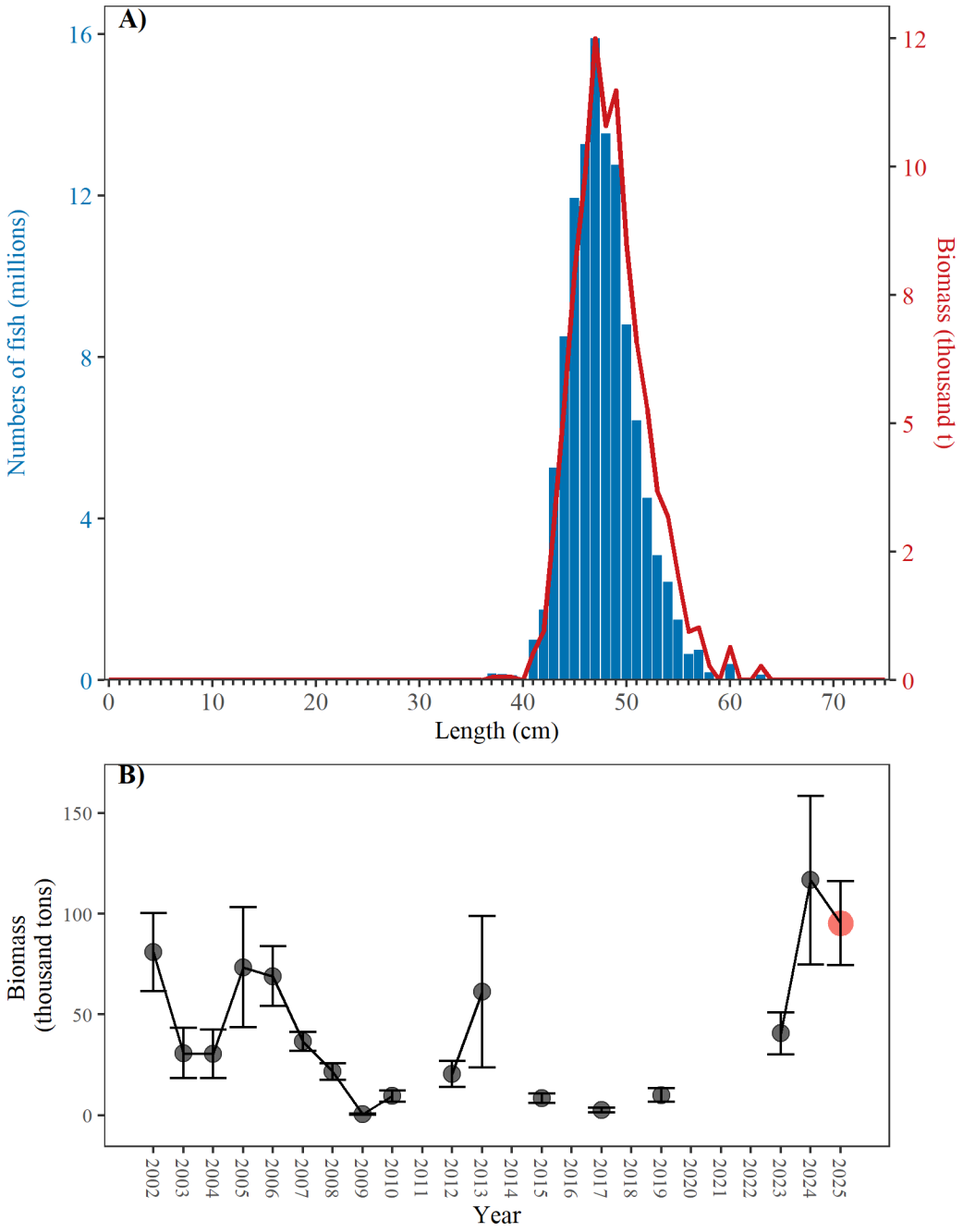


Figure A4.4. 2025 Chirikof Shelfbreak abundance summary. A) numbers- (blue bars) and biomass- (red line) at-length estimates of pollock. B) summary of age-1+ pollock biomass estimates (thousands of metric tons) from 2002-2025. Current survey estimate in red, and shaded area indicates 1-D geostatistical 95% confidence intervals.

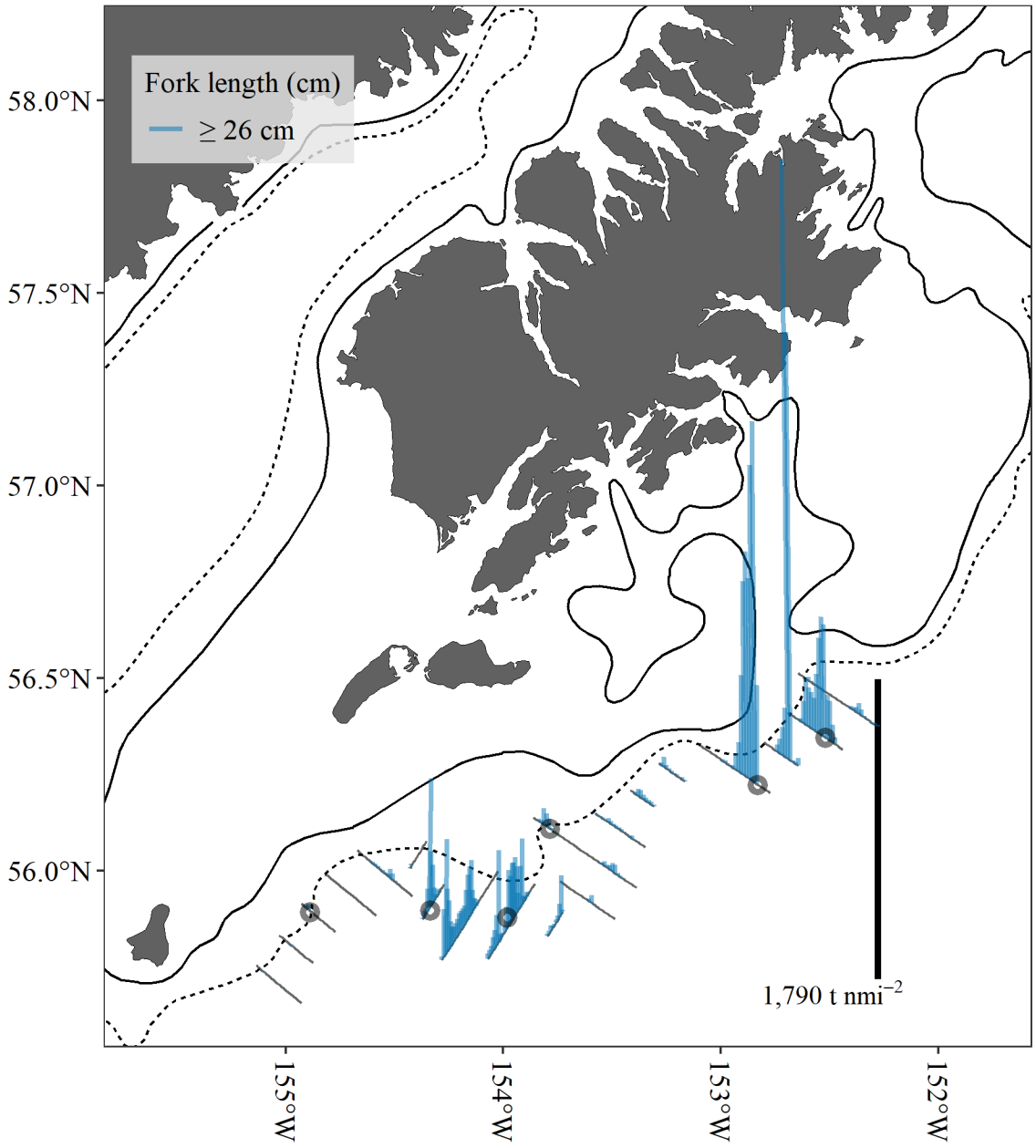


Figure A4.5. Biomass attributed to pollock (vertical lines) along tracklines in the Chirikof Shelfbreak region in 2025. Biomass is categorized as adult (≥ 26 cm FL, blue) pollock. Trawl locations are indicated with black circles.

Marmot Bay

The Marmot Bay region (Fig. 3) was surveyed between 28 March and 30 March. The survey region encompassed 1,014 km^2 (296 nmi^2). Acoustic backscatter was measured along 345.4 km (186.5 nmi) of transects spaced primarily 3.7 km (2.0 nmi) apart with spacing varying from 1.9 km to 3.7 km (1.0 nmi to 2.0 nmi) apart (Fig. 3). Bottom depths in the survey area ranged from 68 m to 275 m.

Sea surface temperatures (SST) measured in the Marmot Bay region indicated relatively warmer thermal conditions during the 2025 survey. SST ranged from 5.1°C to 5.8°C as measured by the ship's flow-through instrumentation along acoustic transects and averaged 5.5°C (Fig. A4.6a). Mean temperature between the surface and deepest trawl (i.e., headrope) depth at all haul locations varied by approximately 0.0°C (Fig. A4.6b). The average SST measured by the SBE 39 at all haul locations was 5.6°C (Table 2), which was 1.6°C warmer than the mean SST in 2023 and 1.6°C warmer than the long-term 1989-2023 historical mean (Fig. A4.7). The average temperature at 100 m depth, used as an indicator of thermal conditions at depth, was 5.6°C, which was 1.5°C warmer than the mean temperature at 100 m depth in 2023 and 1.4°C warmer than the long-term 1989-2023 historical mean (Fig. A4. 7).

Biological data and specimens were collected in the Marmot Bay region from 6 LFS1421 hauls (Table 2, Fig. 3). Pollock were randomly sampled for length (n = 1,864), body weight (n = 367) and maturity (n = 261) measurements (Table 3). Pollock and eulachon were the most abundant species by weight in the LFS1421 hauls, contributing 92.1% and 2.3% of the catch by weight, respectively (Table A4.2). Pollock and eulachon were the most abundant species by number, contributing 90.4% and 4.6% of the catch by number, respectively (Table A4.2).

Pollock observed in the Marmot Bay region were generally in pre-spawning (females) or spent (males) maturity stages. The abundance weighted maturity composition for males > 40 cm FL (n = 23) was 1% immature, 3% developing, 24% pre-spawning, 12% spawning, and 60% spent, and for females > 40 cm FL (n = 78) the abundance weighted maturity composition was 0% immature, 4% developing, 49% pre-spawning, 33% spawning, and 13% spent (Fig. A4.8).

Pollock with lengths < 17 cm FL, indicative of age-1 pollock, accounted for 97.5% of the numbers and 45.3% of the biomass of all pollock observed in the Marmot Bay region (Fig.

A4.9a). Pollock 17-26 cm FL, indicative of age-2 pollock, accounted for 0.2% by numbers and 0.2% by biomass. Pollock ≥ 26 cm FL, indicative of age-3+ pollock, accounted for 2.3% and 54.4% of the numbers and biomass, respectively (Fig. A4.9a). The distribution of pollock in the Marmot Bay region is summarized in Fig A4.10.

A total of 74.6 million pollock weighing 2,256.1 t were estimated to be in the Marmot Bay region. The 2025 biomass was 73.1% less than that observed in 2023 (8,389.6 t) and 83.7% less than the historic mean of 13,877.9 t (Fig. A4.9b). The relative estimation error of the 2025 biomass estimate based on the 1-D geostatistical analysis was 8.3%.

Table A4.2. Catch by species and numbers of length and weight measurements taken from 6 LFS1421 hauls during the 2025 acoustic-trawl survey of pollock in Marmot Bay.

		Catch				Measurements	
Species name	Scientific name	Weight (kg)	%	Number	%	Length	Weight
pollock	*Gadus chalcogrammus*	1,910.1	92.1	45,675	90.4	1,864	367
eulachon	*Thaleichthys pacificus*	47.1	2.3	2,324	4.6	116	55
Pacific ocean perch	*Sebastes alutus*	36.5	1.8	44	<0.1	44	44
arrowtooth flounder	*Atheresthes stomias*	26.1	1.3	15	<0.1	15	15
Pacific cod	*Gadus macrocephalus*	24.0	1.2	7	<0.1	7	7
sculpins	Cottidae (family)	9.4	0.5	456	0.9	31	12
Pacific capelin	*Mallotus catervarius*	8.6	0.4	1,289	2.5	103	72
Chinook salmon	*Oncorhynchus tshawytscha*	2.4	0.1	2	<0.1	2	2
smooth lumpsucker	*Aptocyclus ventricosus*	2.1	<0.1	2	<0.1	2	2
Pacific glass shrimp	*Pasiphaea pacifica*	1.5	<0.1	585	1.2	10	-
Pacific herring	*Clupea pallasii*	1.3	<0.1	144	0.3	14	14
chrysaora jellyfish	*Chrysaora sp.*	1.0	<0.1	4	<0.1	4	4
euphausiids	Euphausiacea (order)	1.0	<0.1	<0.1	<0.1	-	-
aurelia jellyfish	*Aurelia sp.*	0.8	<0.1	2	<0.1	2	2
flathead sole	*Hippoglossoides elassodon*	0.6	<0.1	2	<0.1	2	2
rock sole spp.	Lepidopsetta (genus)	0.5	<0.1	1	<0.1	1	1
sturgeon poacher	*Podothecus accipenserinus*	<0.1	<0.1	1	<0.1	1	1
Total		2,073.2		50,553		2,218	600

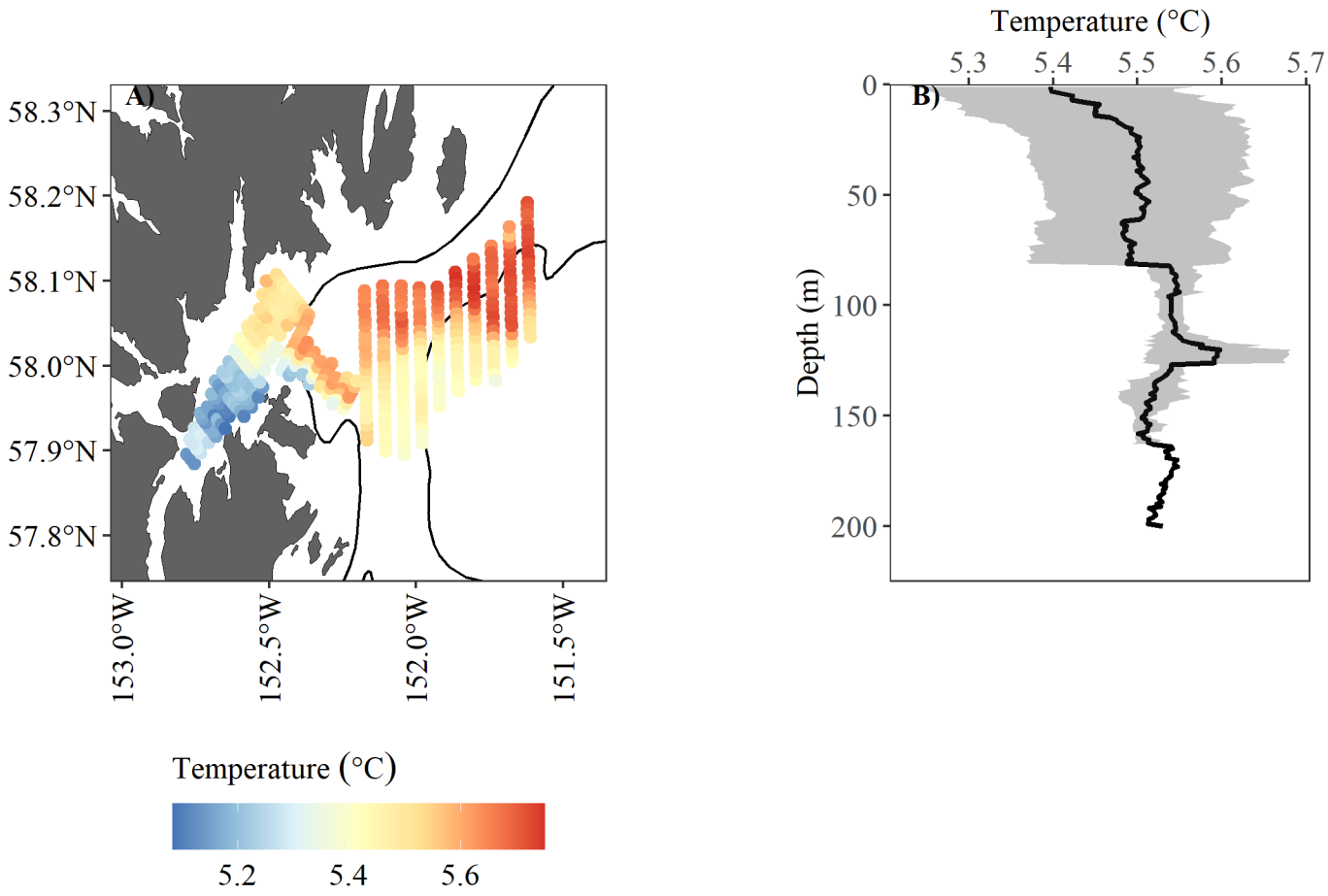


Figure A4.6. 2025 Marmot Bay temperature summary. A) surface water temperatures (°C) recorded at 5-second intervals. B) mean water temperature (°C; solid line) by 1-m depth intervals. The shaded area indicates ± 1 standard deviation.

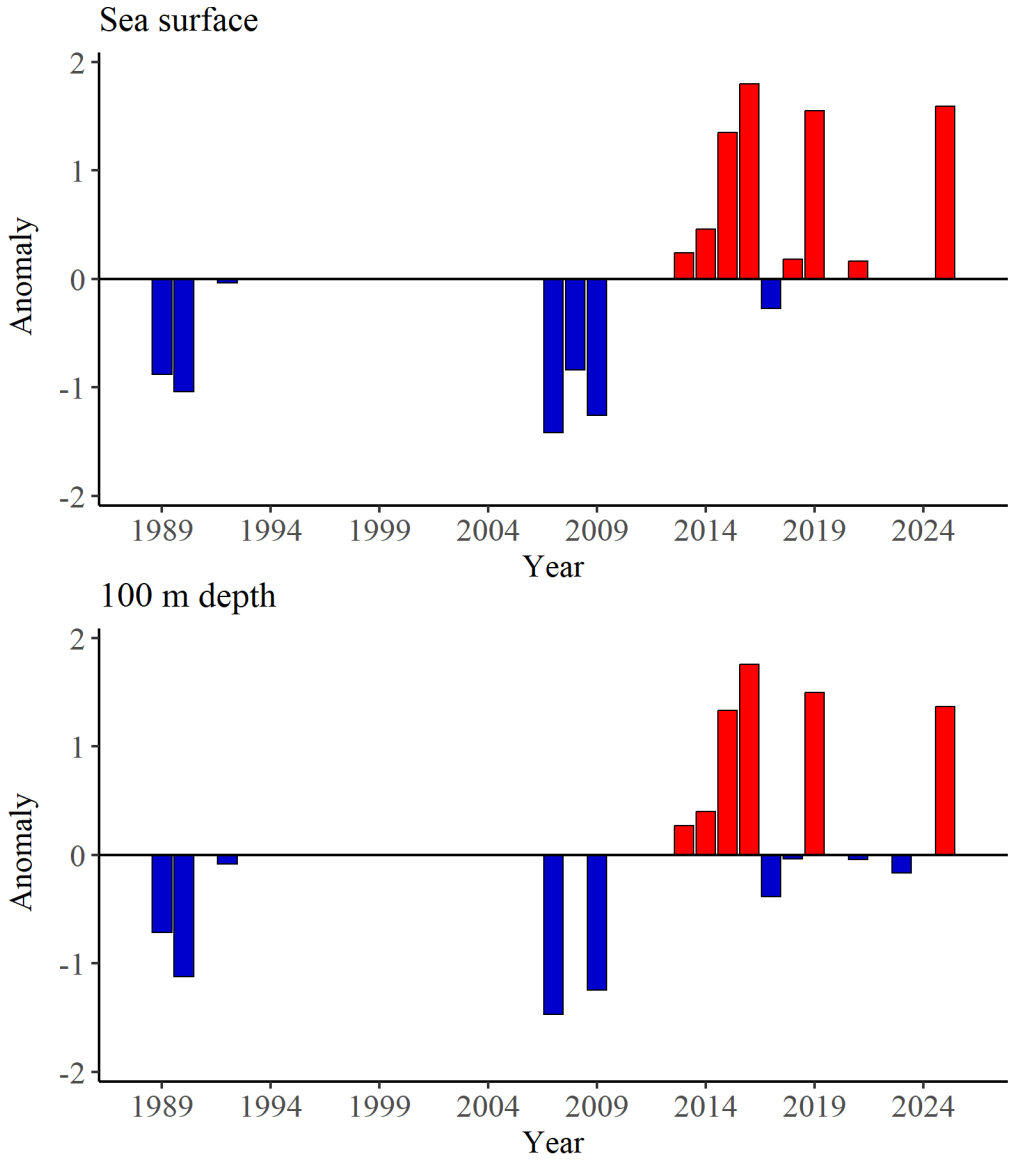


Figure A4.7. Temperature anomalies at the sea surface (upper panel) and 100 m depth (lower panel) in the Marmot Bay region. Anomalies for each temperature source are centered and scaled by their respective mean temperature and standard deviation from the 1989-2023 period. Positive and negative anomalies are indicated by red and blue bars, respectively.

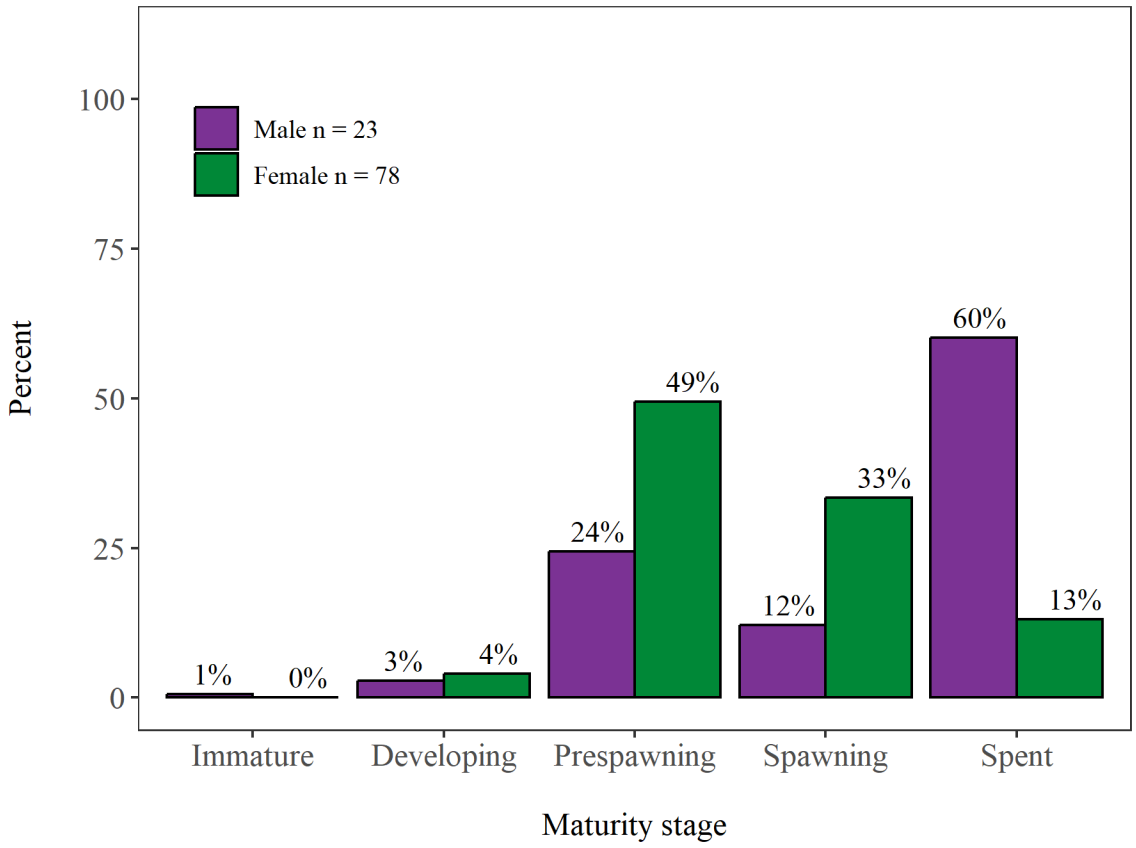


Figure A4.8. Pollock maturity composition for male and female pollock > 40 cm fork length (FL) within each stage in the Marmot Bay region.

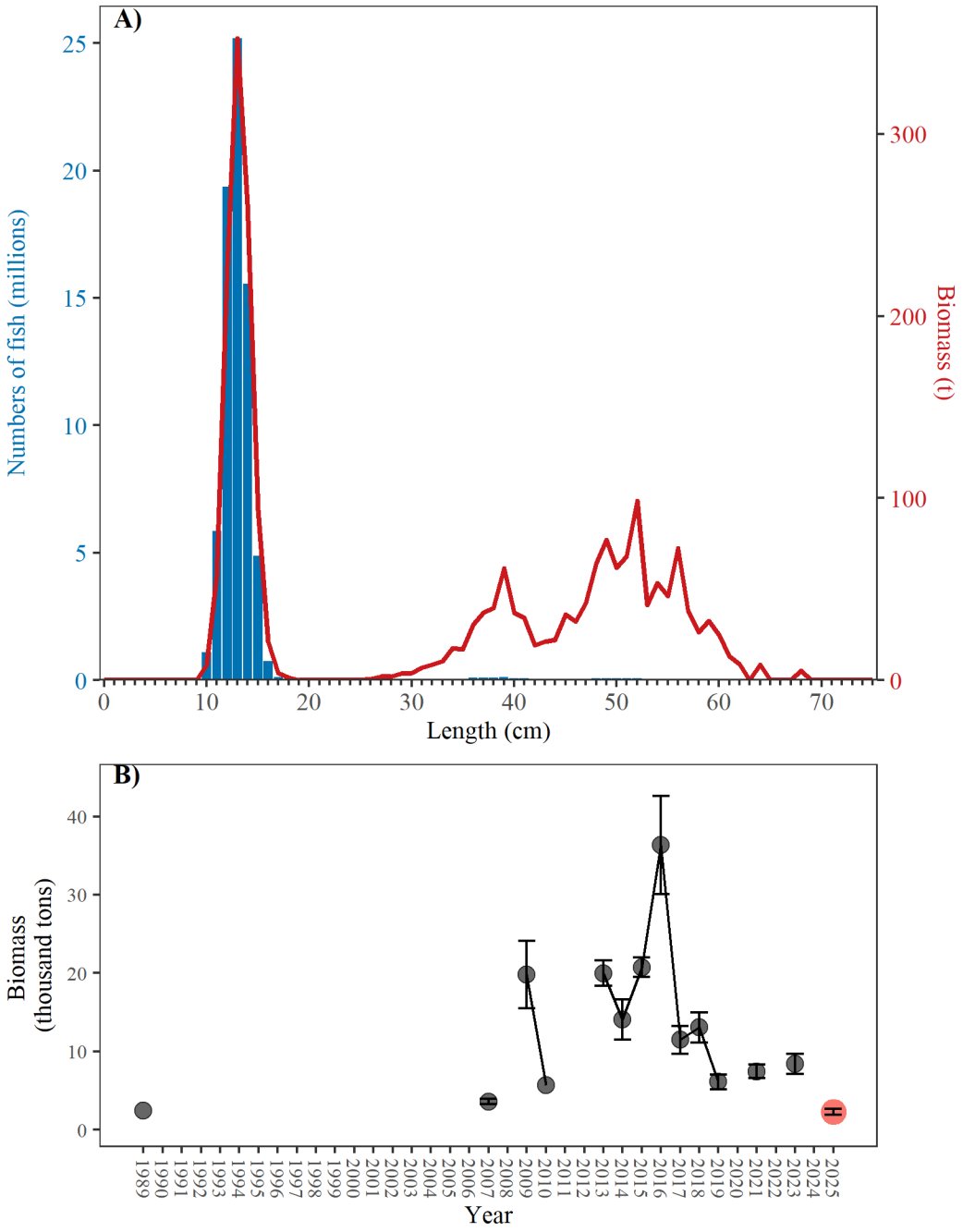


Figure A4.9. 2025 Marmot Bay abundance summary. A) numbers- (blue bars) and biomass- (red line) at-length estimates of pollock. B) summary of age-1+ pollock biomass estimates (thousands of metric tons) from 1989-2025. Current survey estimate in red, and shaded area indicates 1-D geostatistical 95% confidence intervals.

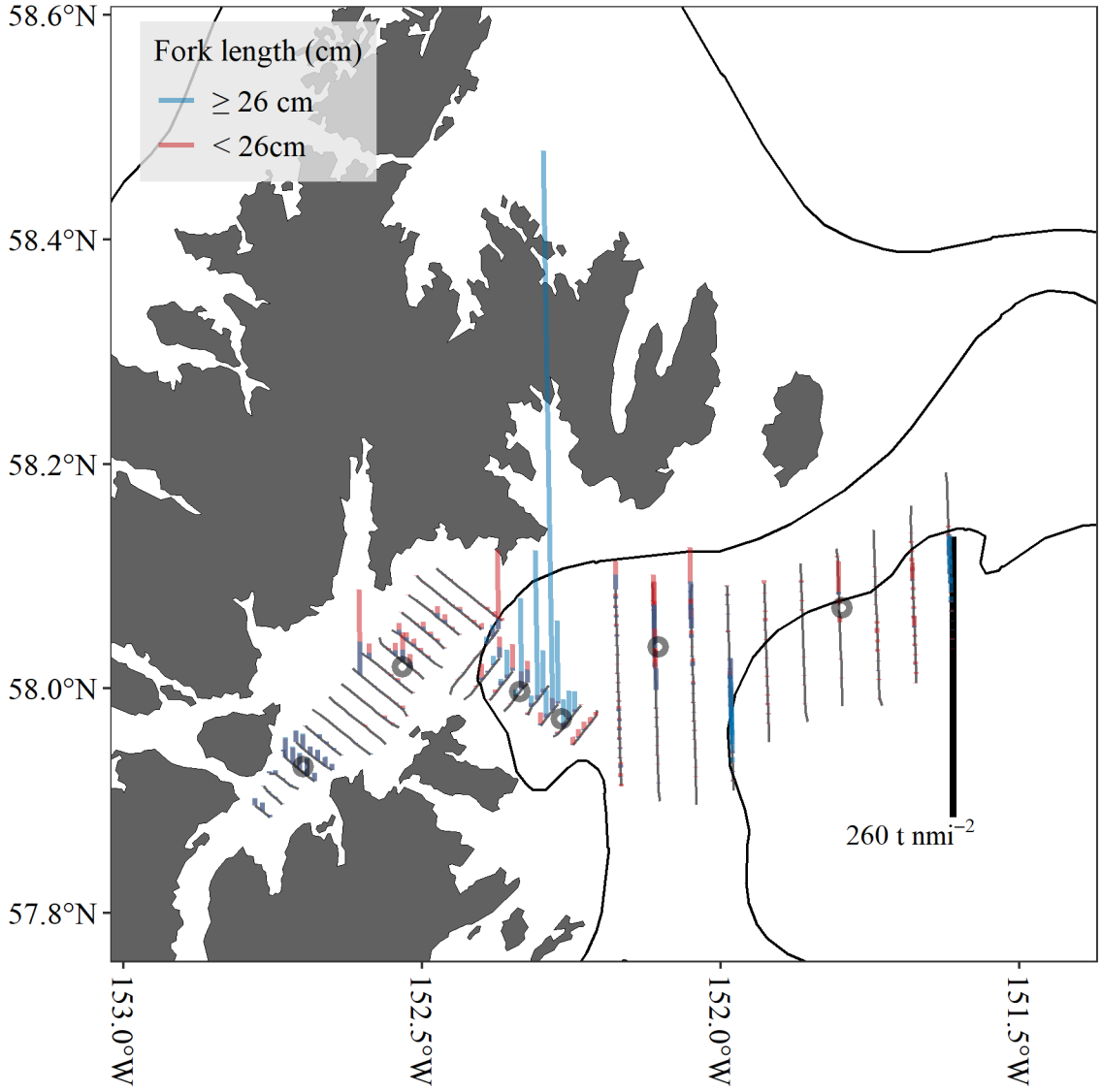


Figure A4.10. Biomass attributed to pollock (vertical lines) along tracklines in the Marmot Bay region in 2025. Biomass is categorized as adult (≥ 26 cm FL, blue) or juvenile (< 26 cm FL, red) pollock. Trawl locations are indicated with black circles.

APPENDIX V. RELATIVE ABUNDANCE OF SHELIKOF AGE-1 POLLOCK

Introduction and Methods

McKelvey (1996) showed that the abundance of age-1 pollock in Shelikof acoustic-trawl surveys 1981-1991 was correlated with age-3 abundance of the same year class, and proposed qualitative scoring of year class strength (low, medium, and high) based on age-1 survey abundance. We have continued to score age-1 survey abundance (without corrections for selectivity or other methodological improvements) in this way as a leading indicator of year class strength in survey reports (e.g., Levine and Jones 2025). We revisited the notion of using age-1 abundance as a leading indicator of year class strength with additional, more recent survey data. We compared age-1 survey abundance to both age-3 survey abundance and to age-3 stock assessment model output (two years later, for the same year class) using functional regression (Ricker, 1973) to allow for error in both series, and by calculating normal deviates ('Z-scores') for annual age-1 survey abundance estimates. A log10(x+1) transformation was applied to stabilize variance before analysis. For consistency with McKelvey (1996), this analysis was done separately on survey results 1981-2021 without correction for escapement of juvenile pollock and other small fishes (Williams et al. 2011, Honkalehto et al. 2024), as well as for 2008-2022 survey results that include this now-standard correction as well as other methodological improvements (McGowan et al. in preparation).

Results and Discussion

Based on survey results from 1981-2021, age-1 survey abundance had a positive relationship with age-3 survey abundance for the same year class, with the regression explaining about 39% of the variability ($r= 0.62$, $r^2= 0.39$, $n= 34$ observations; Fig. 1). The relationship exhibits substantial variability, and in addition, is sensitive to how transformation of the 2015 year class datum is handled: zero age-1 pollock were observed by the survey in 2016, and the +1 part of the data transformation is somewhat arbitrary. Quantitative prediction for any given year class using this relationship would be uncertain. Nonetheless, there is a tendency for high age-1 abundance to be associated with high age-3 abundance.

In a regression fit using only surveys since 2008, to which a consistent set of selectivity corrections and other methodological improvements have been made (as noted in Methods), the

relationship is somewhat stronger ($r= 0.71$, $r^2= 0.51$, n= 13 observations; Fig. 2) but still quite variable. Fitting age-3 stock assessment model output (Monnahan et al. 2024, their Table 1.22) to survey age-1s produced similar results ($r= 0.81$, $r^2= 0.66$, n= 14 observations; Fig. 3). This is one of the reasons that Shelikof survey abundance of age-1 and age-2 pollock is not formally used in the current Gulf of Alaska walleye pollock assessment model at this time (Monnahan et al. 2024). However, we propose that a continued qualitative index of year class strength using survey data is still warranted and suggest using the normal deviate of age-1 survey abundance relative to a running mean since the 2008 survey as the indicator of year class strength: $Z < -1$ indicating 'low', $-1 \leq Z \leq 1$ 'medium', and $Z > 1$ 'high' year class strength (Figs. 1-3). The association between age-1 and age-3 abundance with the addition of new data could continue to be monitored by computing a correlation coefficient.

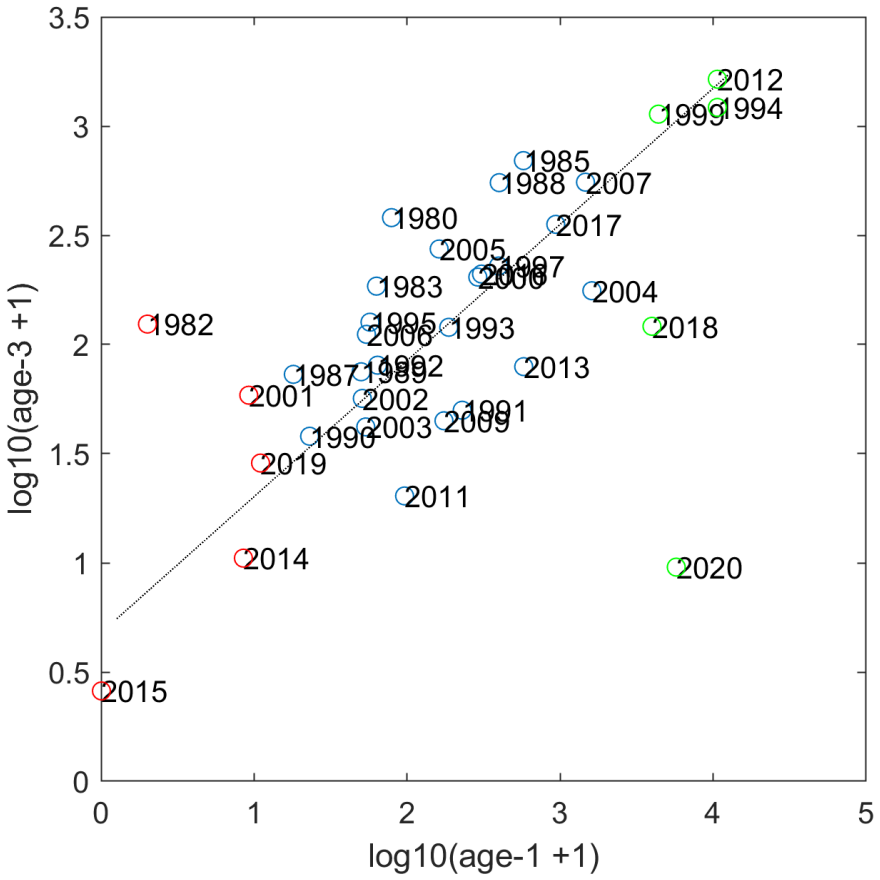


Figure 1. Age-3 walleye pollock abundance (millions of fish) regressed on age-1 pollock abundance in Shelikof Strait acoustic-trawl surveys 1981-2021 (r^2= 0.39, n= 34). A log10(x+1) transformation was applied to stabilize variance. No selectivity corrections for escapement were applied to these data. The year class is indicated next to each data point. Red points are 'low' (Z < -1), blue points are 'medium' (- 1 ≤ Z ≤ 1), and green points are 'high' (Z > 1) based on the normal deviate of age-1 abundance.

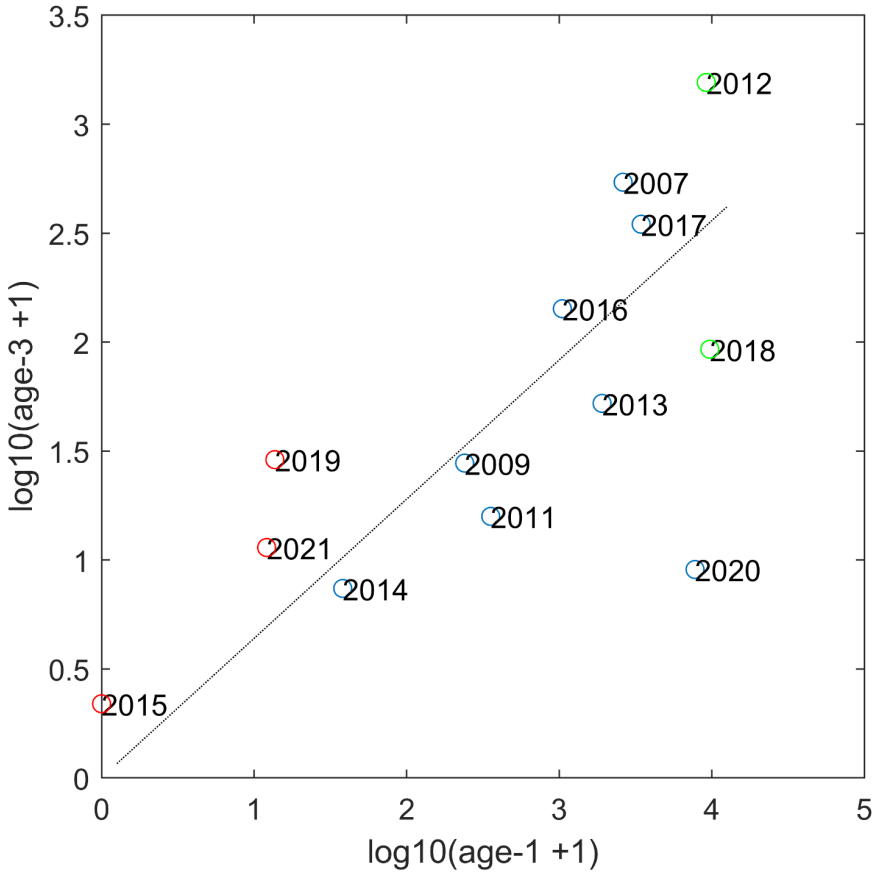


Figure 2. Age-3 walleye pollock abundance (millions of fish) regressed on age-1 pollock abundance in Shelikof Strait acoustic-trawl surveys 2008-2022 (r^2= 0.51, n= 13). A log10(x+1) transformation was applied to stabilize variance. Selectivity corrections for escapement were applied to these data. The year class is indicated next to each datum. Red points are 'low' ($Z < -1$), blue points are 'medium' ($-1 \leq Z \leq 1$), and green points are 'high' ($Z > 1$) based on the normal deviate of age-1 abundance.

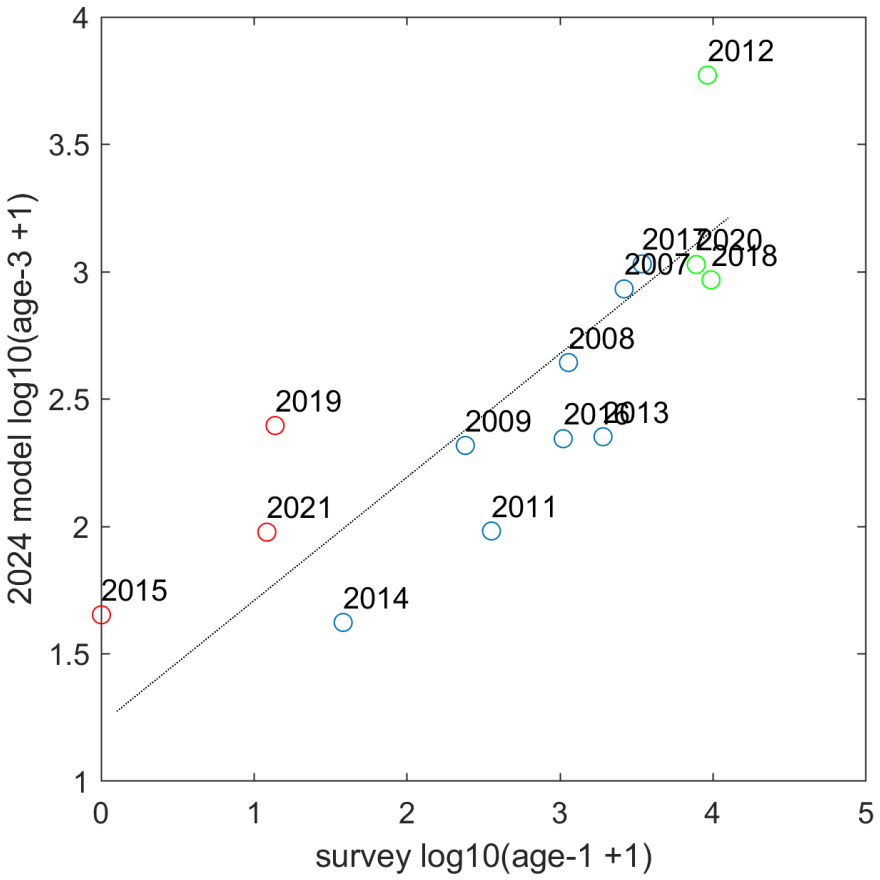


Figure 3. Age-3 walleye pollock abundance (millions of fish) from stock assessment model output (Monnahan et al. 2024, their Table 1.22) regressed on age-1 pollock abundance in Shelikof Strait acoustic-trawl surveys 2008-2022 (r^2= 0.66, n= 14). A log10(x+1) transformation was applied to stabilize variance. Selectivity corrections for escapement were applied to the survey data. The year class is indicated next to each datum. Red points are 'low' (Z < -1), blue points are 'medium' (- 1 ≤ Z ≤ 1), and green points are 'high' (Z > 1) based on the normal deviate of age-1 abundance.